National Library of Canada

Acquisitions and Bibliographic Services Branch

395 Wellington Street
Ottawa, Ontario
K1A 0N4

Bibliothèque nationale du Canada

Direction des acquisitions et des services bibliographiques

395, rue Wellington
Ottawa (Ontario)
K1A 0N4

Your file Votre référence

Our file Notre référence

NOTICE

The quality of this microform is heavily dependent upon the quality of the original thesis submitted for microfilming. Every effort has been made to ensure the highest quality of reproduction possible.

If pages are missing, contact the university which granted the degree.

Some pages may have indistinct print especially if the original pages were typed with a poor typewriter ribbon or if the university sent us an inferior photocopy.

Reproduction in full or in part of this microform is governed by the Canadian Copyright Act, R.S.C. 1970, c. C-30, and subsequent amendments.

AVIS

La qualité de cette microforme dépend grandement de la qualité de la thèse soumise au microfilmage. Nous avons tout fait pour assurer une qualité supérieure de reproduction.

S'il manque des pages, veuillez communiquer avec l'université qui a conféré le grade.

La qualité d'impression de certaines pages peut laisser à désirer, surtout si les pages originales ont été dactylographiées à l'aide d'un ruban usé ou si l'université nous a fait parvenir une photocopie de qualité inférieure.

La reproduction, même partielle, de cette microforme est soumise à la Loi canadienne sur le droit d'auteur, SRC 1970, c. C-30, et ses amendements subséquents.

Canada

University of Alberta

WEAR OF COUPLINGS WITH OILFIELD TUBING

By

GABY H. SONEGO

A Thesis submitted to the Faculty of Graduate Studies and Research in partial fulfillment of the requirements for the degree of Master of Science.

Department of Mechanical Engineering

Spring 1993

National Library of Canada
Acquisitions and Bibliographic Services Branch
395 Wellington Street
Ottawa, Ontario
K1A 0N4

Bibliothèque nationale du Canada
Direction des acquisitions et des services bibliographiques
395, rue Wellington
Ottawa (Ontario)
K1A 0N4

Your file Votre référence

Our file Notre référence

The author has granted an irrevocable non-exclusive licence allowing the National Library of Canada to reproduce, loan, distribute or sell copies of his/her thesis by any means and in any form or format, making this thesis available to interested persons.

L'auteur a accordé une licence irrévocable et non exclusive permettant à la Bibliothèque nationale du Canada de reproduire, prêter, distribuer ou vendre des copies de sa thèse de quelque manière et sous quelque forme que ce soit pour mettre des exemplaires de cette thèse à la disposition des personnes intéressées.

The author retains ownership of the copyright in his/her thesis. Neither the thesis nor substantial extracts from it may be printed or otherwise reproduced without his/her permission.

L'auteur conserve la propriété du droit d'auteur qui protège sa thèse. Ni la thèse ni des extraits substantiels de celle-ci ne doivent être imprimés ou autrement reproduits sans son autorisation.

ISBN 0-315-82149-3

Canada

UNIVERSITY OF ALBERTA

RELEASE FORM

Name of Author: Gaby H. Sonego

Title of Thesis: Wear of Couplings With Oilfield Tubing

Degree: Master of Science

Year This Degree Granted: Spring 1993

Permission is hereby granted to the University of Alberta Library to reproduce single copies of this thesis and to lend or sell such copies for private, scholary or scientific research purposes only.

The author reserves all other publication and other rights in association with the copyright in the thesis, and except as hereinbefore provided neither the thesis nor any substantial portion thereof may be printed or otherwise reproduced in any material form whatever without the author's prior written permission.

Gaby H. Sonego

Gaby H. Sonego

16508 - 79A Avenue
Edmonton, Alberta
T5R 3J3

Date: APRIL 21, 1993

University of Alberta

Faculty of Graduate Studies and Research

The undersigned certify that they have read and recommend to the faculty of Graduate Studies and Research for acceptance, a thesis entitled **Wear of Couplings With Oilfield Tubing** submitted by **Gaby H. Sonego** in partial fulfillment of the requirements for the degree of **Master of Science**.

Dr. D.G. Bellow (Supervisor)

Dr. B.M. Patchett

Dr. J.R. Colbourne

Dr. D.R. Budney

Date: 93/04/20

To my family.....

Abstract

Sucker rod couplings and tubings in a non-vertical oil well are subjected to severe wear as they interact during the cyclic pumping operation. This wear can become excessive in sand environments. Worn couplings and rods can be relatively easily replaced during shutdowns, but tubing is very costly to replace. Therefore, it is important to minimize the wear of these components by choosing a suitable coupling/tubing sliding combination.

A wear testing apparatus was designed in the laboratory to evaluate the wear of couplings and tubing under simulated operating conditions. With this apparatus it was found that the ceramic coated coupling (TiO_2) wore the least and caused the least damage to the tubing in the water environment condition. On the other hand, this coupling showed the worst performance in the presence of sand. When examining the overall performance of the couplings and tubing in the different environmental conditions, the NiW coated coupling yielded the best performance. The influence of the operating variables on the wear of couplings and tubing was studied. Side load, sliding duration, surface roughness and sand flow rate had direct influences on the wear of the couplings and tubing. Surface hardness of the tubing increased due to work hardening and the transfer of harder particles from the coating on the coupling which enhanced the wear resistance of the tubing.

Acknowledgements

I would like to take this opportunity to sincerely thank my supervisor, Dr. D.G. Bellow, for his valuable guidance and support throughout the course of this work. Thanks to my wife, Debbie, for her support, patience and assistance; to my colleagues and the staff at Black Max - downhole tools Ltd. for their support and understanding; to Mr. Dale Harper from Eutectic - Castolin for his help in providing the required coatings and information; to Mr. George Braybrook for his help with S.E.M. A special thanks to Al Muir, Max Schubert, Tony Van Straten, Don Fuhr, Albert Yuen and Bernie Faulkner for their valuable time and for helping keep the test apparatus functioning. I gratefully acknowledge ESSO Resources , NSERC (A-2705) and the Government of the province of Alberta for providing financial support through their scholarship and grant program.

TABLE OF CONTENTS

CHAPTER		PAGE
1	INTRODUCTION	1
	1.1 Nature of The Problem	1
	1.2 Thesis Outline	3
2	COUPLING/TUBING OPERATION	5
	2.1 Introduction	5
	2.2 Sucker Rod Strings	5
	2.3 Coupling/Tubing Environment	7
3	WEAR	8
	3.1 Introduction	8
	3.2 Types of Wear	9
	3.2.1 Adhesive Wear	10
	3.2.2 Abrasive Wear	11
	3.2.3 Delamination Wear	11
	3.2.4 Surface Fatigue Wear	13
	3.2.5 Corrosive Wear	14
	3.3 Factors Affecting Wear	15
	3.3.1 Load	15
	3.3.2 Speed/Temperature	16
	3.3.3 Surface Roughness	17

CHAPTER PAGE

3.3.4 Sliding Distance....18

3.3.5 Material Hardness....19

3.3.6 Lubrication....21

3.3.7 Environment....21

3.4 Wear Modes....23

3.4.1 Mild Wear....23

3.4.2 Severe Wear....23

4 EXPERIMENTAL PROCEDURE....25

4.1 Introduction....25

4.2 Test Apparatus....25

4.3 Material Tested....31

4.3.1 Tubing....31

4.3.2 Coupling....31

Standard....31

NiCr Coated Coupling....32

NiW Coated Coupling....32

TiO_2 Coated Coupling....33

4.4 Data Collection....34

4.5 Statistical Conditioning of Data....35

4.6 Scatter of Experimental Data....38

CHAPTER PAGE

4.7 Uncertainty in Variables....39

5 RESULTS AND DISCUSSION....41

5.1 Introduction....41

5.2 Wear of Coupling and Tubing....41

5.2.1 Coupling Weight Loss....41

Water Environment....41

Water and Sand Environment....43

5.2.2 Tubing Thickness Loss....48

Water Environment....48

Water and Sand Environment....48

5.3 Analysis of Tubing Surface Roughness....51

Water Environment....51

Water and Sand Environment....54

5.4 Analysis of Coupling/Tubing Microhardness....57

5.4.1 Coupling Microhardness....57

Water Environment....57

Water and Sand Environment....60

5.4.2 Tubing Microhardness....62

Water Environment....62

CHAPTER PAGE

Water and Sand Environment....65

5.5 Friction....67

5.5.1 Running-In....67

5.5.2 Frictional Force....69

5.5.3 Apparent Coefficient of Friction....69

Water Environment....71

Water and Sand Environment....73

5.6 Wear Rate....74

Water Environment....74

Water and Sand Environment....77

5.7 Wear Rate and Friction Relationship....77

5.8 Wear Modes....80

5.9 Analysis of Different Wear Mechanisms Using Scanning Electron Micrographs....81

5.10 The Effect of Sand Rates on the Wear of Coupling/Tubing....88

5.11 The Advantages of Coating Materials....93

6 CONCLUSIONS AND RECOMMENDATIONS....97

6.1 Conclusions....97

6.2 Recommendations....100

REFERENCES....101

CHAPTER PAGE

APPENDICES:

APPENDIX 1: Statistical Analysis.....106

APPENDIX 2: Summary of Results.....123

LIST OF TABLES

TABLE		PAGE
4.1	Variable Uncertainties	40
5.1	Sand Rate and the Degree of Wear Relationship	93
5.2	The Cost of Coating Couplings	94
5.3	The Cost of Standard Coupling	95
5.4	Comparison of Coupling Cost vs Performance	94
A.1.1	Coupling Weight Loss	106
A.1.2	Tubing Average Thickness Loss	107
A.1.3(a)	Tubing Surface Roughness -Initial	108
A.1.3(b)	Tubing Surface Roughness - 10 km	109
A.1.3(c)	Tubing Surface Roughness - 100 km	110
A.1.3(d)	Tubing Surface Roughness - 200 km	111
A.1.3(e)	Tubing Surface Roughness - 300 km	112
A.1.4(a)	Coupling Microhardness - Initial	113
A.1.4(b)	Coupling Microhardness - 10 km	114
A.1.4(c)	Coupling Microhardness - 100 km	115
A.1.4(d)	Coupling Microhardness - 200 km	116

TABLE PAGE

A.1.4(e) Coupling Microhardness - 300 km....117

A.1.5(a) Tubing Microhardness - Initial....118

A.1.5(b) Tubing Microhardness - 10 km....119

A.1.5(c) Tubing Microhardness - 100 km....120

A.1.5(d) Tubing Microhardness - 200 km....121

A.1.5(e) Tubing Microhardness - 300 km....122

A.2.1 Coupling Weight Loss [g] vs Distance Travelled at Various Side Loads - Water Environment....123

A.2.2 Coupling Weight Loss [g] vs Distance Travelled at Various Side Loads - Water & Sand Environment....123

A.2.3 Tubing Average Thickness Loss [mm] vs Distance Travelled at Various Side Loads - Water Environment....124

A.2.4 Tubing Average Thickness Loss [mm] vs Distance Travelled at Various Side Loads - Water & Sand Environment....124

A.2.5 Tubing Surface Roughness [µm] vs Distance Travelled at Various Side Loads - Water Environment....125

A.2.6 Tubing Surface Roughness [µm] vs Distance Travelled at Various Side Loads - Water & Sand Environment....125

TABLE PAGE

A.2.7 Coupling Microhardness [VHN] vs Distance Travelled at Various Side Loads - Water Environment....126

A.2.8 Coupling Microhardness [VHN] vs Distance Travelled at Various Side Loads - Water & Sand Environment....126

A.2.9 Tubing Microhardness [VHN] vs Distance Travelled at Various Side Loads - Water Environment....127

A.2.10 Tubing Microhardness [VHN] vs Distance Travelled at Various Side Loads - Water & Sand Environment....127

A.2.11 Frictional Force [N] as a Function of Side Load - Water Environment....128

A.2.12 Frictional Force [N] as a Function of Side Load - Water & Sand Environment....128

A.2.13 Apparent Coefficient of Friction at Various Side Loads - Water Environment....129

A.2.14 Apparent Coefficient of Friction at Various Side Loads - Water & Sand Environment....129

A.2.15 Coupling Wear Rates [cc/Nm] - Water Environment....130

A.2.16 Coupling Wear Rates [cc/Nm] - Water & Sand Environment....130

A.2.17 Summary of Results of Different Variables at Different Sand Rates Using Standard Coupling/J55 Tubing Under 133.5 N Side Load....131

LIST OF FIGURES

FIGURE		PAGE
1.1	Well Production Configurations	2
2.1	Sucker Rod End	6
2.2	Sucker Rod Coupling	6
4.1	Side View of Wear Testing Apparatus	26
4.2	Top View of Wear Testing Apparatus	27
4.3	Sand Dispenser	28
4.4	Bolt-Spring Assembly - Applied Side Load	29
4.5	Coupling Carriage	30
5.1	Coupling Weight Loss at 133.5 N - Water Environment	42
5.2	Coupling Weight Loss at 445 N - Water Environment	42
5.3	Coupling Weight Loss at 890 N - Water Environment	42
5.4	Coupling Weight Loss at 133.5 N - Water & Sand Environment	44
5.5	Coupling Weight Loss at 445 N - Water & Sand Environment	44
5.6	Coupling Weight Loss at 890 N - Water & Sand Environment	44
5.7	Wear of TiO_2 Coated Coupling at 133.5 N Side Load after 10 km	45
5.8	Wear of TiO_2 Coated Coupling and Tubing at 445 N Side Load after 300 km - Water & Sand Environment	46

FIGURE PAGE

5.9 Wear of NiCr Coated Coupling at 445 N Side Load after 300 km - Water & Sand Environment.....47

5.10 Tubing Average Thickness Loss at 133.5 N - Water Environment.....49

5.11 Tubing Average Thickness Loss at 445 N - Water Environment.....49

5.12 Tubing Average Thickness Loss at 890 N - Water Environment.....49

5.13 Tubing Average Thickness Loss at 133.5 N - Water & Sand Environment.....50

5.14 Tubing Average Thickness Loss at 445 N - Water & Sand Environment.....50

5.15 Tubing Average Thickness Loss at 890 N - Water & Sand Environment.....50

5.16 Surface Truncation at Different Levels.....52

5.17 Tubing Surface Roughness at 133.5 N - Water Environment.....53

5.18 Tubing Surface Roughness at 445 N - Water Environment.....53

5.19 Tubing Surface Roughness at 890 N - Water Environment.....53

5.20 Transverse Surface of Tubing under 890 N Side Load after 300 km of Travel (x52, 2% Nital Etchent) Using a) Standard Coupling, b) NiCr Coated Coupling, c) NiW Coated Coupling and d) TiO_2 Coated Coupling.....56

5.21 Tubing Surface Roughness at 133.5 N - Water & Sand Environment.....56

FIGURE PAGE

5.22 Tubing Surface Roughness at 445 N - Water & Sand Environment....56

5.23 Tubing Surface Roughness at 890 N - Water & Sand Environment....56

5.24 Coupling Microhardness at 133.5 N - Water Environment....58

5.25 Coupling Microhardness at 445 N - Water Environment....58

5.26 Coupling Microhardness at 890 N - Water Environment....58

5.27 Wear Path of NiW Coated Coupling at 445 N After 10 km Distance Travelled....59

5.28 Porosity in the Coating - NiW Coated Coupling (Magnification x 44)....59

5.29 Coupling Microhardness at 133.5 N - Water & Sand Environment....61

5.30 Coupling Microhardness at 445 N - Water & Sand Environment....61

5.31 Coupling Microhardness at 890 N - Water & Sand Environment....61

5.32 Tubing Microhardness at 133.5 N - Water Environment....63

5.33 Tubing Microhardness at 445 N - Water Environment....63

5.34 Tubing Microhardness at 890 N - Water Environment....63

FIGURE PAGE

5.35 Tubing Microhardness at 133.5 N - Water & Sand Environment....66

5.36 Tubing Microhardness at 445 N - Water & Sand Environment....66

5.37 Tubing Microhardness at 890 N - Water & Sand Environment....66

5.38 Running-In Friction of NiCr Coated Coupling under 445 N Side Load - Water Environment....68

5.39 Frictional Force as a Function of Side Load - Water Environment....70

5.40 Frictional Force as a Function of Side Load - Water & Sand Environment....70

5.41 Apparent Coefficient of Friction of Tubing with Different Couplings at Various Side Loads - Water Environment....72

5.42 Apparent Coefficient of Friction of Tubing with Different Couplings at Various Side Loads - Water & Sand Environments....72

5.43 Test Sliding Condition as for Tilted Pad Bearing....73

5.44 Wear Rates of all Couplings at 300 km as a Function of Side Load - Water Environment....75

5.45 Wear Rates of all Couplings at 890 N as a Function of Distance - Water Environment....75

5.46 Wear Rates of Standard and NiW Coated Couplings at 300 km as a Function of Side Load - Water and Sand Environment....76

5.47 Wear Rates of Standard and NiW Coated Couplings at 890 N Side Load as a Function of Distance - Water and Sand Environment....76

FIGURE PAGE

5.48 Wear Rate and Friction Relationship for all Couplings at 300 km as a Function of Side Load.....79

5.49 Transverse Surface of Tubing under 890 N Side Load after 300 km (x 240, 2% Nital Etchant).....80

5.50 Coupling Weight Loss at Different Sand Rates.....90

5.51 Tubing Average Thickness Loss at Different Sand Rates.....90

5.52 Tubing Surface Roughness at Different Sand Rates.....90

5.53 Coupling Microhardness at Different Sand Rates.....91

5.54 Tubing Microhardness at Different Sand Rates.....91

5.55 Apparent Coefficient of Friction vs Sand Rate.....92

5.56 Coupling Wear Rate at Different Sand Rates.....92

LIST OF PLATES

PLATE		PAGE
1	Adhesive Wear of Tubing	83
2	Abrasive Wear of Tubing	85
3	Other Wear Mechanisms of Tubing	87

LIST OF SYMBOLS

DR_o -standard deviation ratio

DR -deviation ratio

Xi -data point value

$\overline{X}$ -average data point value of the sample

σ_X -standard deviation of the sample

$\sigma_{\overline{X}}$ -standard deviation of the mean

n -sample size

δY -sensitivity

Y -minimum value measurement

F -frictional force

W -normal load

μ -coefficient of friction

Chapter 1

Introduction

1.1 Nature Of The Problem

Sucker rod strings are devices used to activate pumps located at the bottom of oil wells. The individual rods are connected together by threaded couplings. The couplings, being of a larger diameter than the rods, make contact with the tubing wall causing wear of both the coupling and the tubing during the pumping cycle. Usually, this is no problem unless buckling occurs during the down-stroke, however, this can lead to accelerated wear of the coupling and tubing. In non-vertical wells, (Figure 1.1) the contact is more severe and rapid wear takes place. As a result, the wear of downhole components is a significant problem. Wear can become excessive in the presence of sand. In particularly severe situations, oil field components can wear out in a matter of a few weeks necessitating replacement of components and a general "workover" for the well. Couplings are more easily replaced during shutdowns but it is important to minimize wear of tubing since tubing is very expensive to replace.

The sucker rod coupling and tubing wear problem was recently addressed [1, 2, 3]. These papers describe work in North America to help minimize the problem of coupling-tubing wear to lengthen the

time between shutdowns and reduce the downtime. There are no known studies of coupling-tubing wear in the presence of sand.

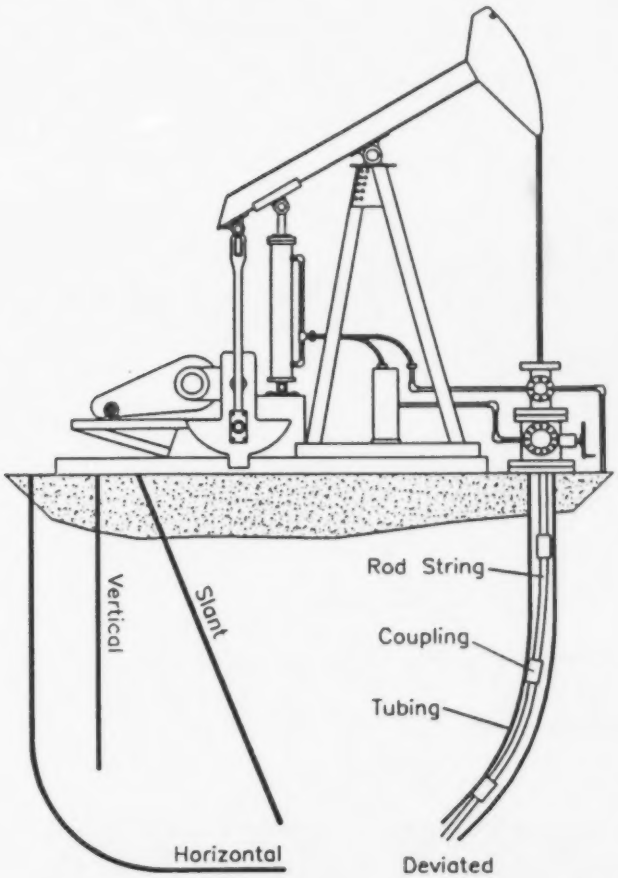

Figure 1.1. Well Production Configurations

Oil companies employ a number of devices to reduce down-hole wear problems. Some of these include the use of continuous sucker rods without couplings (particularly useful in slant wells or deviated wells), injected moulded plastic centralizers placed along the rod to separate the rod from the tubing, plastic coated couplings,

hard metal-coated couplings, and roller couplings. Each of these devices works to a degree, but none has so far been able to eliminate wear completely.

The work described in this thesis was designed to evaluate the performance of various types of couplings versus tubing, the influence of different variables on the wear of couplings/tubing, to show and identify the controlling wear mechanisms, and the influence of sand on wear. Wear tests were performed in two environments; 1) water and 2) water and sand. In each of these environments, actual field components were utilized with the testing variables closely controlled.

1.2 Thesis Outline

The first part of the thesis consists of a general review of coupling/tubing research. In Chapter 2, a general description of sucker rod strings is provided followed by a review of the types of environments to which couplings/tubing are exposed. In Chapter 3, studies of different types of wear are described. The effects of different variables on the wear rate are addressed as well. Chapter 4 describes the experimental procedure, the statistical analyses used in the present study and the uncertainties in individual variables.

The second part of the thesis deals with some experiments conducted on couplings/tubing. This thesis examines (Chapter 5)

the wear of couplings and tubing (weight and thickness loss), work hardening effect, microhardness, wear rates, apparent coefficient of friction and surface roughness. All of the above are compared using different side loads and different environments. Different materials were tested to determine which material caused the least wear in the coupling/tubing. Relative costs of the coatings are shown. Chapter 6 outlines the conclusions of the experimental research.

Chapter 2

Coupling/Tubing Operation

2.1 Introduction

Prior to examining the performance of different couplings, the conditions and constraints of the coupling/tubing operation must be understood. This chapter begins with a brief description of the coupling/tubing operation followed by an explanation of the sucker-rod pumping system and the effects that well fluid properties have on the service life of components.

2.2 Sucker rod strings

Sucker rod strings are made up of 25 foot (7.62 m) steel rods connected by threaded couplings. Sucker rod tubings and couplings are manufactured according to standards set by the American Petroleum Institute (API, 1982) which defines the dimensional geometry and classifies them into various alloy types. The sucker rod is manufactured from bar stock with diameters ranging from 1/2 in (12.7 mm) to 1-1/8 in (28.6 mm). The rod end is forged and machined to create a roll-threaded pin, shoulder, wrench square and upset bead at each end (Figure 2.1).

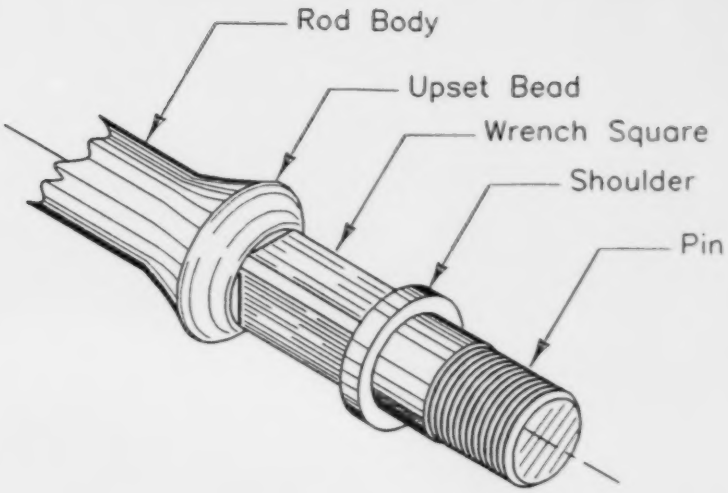

Figure 2.1. Sucker Rod End

The coupling which connects the pins of adjacent rods is usually made out of AISI 8630 from a cold extruded cylinder. The cylinder is bored through and machined with an inside rolled thread (Figure 2.2). The coupling has an outer diameter of 1-3/4 in (44 mm) and is 4 inches long (100 mm) according to API dimensions. The tubing has an outer diameter of 2-7/8 in (73 mm) electrical resistance welded (ERW) tubing.

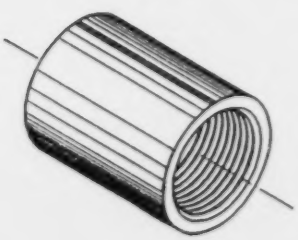

Figure 2.2. Sucker Rod Coupling

2.3 Coupling/Tubing Environment

The properties of oil well fluids have a large influence on the service life of coupling/tubing. When the water component of the pumped fluids is corrosive, a mechanism known as corrosive wear can greatly reduce the service life. Furthermore, the wear is more severe in an environment where sand and fluid are combined. It is this latter environmental combination which is discussed in detail in this thesis.

Chapter 3

Wear

3.1 Introduction

Wear is the progressive loss of material from the surface of a body due to the relative motion of two bodies in contact [4]. In recent years due to many attempts to control and understand the wear process, a broader definition was adopted. Wear is defined as "the gradual damage which may result when two materials in contact move relative to each other" [5]. This definition can be further subdivided into two categories;

I. Material may be displaced or changed in shape or in mechanical property with little or no material loss.

II. An observed net change of mass from at least one of the interaction components and loose wear debris.

These distinctions are important. If there is no apparent change in volume or mass it might be concluded that no wear has taken place. However, wear might have occurred as a result of material displacement from one part of a body to another without any material loss.

3.2 Types of Wear

In the oil industry the wear of the coupling/tubing is primarily caused by impacting and sliding motions. The environment plays an important role in this process. The environment can contain sand, water, gas, slurry, corrosive media and these may act as carriers for particle asperities. These particles that have broken off, slide and plow into the surface material. Such wear debris (broken asperities due to cyclic loading system) is the dominant cause of the wear.

In order to study and to gain a better understanding of wear, it is essential to recognize that several distinct and independent mechanisms may be involved. Wear may be characterized by the appearance of the worn surface or based upon the mechanisms and conditions which prevail during material removal [6]. Such classifications as mild wear and severe wear are based upon the observation of worn surfaces. However, other terminologies such as adhesive wear, abrasive wear and delamination wear are based upon the mechanism of material removal or the conditions which exist during the wear process. The following types of wear have been classified.

3.2.1 Adhesive Wear

Adhesive wear occurs as a result of the relative sliding between two surfaces under a normal contact load. As a normal load is applied, the local pressure on the asperities becomes extremely high. The yield point stress is exceeded and the asperities deform plastically. This process continues until the real contact area has increased enough to support the applied load.

Continued sliding causes the junctions to be sheared and new junctions to be formed. Some of the ruptured junctions transfer from one surface to the other [7], others are discarded as debris.

The transfer of material from one surface to another by adhesion has been studied by several investigators. For example, Kerridge and Lancaster [8] used a radioactive pin of 60:40 brass rubbing against a ring of tool steel. The transfer of material was demonstrated by placing a photographic film in contact with the tool steel after rubbing. An autoradiograph of the transferred brass from the wear track was subsequently obtained. Another example of the transfer of material was conducted by Bellow et. al. [1]. In their study, a scanning electron micrograph was used to show nickel platelets deposit from coated couplings on to the softer oilfield tubing.

3.2.2 Abrasive Wear

Abrasive wear occurs in one of two ways. First, the wear is caused by the ploughing out of softer material by a harder surface. This is known as two-body abrasive wear. In the second case, abrasion is caused by loose hard particles sliding between rubbing surfaces. This is known as three-body abrasive wear [9]. The mechanism of abrasive wear has been shown to be microcutting of small chips by the harder particles acting as cutting tools [10]. These particles slide and deform the surface and the subsurface by plowing. The subsurface deformation is due to the process of subsurface void and crack formation similar to delamination which is more fully described below.

Surface hardness is an important parameter in abrasive wear. Kruschov [11] showed there was a linear relationship between resistance to wear with hardness, for a range of annealed pure metals. It was also found that prior work-hardening of the pure metals had no effect on the wear rate. The conclusion reached was that during abrasion, a metal surface work-hardens to a maximum value which determines the abrasion resistance of the material.

3.2.3 Delamination Wear

Delamination wear takes place by deformation of the surface layer, nucleation of cracks at the subsurface and the propagation of these cracks parallel to the surface along the sliding direction. The

wear particles generated by this wear mechanism differ in shape from those generated by the deformation and fracture of asperities and by plowing. The wear particles generated by the removal of the surface asperities are small whereas those associated with plowing tend to be long by one order of magnitude [12].

The delamination theory of wear [13] describes the following sequence of events which lead to loose wear sheet formation:

a) When two sliding surfaces come in contact, normal and tangential loads are transmitted through the contact regions by adhesive and plowing actions. The asperities of the softer surface are easily deformed and some are fractured by the repeated loading. A relatively smooth surface is formed while these asperities are deformed or are being removed.

b) Once the surface becomes smooth, the contact is not just asperity to asperity contact, but rather an asperity to plane contact. Each point along the softer surface experiences cyclic loading. The surface traction exerted by the harder asperities on the softer surface induces plastic deformation which accumulates with repeated loading.

c) As the subsurface deformation continues, voids and cracks are nucleated below the surface.

d) Upon further deformation and with repeated loadings, cracks propagate, joining the neighboring ones. Cracks tend to propagate parallel to the surface governed by material properties and the state of loading.

e) When these subsurface cracks reach a critical length they become unstable and propagate to the surface generating thin wear sheets. The thickness of these sheets depends upon the material properties and the magnitude of the normal and tangential loads at the surface, since they control the magnitude and the depth of the maximum tensile stress behind the moving asperities.

3.2.4 Surface Fatigue Wear

When two sliding surfaces make contact via asperities, it follows that wear can occur by adhesion or abrasion. It is possible however, that these asperities can make contact without adhering or abrading and can pass each other leaving one or both asperities plastically deformed. After a critical number of such contacts, an asperity would fail due to fatigue, producing a wear debris. Archard and Hirst [14] have suggested that the metal transferred by adhesion is finally removed by a fatigue process. It is difficult to prove directly that asperity fatigue is a major cause of wear under any given set of conditions [15].

Surface fatigue is usually associated with surfaces in rolling contact. This type of wear is caused by surface and subsurface cracks and fatigue crack propagation [6, 16]. Lancaster [4] defined fatigue wear as "the detachment of particles as a result of cyclic stress variations usually associated with rolling, but localized fatigue on an asperity scale is becoming increasingly recognized as a factor in sliding wear also".

3.2.5 Corrosive Wear

Corrosive wear is a process in which a chemical reaction with the environment is the rate-determining factor. When rubbing takes place in a corrosive environment which may be either gaseous or liquid, surface reactions take place and reaction products are found on one or both surfaces. These reaction products are commonly poorly adherent to the surfaces and further rubbing causes their removal [15]. This process is then repeated. Corrosive wear requires both corrosion and rubbing. The reaction products depend upon the exact composition of the environment. For instance, small quantities of water vapor in air cause the reaction product to be the hydroxide rather than the oxide. The most common liquid environment is water and here small amounts of dissolved gases, commonly oxygen or carbon dioxide, influence corrosion. Corrosion is also influenced by the relative electropotential of rubbing metals. High contact stresses can cause enhanced corrosion locally leading to pitting. The pitting may lead to surface cracking and this combined with surface rubbing may result in catastrophic wear. The presence of a lubricant usually protects the surfaces from the corrosive environment. However, it is not uncommon for corrosive elements to be dissolved in lubricants like water in oil. Lubricants can be degraded in time and can become progressively more corrosive.

3.3 Factors Affecting Wear

Wear in sliding contact depends upon parameters such as the material properties, the load, the temperature surface topography, lubrication, and speed [17]. The following sections will describe those factors which can cause considerable variation in the wear rates of rubbing surfaces.

3.3.1 Load

Teer and Arnell [15] suggested that an increase in load causes an increase in the frictional force, and hence, a rise in temperature. An increase in load can also cause a transition from mild wear to severe wear. This point was supported by Bellow et al. [1]. This work showed a change in wear mode of couplings and tubings i.e. a change from mild wear to severe wear, while increasing the contact pressure from 370 kPa to 1380 kPa. It was also suggested that the wear rate/weight loss of the standard coupling increased in a non-linear fashion with an increasing load. The wear rate was measured as $g/10^5 m$. The load increase caused an increase in the hardness of the surfaces in contact [1]. Ko et al. [2] showed that the coupling/tubing wear rates tend to increase with high normal loads and faster sliding speeds.

3.3.2 Speed/Temperature

In general, the effect of speed is to cause an increase in the temperature of the sliding interface and facilitating oxide formation. If the increase in the temperature is high enough the hardness of the metal will decrease so that an increase in the wear rate should be expected.

The general effect of increasing surface velocity is a reduction in the rate of wear. This was shown in a detailed study of wear of 60/40 brass on steel over a speed range of 0.01-500 cm/s using a pin-ring machine [18]. These experiments showed that the size of the transferred material decreased as the speed increased. Since time was not available for junction growth, it caused a progressive fall in the rate of wear. The other effect of speed was to cause a progressive rise in temperature with a concomitant fall in the shear strength of the brass. This resulted in an increase in junction size. A progressive rise in temperature with increased speed increased the amount of brass which was deposited. When this overcame the effect of the frequency of transfer, wear rate increasesd.

Ko et al. [2] showed that the coupling/tubing wear rates tended to increase with higher normal contact load and faster sliding speed. However, at the slowest stroke rate tested (5 strokes/min; stroke=0.9m), wear rates were much less sensitive to normal contact load. The high sliding rate might also have increased the vibration level of the test apparatus. These conditions are prone to promote

the dispersion of wear debris and the breakdown of surface oxide leading to metallic contact and transfer, and hence more severe wear damage.

3.3.3 Surface Roughness

Surface roughness is "the geometrical detail of a solid surface, relating particularly to variations in height" [19]. This definition would refer and include any change in the actual surface level from the ideal datum level.

Since wear is a process of fatigue occurring at the material surface, the initial surface roughness may be considered a factor which may influence the rate of wear and friction. The wear of different surface finishes in the range 0.1μm - 4.8μm were observed by Jahnmir and Suh [20]. The results of the experiments indicated that under very light loads, rough surfaces tend to wear less initially than smooth surfaces while the opposite appears to be true under high load. However, the results observed appear to be limited to the first 100 m of sliding. During this sliding distance, the geometry of the asperities was changed by plastic flow and the surface became relatively smooth.

In another study on cam wear conducted by C. Alamsyah et al. [21], initial surface profiles did not play a predominant role in the run-in wear of the cams. Rather, the wear occurred in the initial minutes of testing, apparently at wear initiation sites provided by

the microstructure and initial finish.

In a discussion on Argon's paper [22], S. Jahnmir said that the effect of surface roughness is present only at the initial stages of wear. Once the original roughness of the surface is removed by the wear process, the steady-state wear does not depend on the initial surface roughness. The behavior at low loads was controlled by the gradual removal of the asperities, so the total wear of the surface which had the roughest surface, was larger than the total wear of the smoothest surface. The steady-state wear rate of both surfaces was the same. When the load was increased, asperities of the smooth surface could not support the load and thus were broken up very quickly in the sliding process, starting the steady-state delamination wear processes immediately. However, for rough surfaces, it took some time before the rough, hard asperities could be removed and the delamination process could start. In all cases, the steady-state wear rate did not depend upon the initial surface roughness [23, 24]. It is important to note that these observations were obtained for metal-metal contact. The same observations are not necessarily true for metal-polymer contact [25].

3.3.4 Sliding Distance

The sliding wear of metals with typical machined surfaces is dependent upon the history of sliding, the environment, the applied load and the surface roughness as well as on the microstructure and the basic properties of metal. To a first approximation, the wear

volume of a typical metal may be plotted as a function of the sliding distance. The sliding wear rate is a linear function of sliding distance except for the first 500 run-in cycles (30m) [26]. Initially, very high wear rates are observed as the original surface asperities are removed. When the surface is lubricated or when the load is low, the surface becomes smooth and no wear is observed. As distance increases, the subsurface is subjected to changes which lead to the delamination process [12]. This wear mechanism causes the wear rate to increase rapidly and the cycle starts again. The wear rate decreases with increasing distance. On the other hand, the wear (loss of material) increases with distance [1, 2].

3.3.5 Material Hardness

The removal of material from metallic surfaces by any wear mechanism occurs by deformation and fracture of wear particles from the wearing material. Therefore, the wear rate must depend on such mechanical properties as hardness, ductility, plastic flow stress etc.. The hardness of a material is a measure of its resistance to plastic flow.

As a general rule, the adhesion, delamination and abrasion rates are inversely proportional to the hardness [6]. Poggie et al. [26] and Czichos et al. [27] also showed that the wear rate decreased as the hardness increased. The experimental results of the Bellow et al. [1] study indicated that the hard-metal coated coupling had greater resistance to wear than the standard coupling. On the other

hand, Jahnmir et al. [28] observed that increasing hardness by introducing many inclusions or hard second phase particles may increase the delamination rate because the hard particles act as void nucleation sites.

By examining abrasive wear as a function of the hardness ratio (hardness ratio between abrading species and abraded material), Peterson & Ramalington [29] suggested that the hardness ratio of the order of 0.4 is desirable to obtain negligible wear. Therefore, in order to provide wear protection in sliding against a material that possesses Vickers hardness between 600 and 800 counterface hardnesses in the Vickers range of 1500 to 2000 are sufficient.

The effect of ductility on wear has not been studied extensively. It may be expected that an increase in ductility decreases the wear rate [6]. However, this would not be the case if increasing ductility causes the hardness of the material to decrease, thereby may increase the wear rate.

The relation between wear and material hardness is more complicated in three body abrasion than in two body abrasion. When material hardness changes, the ratio of cutting wear to plastic deformation wear changes [30]. Rabinowicz et al. [31] and Misra [32] conducted three body abrasion tests and showed that the wear resistance of metals increased with increasing hardness almost linearly and the relation obtained by them was similar to that in two body abrasion.

3.3.6 Lubrication

Most lubricants are introduced into a sliding system with the aim of 1) separating the two surfaces, 2) reducing the friction force, and 3) reducing the degree of surface adhesion. Sometimes, however, lubricants will be used to reduce the interfacial temperature. All of the above usually lead to a reduction in the wear rate [33].

Metallic films can serve as a lubricant. They can cause smooth sliding and they can also protect the underlying metal surfaces. In addition, these films are worn off the surface by successive sliding over the same track in a manner similar to that of a lubricant film, except that the metallic films are worn away at a higher rate than long-chain paraffins or fatty acid films. The difference between metallic and lubricant films is, that on rough surfaces, a lubricant film needs to be only one or two molecules thick in order to be effective as a boundary lubricant. However, a metallic film must be of the order 10^{-4} mm [34] in order to be effective.

3.3.7 Environment

Moisture in the environment can have a large effect on the fracture mechanisms of steel with or without oxygen present [35]. Dahlberg [36] reported that moist air increased the crack propagation rate about 10 times over dry air for 4340 steel.

Wear behavior in aqueous environments parallels that of many other types of conjoint chemical-mechanical interacting systems such as corrosion fatigue or stress corrosion cracking. For some metals, this environment can be most detrimental in corrosion fatigue and causes wear damage. For example, Appledorn et al. [37] showed that by making the environment more corrosive, wear was increased. Most metals are covered by an oxide film and even after cleaning by machining or grinding acquire a film of oxide of between 5 and 50 molecular layers in five minutes or less [15]. When an oxide film covering an asperity is removed by rubbing, the clean metallic surface will be immediately covered by a monomolecular layer. This should be taken into account in the wear of metals under atmospheric conditions. The properties of the oxide film are also important. For instance, the hard brittle oxide formed on aluminium provides poor protection against heavy wear. Barwell [48] showed that the wear of two steel surfaces in a vacuum of 10^{-4} mmHg was lower than their wear when air was allowed into the apparatus. The explanation of these results is that a thin tough and tenacious oxide film was formed on the steel at 10^{-4} mmHg whereas when air was admitted, the oxide film formed was thicker but less protective. Corrosion products (eg. oxide film) prevent the junction growth which occurs in vacuo and thus lower the coefficient of friction and reduce wear unless the corrosion itself is so severe that it wears the surface. Corrosion products can act as lubricants, lower the coefficient of friction and reduce wear unless the corrosion itself is so severe that it wears the surface.

3.4 Wear Modes

Two broad types of wear are identified when relatively soft metals are sliding against a smooth harder counterface. These wear types are described as mild and severe.

3.4.1 Mild Wear

Lancaster [39] identified mild wear with low wear rates, minimal plastic deformation, surface film deformation protecting against metal to metal surface and oxide wear debris. In fact, this wear process involves three stages: 1) transfer of metal fragments to the counterface, 2) oxidation of these fragments, and 3) removal of this oxide by attrition. The rate determining stage is the rate of oxidation. Bowden and Tabor [34] described the mild wear debris as a fine powder. The transition between mild to severe wear is associated with the merging, by subsurfaces deformation, of local asperities [40]. Metal oxide is removed in the mild regime while large metal particles are removed in the severe region.

3.4.2 Severe Wear

Severe wear is characterized by high wear rates, extensive plastic deformation and transfer to the harder counterface [39]. This wear mode is typically found at high loads and low speeds. Initially, relatively small fragments are transferred to the harder counterface. These fragments then increase in size and successive preferential

transfer until a critical size is formed and then they are detached as flake-like debris.

Archard's model [40] for oxidation time describes a wear particle 10^{-5} mm in diameter coming off the surface at 727°C. The time for complete oxidation is 0.001 s. For a particle of 10^{-4} mm in diameter, the time is still only 0.1 s. Bellow et al. [1] indicated that the mild and severe wear modes were dependent on the nature of the rubbing surfaces and the amount of side load present.

It is known that the wear rate of coupling/tubing increases as normal contact load, sliding speed [2] and distance [1] increases. It is also known that wear rates are lower in a water/oil emulsion environment than in an aerated water environment [2], and that the wear of hard metal coupling on the J55 tubing is considerably lower than that of standard coupling [1]. However, it is not known why the hard metal coupling wore less than the standard coupling [1]. The effect on the wear of coupling/tubing in the presence of sand and the controlling wear mechanisms are unknown.

Chapter 4

Experimental Procedure

4.1 Introduction

Wear is an interdisciplinary subject and its complex mechanisms are not easily clarified. The progressive nature of wear destroys the evidence of its initial stages as cumulative action develops toward surface fatigue. Test results from field studies can be inconclusive due to difficulties in controlling the test variables and they are also costly.

A specific wear testing apparatus was designed in the laboratory to evaluate coupling and tubing wear. Different controlled variables were examined. All tests were carried out using actual oil field components.

4.2 Test Apparatus

Since there are not standard testing machines for evaluating the wear of oil field components, a special wear apparatus was developed to simulate downhole operations using actual oil field components.

The test apparatus was activated by a hydraulic piston that drove four specimen carriages, each holding one coupling specimen back and forth along four stationary tubing test sections. Each test section was sloped to allow fluid to flow down all tubings (Figure 4.1 - 4.2). The wear of actual downhole components is accelerated by corrosion, therefore, the test apparatus was designed to incorporate fluid flow to wet the contact surfaces continuously. Water was used to represent the above environment, rather than salty water or other fluid combinations because each well contains water with different salinity. The water flow rate was set at 0.5 l/m using fresh non-recirculated tap water at 18°C, pH 7.8-7.9.

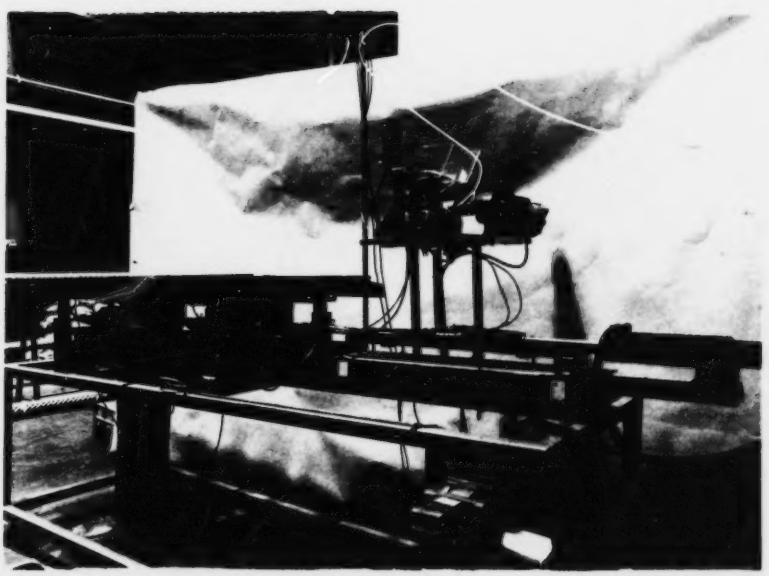

Figure 4.1. Side View of Wear Testing Apparatus

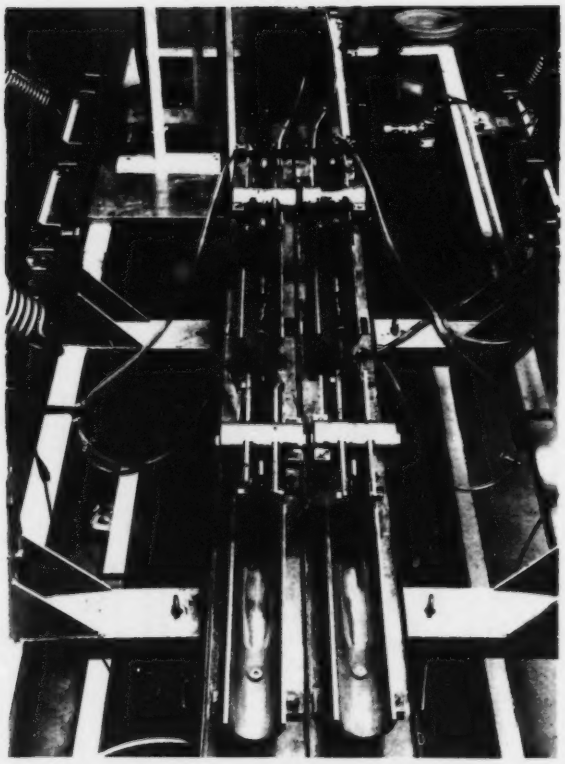

Figure 4.2. Top View of Wear Testing Apparatus

In order to simulate the third body abrasive environment, a special sand dispenser (Figure 4.3) was developed and used to meter out minute quantities of sand into the water stream. Ottawa 50-70 testing sand was used. This has a grit size of 50-70. The sand flow rate was set at 165 g/day and was steady. Other flow rates were applied to the standard coupling to compare the effects of different sand rates.

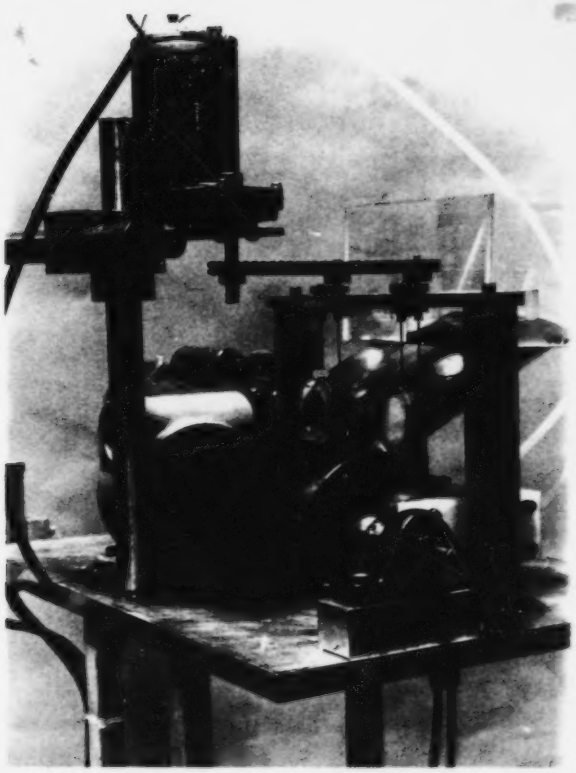

Figure 4.3. Sand Dispenser

The stroke length was set at 0.41 m. The stroke rate was 44 strokes/min. and the speed was constant while conducting all tests. The stroke length used in the field ranges from 1 ft to 5 ft (0.3 m - 1.5 m) and can change depending on the amount of fluid pumped. The stroke rate applied in the field ranges from 5 (slow) to 25 (fast) strokes/min. Hence, speed is from 1.5 m/min. to 37.5 m/min. The speed used in the lab represents the average speed used in the field. The stroke length used in the lab was comparable to the short stroke lengths used in the field.

Calibrated bolt-spring assemblies (Figure 4.4) applied normal contact loads (side load) between the coupling specimens and longitudinally-split tubing specimens as the carriage (Figure 4.5) reciprocated along linear motion bearing rails. Three different loads, 133.5 N, 445 N and 890 N, were applied. Ko et al. [2] used loads ranging from 223 N to 890 N. Bellow et al. [1] used loads ranging from 445 N to 1335 N. These magnitudes of loads were chosen after consulting with the above investigators and workers in the oil producing industry and are comparable to the actual loads found in rod strings in the field.

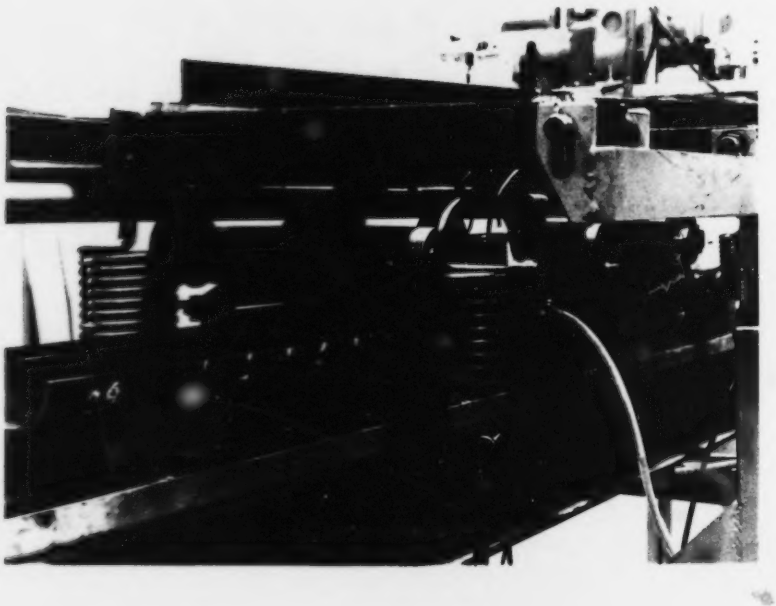

Figure 4.4. Bolt-Spring Assembly - Applied Side Load

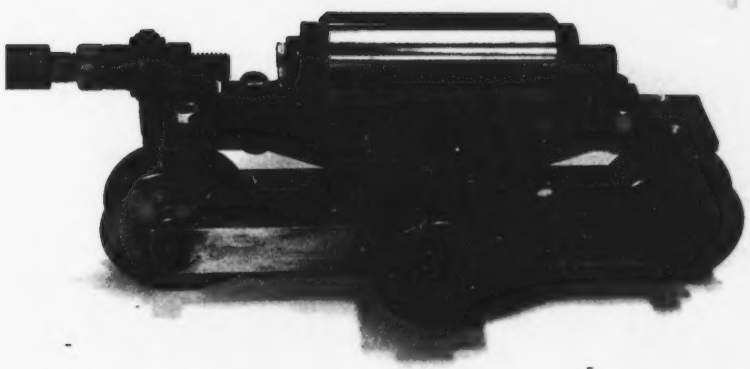

Figure 4.5. Coupling Carriage

The test length was measured by distance travelled along 300,000 m in a period of 11.5 days. This period is comparable to the time to failure observed in actual oil wells which vary from a few days (high contact load and corrosive environment) to 3-4 weeks (low contact load and non-corrosive condition).

4.3 Material Tested

4.3.1 Tubing

All experiments used new J55 tubings with an outer diameter of 73 mm and were 400 mm long. All tubings were cut in half longitudinally along the welding seam. The tubing was then honed in order to obtain an initial uniform surface roughness. The J55 tubing had an initial hardness of 180 HV 785g (Vickers' hardness number and the applied load). The J55 tubing consists of 0.06-0.1% C, 1.1-1.3% Mn, 0.033-0.047 % Co and 0.015-0.125 % Ti.

4.3.2 Coupling

Standard

One of the test couplings used in this study is the common coupling supplied with sucker rods. For the purpose of this study, it will be called the standard coupling. This coupling had an outer diameter of 46 mm and was 100 mm long. It was made from cold extruded tube out of AISI 8630 (typical density is 7.85 g/cc). The surface hardness was 190 HV 785g.

Three types of coated couplings were used in the present study. The coated couplings were supplied by "Eutectic Castolin". Their description, chemical composition and physical properties were supplied by the manufacturer. Standard couplings were used as the base and were coated with the following powders:

NiCr Coated Coupling

Metaceram 23045 is a trade name for a nickel based spray and fuse powder. The ground coating is designed to combat severe friction, abrasion, heat and corrosion. 23045 produces one of the hardest metallic coatings available with the exception of powders containing tungsten carbide. For purposes of this study, this coating will be referred to as NiCr.

Chemical composition: Ni 73.603%; Cr 14.52%; Si 3.92%; Fe 3.81%; B 3.45%; C 0.697%.

Physical properties:
- -melting temperature: 1895°F (1035°C)
- -maximum operating temperature: 1400°F (760°C)
- -typical hardness: Rc 58
- -thickness limit: 0.060 in (1.5 mm)
- -density: 8.0 g/cc approx.
- -typical porosity (fused): less than 1%
- -bonding mechanism: metallurgical*

NiW Coated Coupling

Metaceram 23075 is a trade name for a nickel spray and fuse powder containing tungsten carbide particles. The Metaceram alloy

---

* metallurgical i.e. thermal spray technology.
Thermal spraying is an overlaying process in which energy is used to atomize the coating material (usually metallic) to produce a spray of small droplets which is allowed to impinge on and adhere to a prepared substrate.

when ground finished provides optimum resistance to fine particle abrasion and erosion.

Chemical composition: Ni 44.91%; W 32.8%; Cr 7.8-9.0%; Co 4.4-5.2%; C 2.39-2.65%; Si 2.1-2.7%; Fe 1.65-2.48%; B 1.65-2.1%; Nb 0.06%; Ta 0.06% and Ti 0.04%. For purposes of this study this coating will be referred to as NiW.

Physical properties:
- -melting temperature: 1895°F (1035°C)
- -maximum operating temperature: 1000°F (538°C)
- -typical matrix hardness: Rc 58
- -typical WC hardness: Rc 75
- -thickness limit: 0.025 in (0.6 mm)
- -density: 10.8g/cc approx.
- -typical porosity (fused): less than 1%
- -bonding mechanism: metallurgical

TiO_2 Coated Coupling

Metaceram 25040 is a trade name for a ceramic powder (Titania, TiO_2) which can be deposited on metal substrates by flame spraying. A nickel based bond coat is required and provides a bond strength of 5000-6000 psi (34475-41370 kPa). Grinding or lapping produces an excellent finish which is highly resistant to frictional wear. In addition, the coating is extremely hard and dense which provides for good wear resistance to abrasive particles and hard surfaces.

Chemical composition: TiO_2 99.787%; SiO_2 0.11%; Al_2O_3 0.06%; CaO 0.03%; Fe_2O_3 0.003%; and MgO 0.002%. For purposes of this study the coating will be referred to as TiO_2 .

Physical properties:
- -melting temperature: 3400°F (1871°C)
- -maximum operating temperature: 1000°F (538°C)
- -typical hardness: Rc 57
- -thickness limit: 0.020 in (0.5 mm)
- -typical density: 5.6 g/cc
- -typical porosity (fused): 3-5%
- -bonding mechanism: mechanical*

4.4 Data Collection

Prior to a test, the couplings and tubings were weighed, their hardness was measured with an ultrasonic hardness tester which used a 7.7 N (785g) load on a 136° angle diamond indenter. The tubings were measured for thickness along the longitudinal center line and their surface roughness was recorded.

During the test, the axial force as measured by strain gauges attached to the push rod was plotted on a chart recorder. The coefficient of friction during the test was determined using these

---

* mechanical i.e. brazing
Brazing is an adhesion process in which the materials being joined are heated but not melted; the brazing filler metal melts and flows at temperatures above 800°F(427°C).

plots. The test was set up to stop at intervals of 10, 100, 200 and 300 km. At each intermediate distance, the specimen surfaces were cleaned dry and all of the following measurements were taken; fifty hardness readings were taken along the wear path of both coupling and tubing, and ten readings of surface roughness were taken along a selected length of the tubing. Weight loss of the coupling was determined by measuring the weight at each stage of the test. Weight loss of the tubing could not be accurately measured since the wear path surface was corroded and the wear was a combination of corrosion and sliding contact between the two surfaces. Therefore, tubing wear was determined by measuring the wall thickness at 10 equally spaced locations along the center line of the wear path. The tests were repeated three times for concurrency in results. While conducting the tests, the water (and sand when applied) flow rate was kept constant. A series of tests were conducted by varying the side loads while keeping the other variables constant.

Surface topography of cross section specimens cut perpendicular to the wear path were examined with a microscope. The tubing wear path was inspected using a scanning electron microscope (SEM) and Energy-Dispersive X-Ray (EDXA).

4.5 Statistical Conditioning of Data

Based on previous findings as noted in Section 3.4, and based on the fact that more than one test was conducted in the present study, using the same controlled variables, variations in measures

were expected. Since numerous hardness readings were taken (50 per each intermediate distance), and because of the expected variations in data, an arithmetic average was utilized.

Environmental factors are crucial in the determination of wear and concurrent tests suggested that environmental variations (temperature, humidity) may be responsible [42]. Often a data point appeared questionable when compared with the rest of the data. A decision had to be made whether the deviation of the data point was due to a mistake (resulting from errors in measuring or recording) and whether it could be rejected or retained.

A statistical procedure known as Chauvenet's criterion provides a consistent means for making the decision to reject or retain such a point. Application of Chauvenet's criterion requires a comparison between DR and DR_0. DR is the deviation ratio and is computed for each data point. DR_0 is the standard deviation ratio and it depends upon the number of measurements. Values for DR_0 are listed by Dally et al. [41].

The deviation ratio DR for a point is defined as :

$$DR = \frac{x_i - \bar{x}}{\sigma_x} \qquad (4.1)$$

where: x_i – data point value

$\bar{x}$ – average data point value of the sample

σ_x – standard deviation of the sample

The data point is rejected when

$$DR > DR_0 \tag{4.2}$$

and retained when

$$DR \leq DR_0 \tag{4.3}$$

If the statistical test of equation (4.2) indicates that a single data point in a set of readings should be rejected, then the data point should be removed from the set and the mean x and the standard deviation σ_x should be recalculated. Chauvenet's criterion can be applied only once on each set of data points.

All the measurements and the data from the tests were examined using this criterion. A complete sample of statistical analysis of the experimental data for the tests using tubing versus standard coupling with 133.5 N side load is shown in Appendix 1: Tables A.1.1-A.1.5 .

The statistical analysis included the following:

a) The mean value of the sample.

b) The standard deviation σ_x of the sample.

c) The standard deviation of the mean (SDOM) $\sigma_{\bar{x}}$ and

$$\sigma_{\bar{x}} = \frac{\sigma_x}{\sqrt{n}} \qquad (4.4)$$

where: n is the sample size.

This determines the standard error of the mean value which was used in the applicable graphs and is presented in Appendix 2.

d) The percentage error is calculated from the standard deviation of the mean and presented as:

$$\%\text{error} = \sigma_{\bar{x}} / \bar{x} \qquad (4.5)$$

Thus the final mean value of the sample is expressed as:

$$X_{\text{final}} = \bar{X} \pm \%\text{error} \qquad (4.6)$$

e) In all the statistical analyses, Chauvenet's criterion was used as the statistical conditioning of the experimental data.

4.6 Scatter of Experimental Data

Scatter in laboratory wear data is most often apparent when the results of different investigators working on similar materials are

compared and test conditioning and material properties are the accepted explanation for the scatter data [42]. Varying experimental conditions clearly play an important role in the scatter of wear rates, but even when identical experiments have been conducted and repeated by the same investigators, scatter was still found [43]. Under these circumstances, most investigators choose to quote the mean value of their measured wear rates [42].

4.7 Uncertainty in Variables

The uncertainties of all measured variables depend upon the sensitivity of the applicable equipment used to take the measurement. All the following uncertainties were carried out using the minimum value for each variable family (eg. the weight of couplings and tubings ranged from 625g to 3200g respectively, hence 625g was used for uncertainty purposes). All calculations were carried out using the following formula:

$$\text{uncertainty of variable} = \delta Y / Y \qquad (4.7)$$

where: δY- sensitivity of the applicable apparatus used to measure the variable.

Y- minimum value measured i.e. load, weight etc.

and are presented in Table 4.1 .

Table 4.1. Variable Uncertainties

Apparatus	±Δ	Min. value	Units	Uncertainty
Digital balance	0.1	625	g	1.60E-04
Micrometre	0.01	2.98	mm	3.36E-03
Talysurf	0.2	4	μ in	5.00E-02
Ultrasonic hard. tester	1	101	hv	9.90E-03
Load cell	0.1	30	lb	3.33E-03
x-y recorder	0.2%*	10	lb	2.00E-02
Counter	1	44	stroke/m	2.30E-02
Piston	10	410	mm	2.40E-02
Flow metre/regulator	0.02	0.5	l/m	4.00E-02
Sand dispencer	0.5	15	g/day	3.30E-02

* the sensitivity of an x-y recorder depends upon the design of the input amplifiers which includes deadband error and typically is 0.2% [41].

Chapter 5

Results and Discussion

5.1 Introduction

Comparison of results of four different couplings sliding on stationary tubings are presented. Wear of the tubing and couplings was the prime area of investigation. The following discussion covers the effect of varying side load and environmental conditions. Other observations such as changes in surface hardness, roughness, wear rates, wear modes and wear mechanisms are discussed. Since the definition of wear is the progressive loss of material from a surface body, weight loss is discussed first.

5.2 Wear of Coupling and Tubing

5.2.1 Coupling Weight Loss

Water Environment

As expected, coupling weight loss increased as the applied side load increased. The results shown in Figures 5.1 - 5.3 demonstrate an increase in the coupling weight loss trend while distance

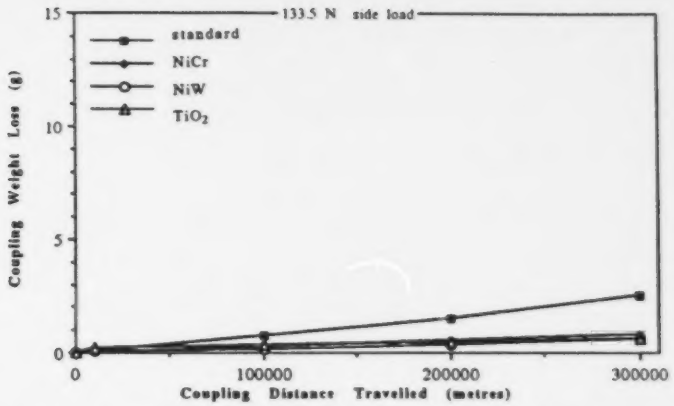

Figure 5.1. Coupling Weight Loss at 133.5 N -Water Environment

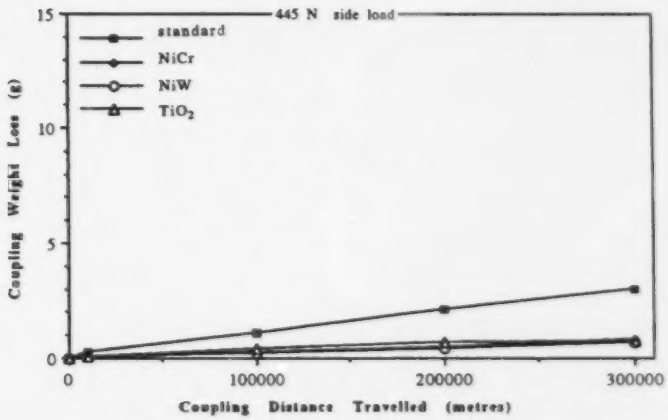

Figure 5.2. Coupling Weight Loss at 445 N - Water Environment

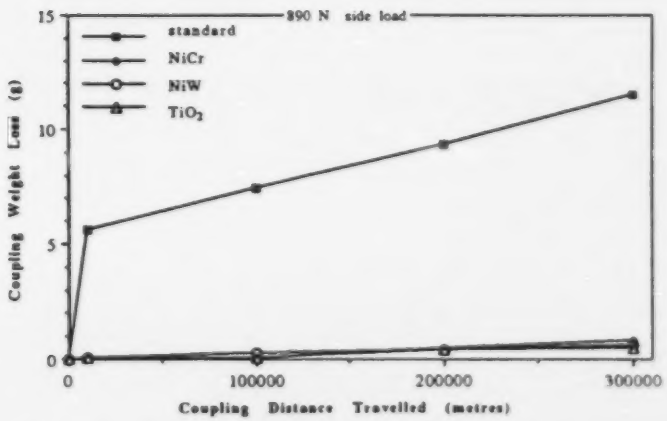

Figure 5.3. Coupling Weight Loss at 890 N -Water Environment

increased under constant load. The standard coupling had the worst performance under all side loads. The coated couplings showed minimal wear and at 890 N side load (Figure 5.3) the weight loss of the TiO_2 coated coupling was 4.3% of that of the standard coupling. The weight loss of NiW and NiCr coated couplings was 5.3% and 7.1% (respectively) of that of the standard coupling. The weight loss rate of the standard coupling during the first 10 km was much higher than that obtained for the rest of the test. This can be seen clearly in Figure 5.3. Changes in the weight loss rate may have been due to the work hardening of the material surface. Surface hardness increased noticeably after 10 km and then remained more or less constant. This also explains why the weight loss rate from 10 km to 300 km was quite constant. A similar standard coupling weight loss trend was found in Bellow's study [1].

Water and Sand Environment

Grooving wear can be defined as wear due to penetration of hard particles or surface asperities of a harder counterbody into a softer surface i.e. tubing in sliding contact. It is often observed in grooving wear on different materials that wear loss increases significantly with increasing size of abrasive particles [44]. Therefore, adding sand to the water was expected to cause more wear and might change the wear mechanism.

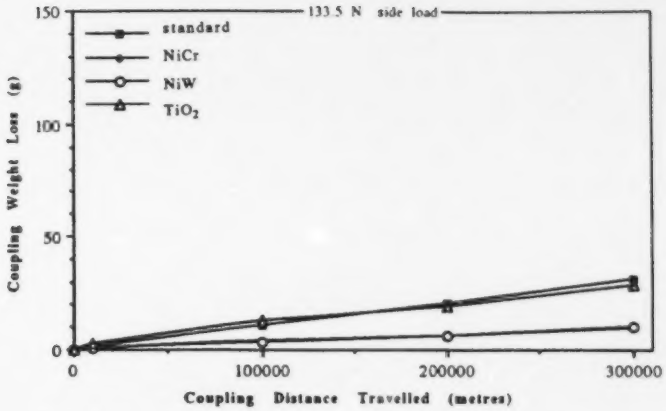

Figure 5.4. Coupling Weight Loss at 133.5 N -Water & Sand Environment

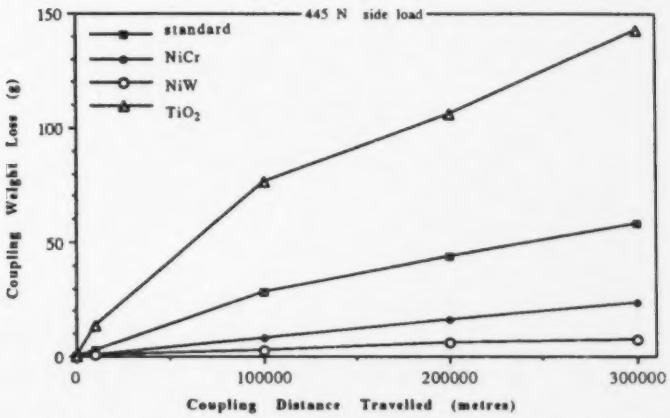

Figure 5.5. Coupling Weight Loss at 445 N -Water & Sand Environment

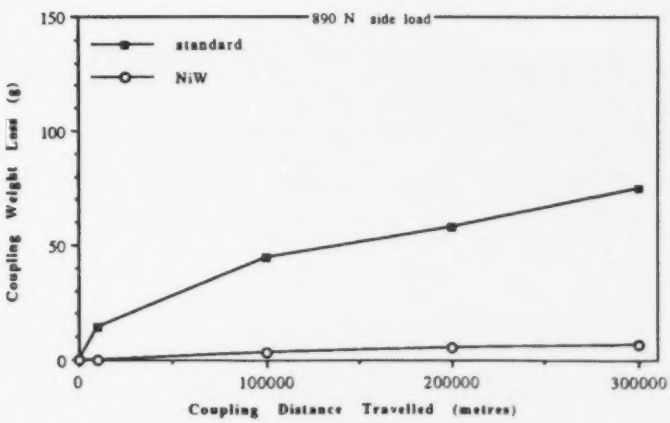

Figure 5.6. Coupling Weight Loss at 890 N -Water & Sand Environment

The weight loss of the couplings was much greater with sand than without sand. However, the performance of the couplings was not quite the same compared to a sand free condition.

The performance of the TiO_2 coated coupling was better than the standard as long as the coating was intact. But once the coating wore off, the performance of TiO_2 coated coupling was the same as a standard coupling as this will be explained further on.

Figure 5.7 shows the TiO_2 coated coupling under a load of 133.5 N after 10 km with most of the coating worn off. The performance of the TiO_2 coated coupling worsened at higher loads causing vibrations in the apparatus and between the coupling and the tubing. At a 445 N load (Figure 5.5) the weight loss was noticeably higher than observed with the other couplings.

Figure 5.7. Wear of TiO_2 Coated Coupling at 133.5 N Side Load After 10km

The ceramic coating of the TiO_2 coated coupling was hard and brittle and did not withstand the sand. It chipped off the surface. The debris of the coating became a hard third body abrasive particle which caused accelerated damage to the coupling and tubing (Figure 5.8). Another reason why the coating chipped off the surface may be due to the under layer bonding material being unable to withstand the loading condition and environment.

Figure 5.8. Wear of TiO_2 Coated Coupling And Tubing at 445 N Side Load After 300 km - Water & Sand Environment

The NiCr and NiW coated couplings showed better performance and wore less than the standard and TiO_2 coated couplings. Since the coating on the NiCr coated coupling wore off at the end of the tests using 445 N (Figure 5.9), and the base material was a standard

coupling, the next tests were run using 890 N with only a NiW coated coupling.

Figure 5.9. Wear of NiCr coated Coated Coupling at 445 N Side Load After 300 km - Water & Sand Environment

The NiW coated coupling yielded the best performance i.e. the least weight loss during all tests in the presence of sand. As shown in Figure 5.6, the weight loss of the NiW coated coupling was 10% of that of the standard coupling. Although the coating was worn it was not completely worn through to the base metal by the end of the test (300 km).

5.2.2 Tubing Thickness Loss

Water Environment

Tubing wear was indicated by thickness loss (decrease, see Section 4.4). As shown in Figures 5.10 - 5.12, the TiO_2 coated coupling caused the least wear in a tubing. The surface of the tubing was smooth (see Section 5.3) and on some areas along the sliding path there was no indication of wear.

An example of the effect of work hardening on the wear rate is shown in Figure 5.12 where the wear rate of the tubing in contact with the standard coupling was high, up to 10 km. Subsequently, minimum wear rate was observed until the end of the test.

Water and Sand Environment

Figures 5.13 - 5.15 show the thickness loss of tubings under different environmental conditions. As expected, the wear rate was found to be higher when sand was added to the water.

For a side load of 133.5 N, the standard coupling caused the greatest wear of the J55 tubing compared with the coated coupling under the same load. However, at a side load of 445 N (Figure 5.14), TiO_2 coated coupling wore more than the rest of the couplings due to a hard third body abrasive in the form of ceramic chips.

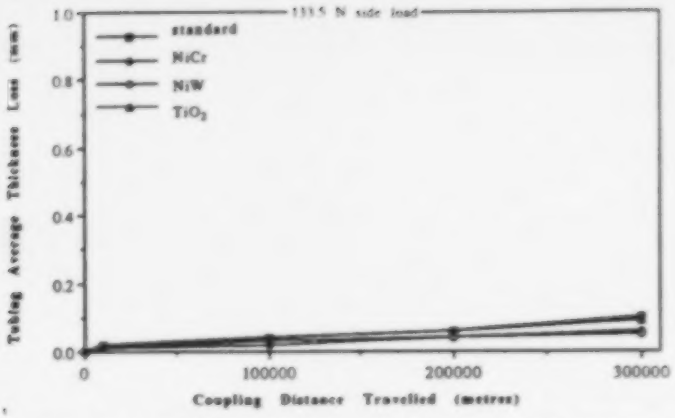

Figure 5.10. Tubing Thickness Loss at 133.5 N - Water Environment

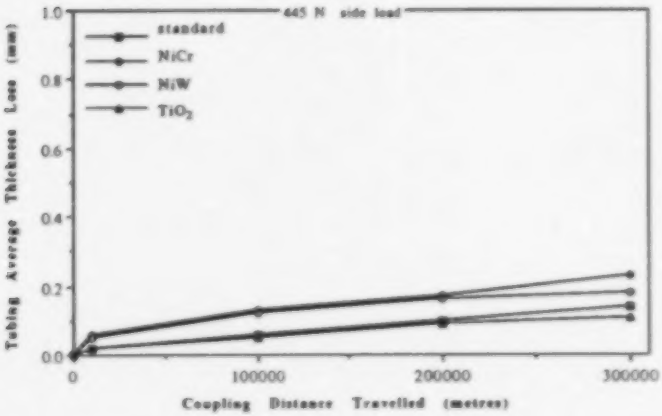

Figure 5.11. Tubing Average Thickness Loss at 445 N - Water Environment

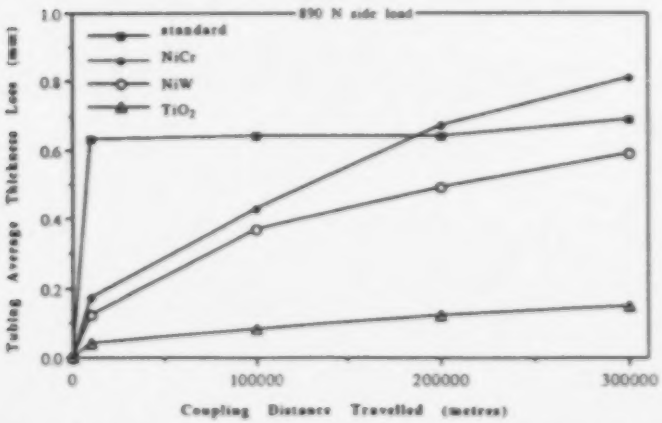

Figure 5.12. Tubing Average Thickness Loss at 890 N -Water Environment

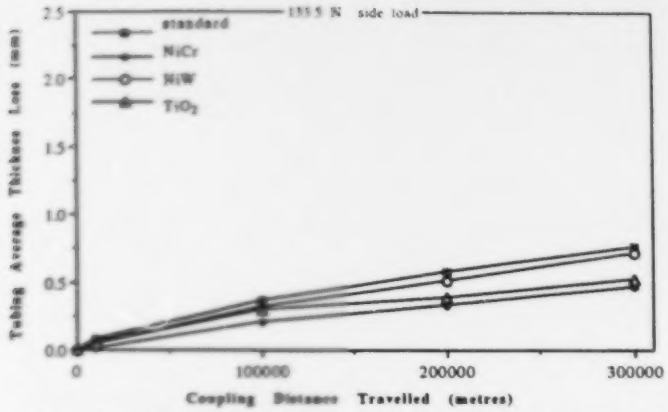

Figure 5.13. Tubing Average Thickness Loss at 133.5 N - Water & Sand Environment

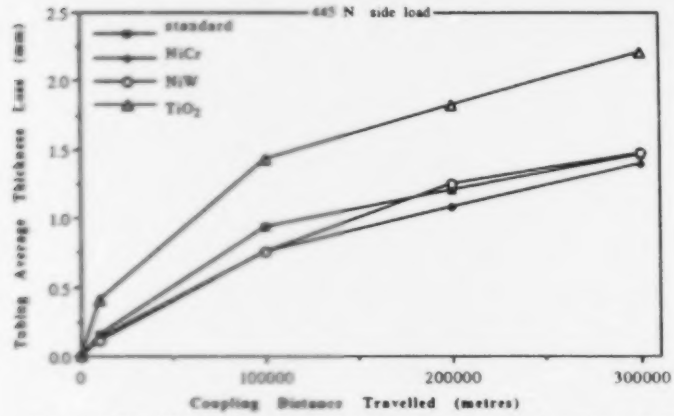

Figure 5.14. Tubing Average Thickness Loss at 445 N - Water & Sand Environment

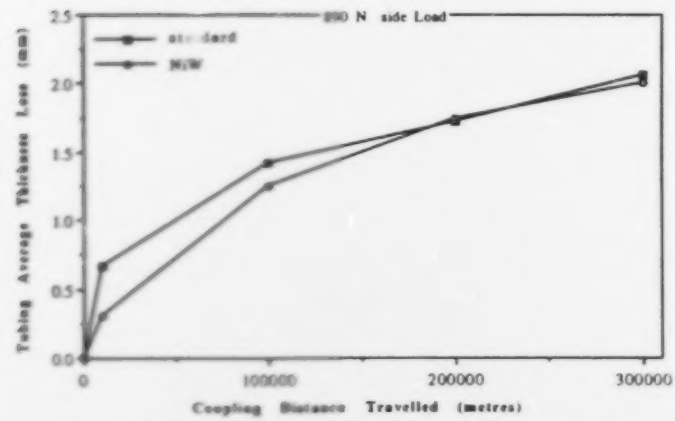

Figure 5.15. Tubing Average Thickness Loss at 890 N - Water & Sand Environment

Figure 5.15 shows the thickness loss of the tubings in contact with standard and NiW coated couplings. The latter combination yielded less wear of both tubing and coated couplings.

While demonstrating the performance of the tubing in Figures 5.10 and 5.15, the average thickness loss was used as the indication of the wear rate. The values of thickness loss did not indicate the critical points along the tubing's wear path. The critical points refer to the points along the wear path where the thickness loss of the tubing was greater than the average value. The range of thickness loss differed from the average by 25%.

5.3 Analysis of Tubing Surface Roughness

Water Environment

As indicated in section 4.3.1, the tubings were initially honed in order to get a uniform surface finish prior to the start of all tests. At 133.5 N, the tubing surface roughness tended to decrease i.e. the surface became smoother as time and distance increased. The smoothing action was basically rubbing off the higher asperities. This mechanism is called "truncating" [45] or "censoring" the height distribution over a period of time. In this type of wear the bottom of the profile remains the same while the upper is progressively removed (Figure 5.16).

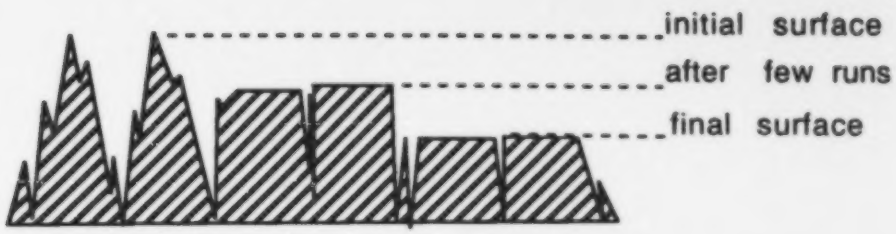

Figure 5.16. Surface Truncation at Different Levels.

Jahnmir's observation (Section 3.3.3) stated that at lower loads between two surfaces of different roughnesses, the total wear of the rougher surface is greater than the one with the smoother surface. This is in agreement with the results shown in Figures 5.17-5.19. The least material loss was found in the tubing when in contact with a TiO_2 coated coupling (Figures 5.10-5.12). It also had the smoothest surface. At the highest load (Figure 5.19), the surface roughness of the tubing worn by a TiO_2 coated coupling decreased with increasing distance travelled. It should be noted that the other couplings did not cause the same wear of the tubings. For those, the surface roughness changed in a sinuous fashion. This may have been due to different wear modes for each different coupling/tubing combination.

Transverse surface topography of tubings for all couplings under 890 N side loads are presented in Figure 5.20. As can be seen, the surface topography of the tubing using a TiO_2 coated coupling (Figure 5.20d) was more leveled than the rest of the tubings (Figure 5.20a-c).

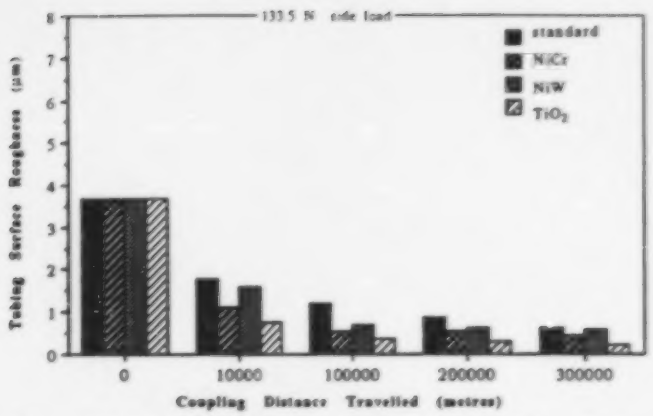

Figure 5.17. Tubing Surface Roughness at 133.5 N -Water Environment

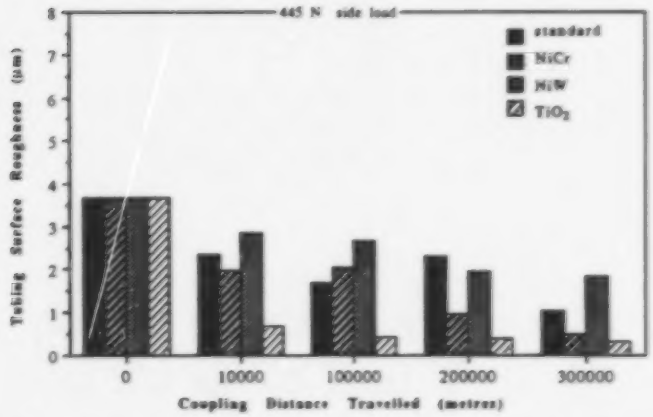

Figure 5.18. Tubing Surface Roughness at 445 N -Water Environment

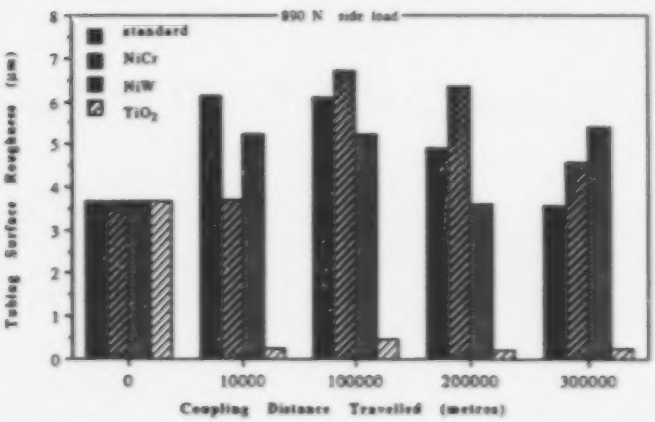

Figure 5.19. Tubing Surface Roughness at 890 N - Water Environment

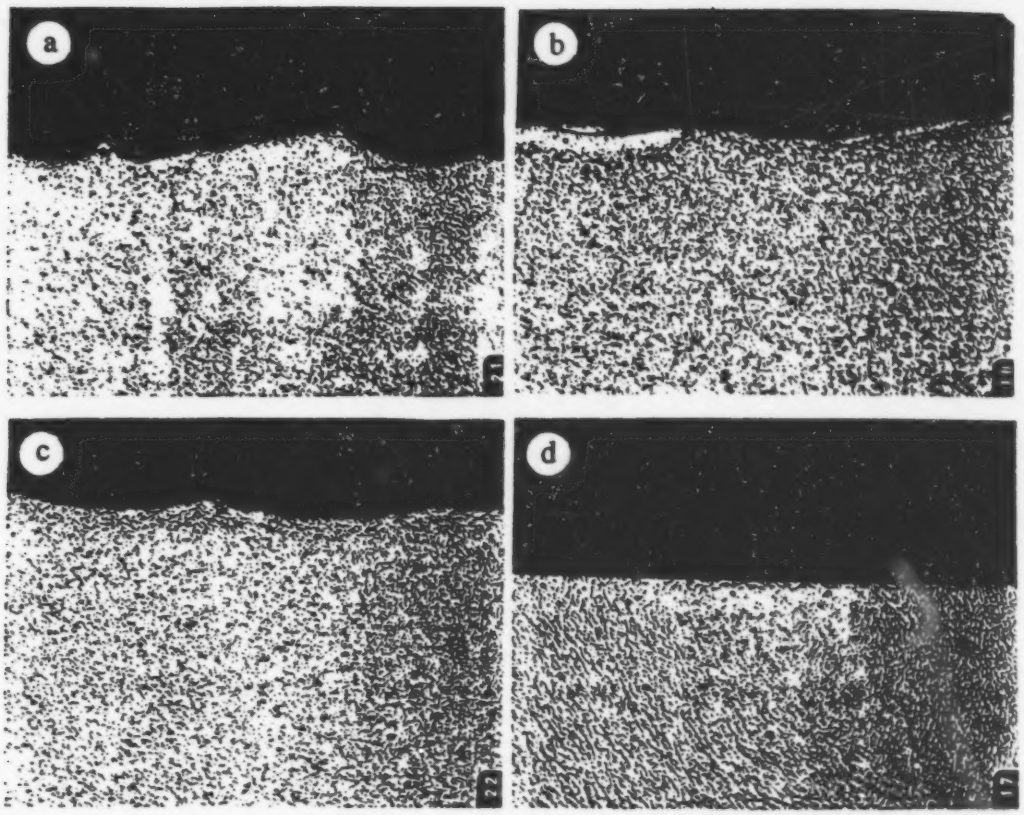

Figure 5.20 Transverse surface of tubing under 890 N side load after 300 km of travel (x52, 2% Nital etchant).
Using a) Standard coupling
b) NiCr coated coupling
c) NiW coated coupling
d) TiO_2 coated coupling

Water and Sand Environment

The tubing surface roughness results obtained when using a TiO_2 coated coupling (Figure 5.21) were smoother in water

environment than in water and sand environment. Since the broken coating damaged the surface of both the coupling and the tubing, these results were to be expected.

Figure 5.21 shows the decreasing surface roughness trend for all tubing using different couplings (compared to initial value). When the sliding system was loaded with 445 N (Figure 5.22) the tubing surface roughness using standard coupling and TiO_2 coated coupling was higher than the initial value. Using sand under the 445 N side load caused the sand to anchor, or become embedded, in the tubing and the standard coupling. Note that the hardness of the tubing and the standard coupling is similar. Whereas in the tests using NiW and NiCr coated couplings, the sand grains were embedded only in the tubing since it was hard to penetrate the coating. Figure 5.23 illustrates the surface roughness of the tubing using standard and NiW coated couplings. The sand did not appear to have influenced the surface roughness. This appears to be the case because the high contact load did not allow sand to flow between both surfaces as was the case with much lower loads. If sand got trapped between the surfaces, it got crushed and washed away. Adding sand to the water had a significant effect on surface roughness only in the case where the 445 N load was used. When 133.5 N and 890 N were used there was no significant change in the surface roughness of the tubing. At 133.5 N the sand rolled down the tubing without causing severe damage and at 890 N, not enough sand got trapped between the surface or got crushed and washed away.

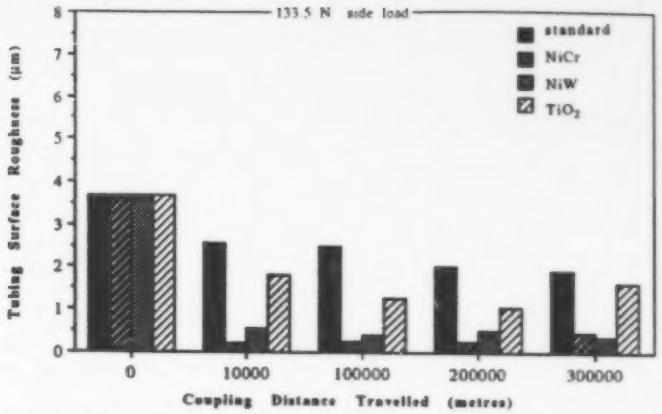

Figure 5.21. Tubing Surface Roughness at 133.5 N - Water & Sand Environment

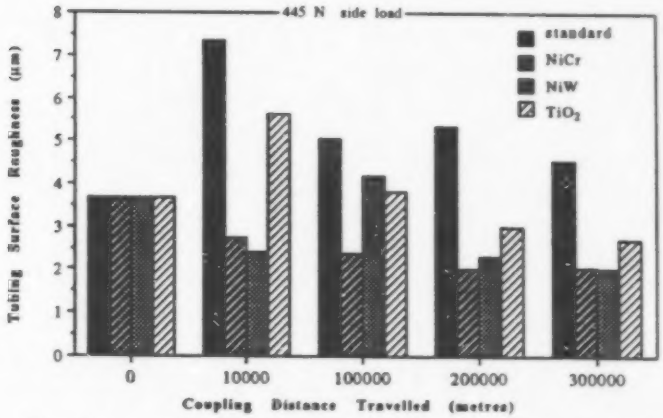

Figure 5.22. Tubing Surface Roughness at 445 N - Water & Sand Environment

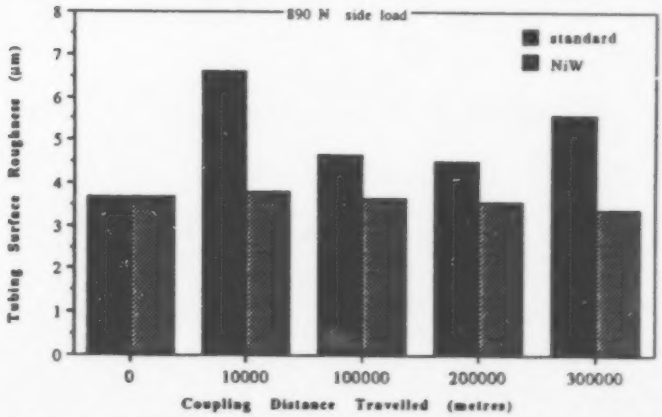

Figure 5.23. Tubing Surface Roughness At 890 N - Water & Sand Environment

In general, as the value of surface roughness increased, the wear of all tubings and couplings increased. The wear surfaces at the end of the test were found to be similar to those of couplings/tubings taken from the field. This suggests that the testing apparatus provided a reasonable duplication of the type of wear process occurring in an oil well.

5.4 Analysis of Coupling/Tubing Microhardness

5.4.1 Coupling Microhardness

Water Environment

Figures 5.24-5.26 show little change in hardness of the coated coupling under all side loads. The hardness of the standard coupling increased with distance travelled which indicated the effect of work hardening. On the other hand, the hardness of the NiW coated coupling decreased with distance travelled.

Figure 5.27 shows that the coating of the NiW coated coupling did not wear off. A closer look, however, at the coupling surface (Figure 5.28) revealed air pockets (voids) along the wear path which indicates porosity in the coating. The density of the worn coated surface at 10 km was lower than that found at the beginning of the test. The reduction in the density of the coating is believed to be the cause of the reduction in overall hardness of the surface of the coupling.

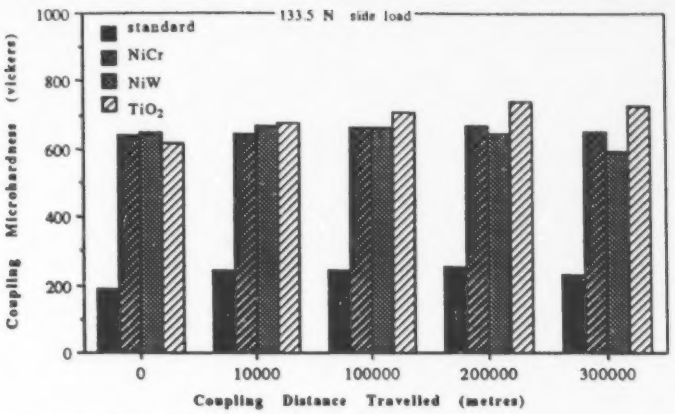

Figure 5.24. Coupling Microhardness at 133.5 N - Water Environment

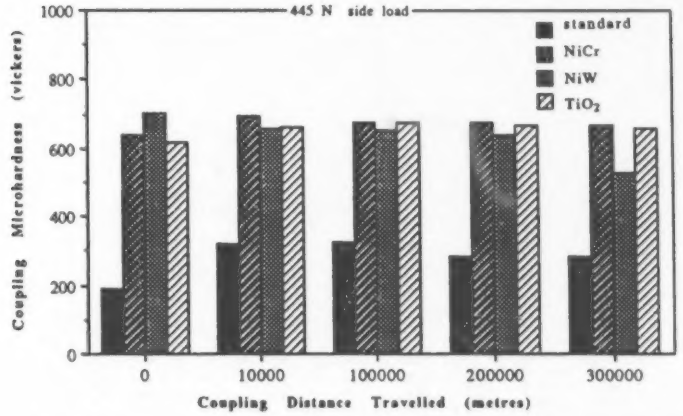

Figure 5.25. Coupling Microhardness at 445 N - Water Environment

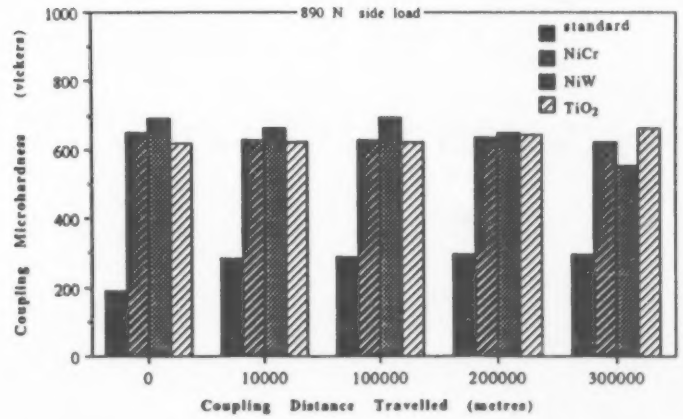

Figure 5.26. Coupling Microhardness at 890 N - Water Environment

Figure 5.27. Wear Path of NiW Coated Coupling at 445 N after 10 km distance travelled

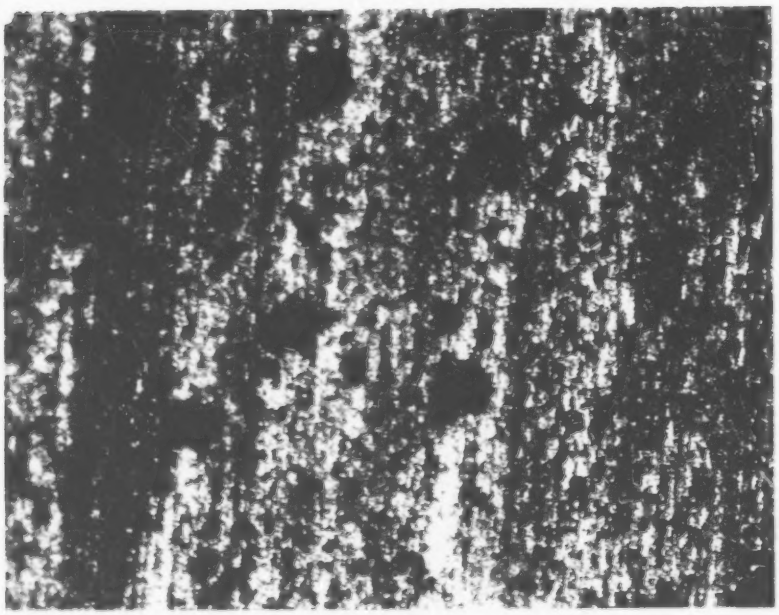

Figure 5.28. Porosity In The Coating -NiW Coated Coupling (magnification x44)

Figure 5.29 shows the similarity in hardness between a standard coupling and a TiO_2 coated coupling after 10 km and 133.5 N. Since the coating wore off during the first 10 km, the TiO_2 coated coupling behaved almost the same as the standard coupling at 445 N (Figure 5.30). The hardness of the NiCr coated coupling was constantly reduced due to changes in the surface coating. The coated coupling surface was examined with a microscope at each intermediate distance and the surface coating was found to be less dense. By the end of the test (445 N, 300 km), the coating wore off completely and the hardness was found to be similar to the standard and the TiO_2 coated coupling. Figure 5.31 shows the hardness of the standard and NiW coated couplings. Work hardening can be explained from the stress-strain diagram for steel and can be seen in the case of the standard coupling. Basically, metallic powders can also be work hardened providing the coating wore minimally as can be seen in the tests using water only. Once sand was introduced to the coated coupling, the coating wore more than without sand and the density decreased which in turn caused an overall decrease in surface hardness. In the case of the TiO_2 coated couplings and since the ceramic coating is brittle, work hardening should not take place. However, it would appear to have done so (Figure 5.24). The surface of the TiO_2 coated coupling was examined with a microscope at each intermediate distance and it was observed that the coating density increased while wearing off. This is contrary to what was observed with the metallic powders.

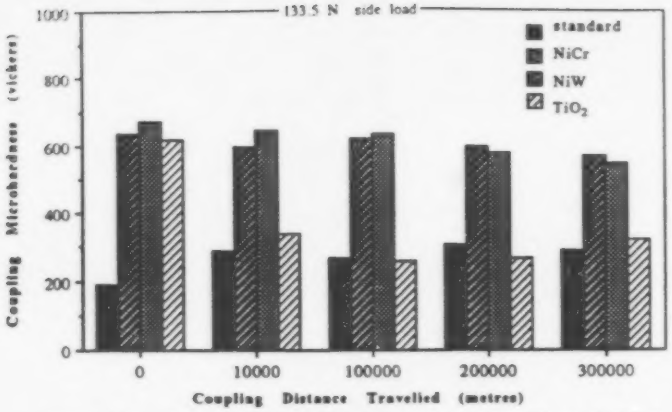

Figure 5.29. Coupling Microhardness at 133.5 N - Water & Sand Environment

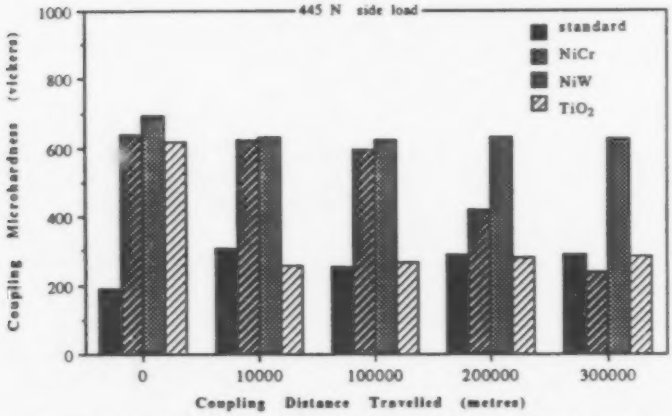

Figure 5.30. Coupling Microhardness at 445 N - Water & Sand Environment

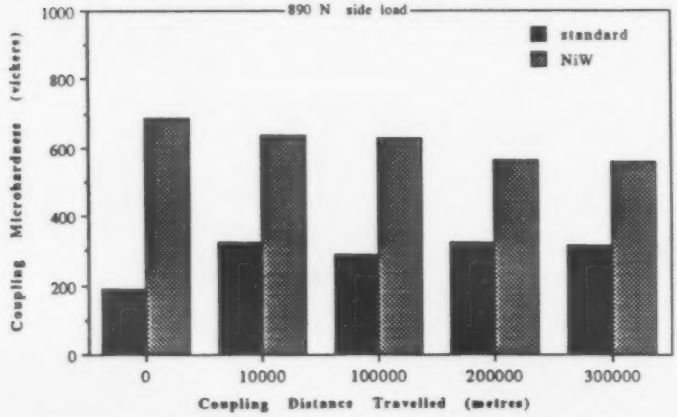

Figure 5.31. Coupling Microhardness at 890 N - Water & Sand Environment

The TiO_2 is applied by a brazing process which is used to join similar or dissimilar metals by using a metal or alloy of a lower melting point than either of the components to be joined. The melted alloy wets the surfaces between the parts to be joined. For the purpose of the study, the alloy will be refered to as the bonding coat. As previously mentioned, the density of the TiO_2 increased at each intermediate distance as the surface coating got closer to the bonding coat. This explains the reason for the so called 'work hardening' even though it does not occur in a brittle material such as ceramic. Again, the density of the coating affected the level of surface hardness.

5.4.2 Tubing Microhardness

Water Environment

Because the J55 tubing was all from the same heat of steel, the initial surface hardness of all tubings were similar (approximately 180 HV 785G). The test results show (Figure 5.32-5.34) that the higher the applied side load the harder the surfaces of the tubing becomes due to the work hardening. The hardness of the tubings during the tests increased to double its original value while using the Ni coated couplings (NiCr and NiW coated couplings).

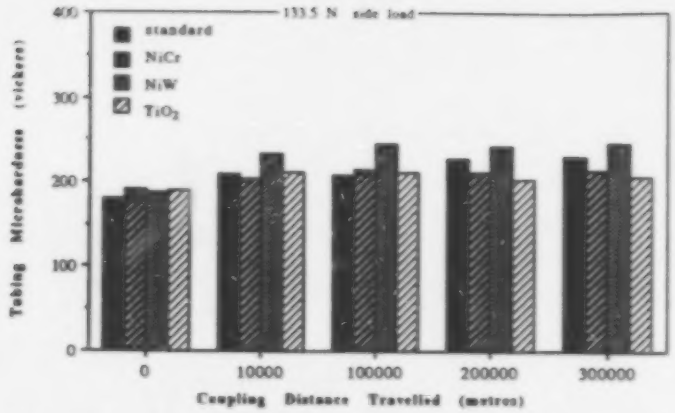

Figure 5.32. Tubing Microhardness at 133.5 N - Water Environment

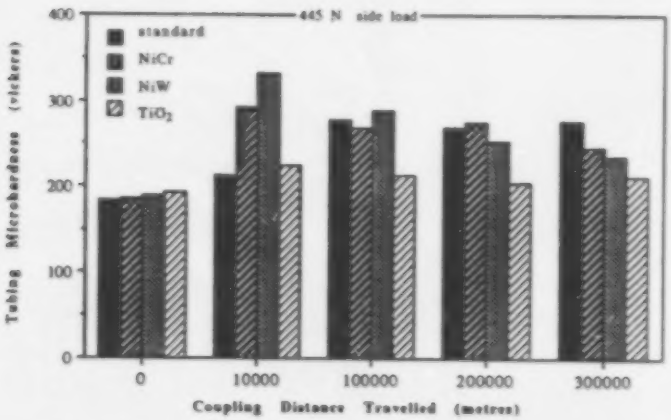

Figure 5.33. Tubing Microhardness at 445 N - Water Environment

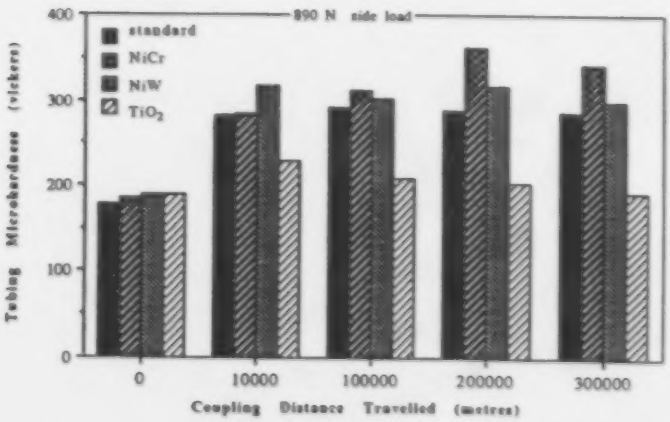

Figure 5.34. Tubing Microhardness at 890 N - Water Environment

Scanning electron micrographs showed a transfer of nickel and tungsten in the shape of platelets or smeered nickel onto the surface of the tubing. The use of EDXA spot analysis showed that the particles were nickel and tungsten. Figures 5.32-5.34 show hardness variations (increasing) which confirmed that work hardening of the surface was occurring. The hardness of the surface of the tubing with the standard coupling increased but not as high as with NiCr/NiW coated couplings. This suggested that the hardness increase was not only due to work hardening, but also due to a transfer of harder materials from the coated couplings.

The hardness of the surfaces influenced the wear and the wear resistance of the tubings. During the first 10 km, the wear (thickness loss) of the tubing was high. With distance travelled, the tubing surface became harder. This increased the wear resistance and resulted in a reduction in the amount of wear. This can be seen clearly in the test using the standard coupling (Figure 5.12).

In measurements of J55 tubing specimens, Ko et al. [2] showed that for higher normal loads the hardness of the worn surfaces at the end of the test was about four times its original value. This shows that work hardening took place in the process and supports the results of the present study and the results of Bellow et al. [1].

Ko et al. [2] suggested that the work hardening effect may make the surface more susceptible to brittle fracture by the long cyclic loading. Subsequently, it would be susceptible to severe

damage. When looking at the hardness values obtained at intermediate distances (Figure 5.32-5.34) there is a lack of consistency. For example, the tubing surface microhardness using NiCr coating couplings under a 445 N side load (Figure 5.33) was increased from 186 HV 785g (initial) to 291 HV 785g at 10 km, then was reduced to 269 HV 785g at 200 km and finally decreased to 245 HV 785g at the end of the test (300 km). Work hardening was in effect, but as the surface became harder and hence more brittle, the cyclic loading broke off the top layer and exposed a softer subsurface. The subsurface may even be equal to the original hardness value. The cycle of surface work hardening begins again. The measurements could have been taken at any given time during this cycle and work hardening would have been found.

Water and Sand Environment

When sand was added to the water at the rate of 165 g/day, it was present between the wear surfaces and prevented the effective transfer of metal particles. This diminished the beneficial effects of the coated coupling as previously shown and as predicted by Bellow et al. [1]. Nevertheless, work hardening was still in effect as shown in Figures 5.35-5.37. The value of hardness was higher in these tests than in those in which sand was not present. The sand caused grooving wear. Grooving wear is similar to 'indentation wear' since in both mechanisms the abrasive penetrates the metal surface. The metal surface is displaced and severely cold worked.

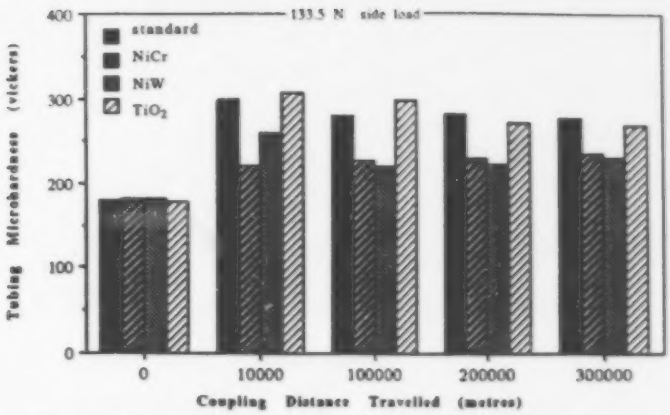

Figure 5.35. Tubing Microhardness at 133.5 N - Water & Sand Environment

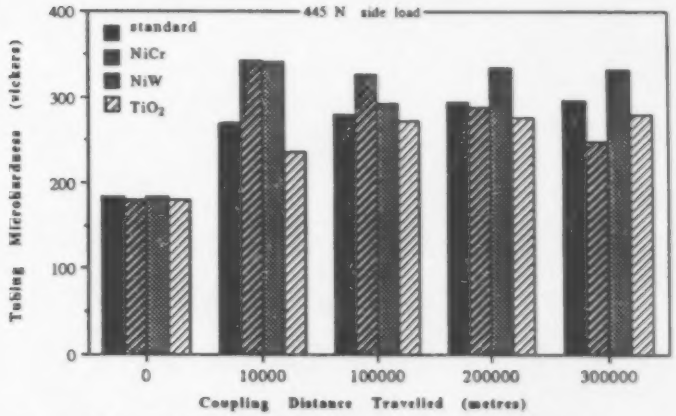

Figure 5.36. Tubing Microhardness at 445 N - Water & Sand Environment

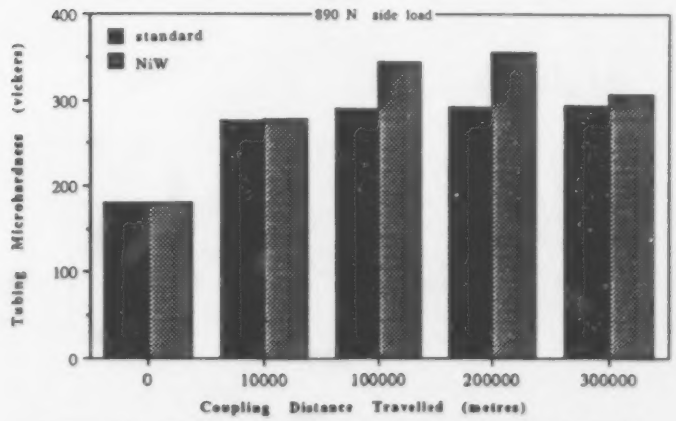

Figure 5.37. Tubing Microhardness at 890 N - Water & Sand Environment

The indentation process itself produces work hardening [34]. In general, there were more grooves in the wear path of the tubing surfaces in the presence of sand than occurred in the presence of water alone. The indentations were deeper and resulted in higher hardness values.

5.5 Friction

Friction between two metal surfaces in contact sliding is generated by adhesion, plowing by wear particles and asperity deformation. In the work published by Kim and Suh [46] the plowing component of friction contributed more to the frictional force than adhesion in the absence of a lubricant. This suggests that mechanical interactions at the sliding interface are the primary causes of friction between two surfaces with asperities. If the mechanical interaction can be reduced, then the frictional force will be significantly reduced.

5.5.1 Running-In

Figure 5.38 illustrates the apparent coefficient of friction versus distance travelled using a NiCr coated coupling. However, this behavior was typical for all couplings in a water environment. The points in Figure 5.38 indicated by the arrows show running-in. These running-in values occurred at the beginning of each stage

(during the first 100 cycles) in the test. Running-in is characterized by more intensive wear of sliding surfaces and by higher heat generation. These are accompanied by changes in both surface geometry and in the physical and mechanical properties of the materials surface layers [17]. One data point (Figure 5.38 at 100 km) did not describe running-in, it was assumed that the coupling seated itself back into its original tracks. In the process of running-in, the asperities are destroyed and new asperities differing from the original in shape and size are formed. After the initial run-in, a stable surface roughness develops. The stable surface roughness of a solid depends upon the strength of bonds due to contact molecular interactions, elastic properties of the solid and load.

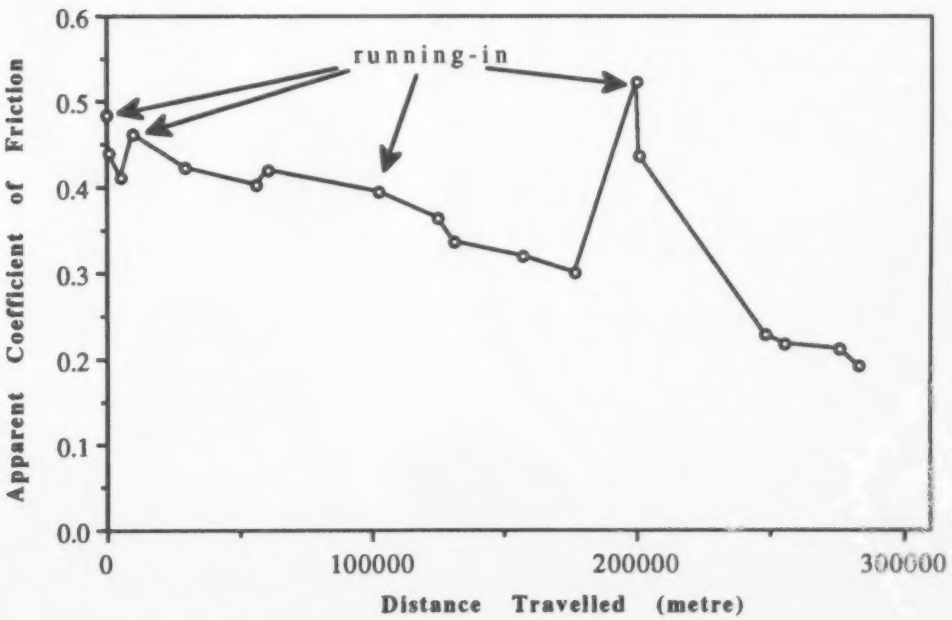

Figure 5.38. Running-In Friction of NiCr Coated Coupling Under 445 N Side Load - Water Environment

5.5.2 Frictional Force

Frictional force was defined as the force required to slide the coupling along the tubing as a function of the side load and the wear mode. It is not difficult to monitor the friction force with most sliding test geometries. It is generally advisable to measure friction even when the primary goal is to obtain wear data. The reason for this is that the measurement of friction may assist in interpreting wear data at different stages. One needs to be cautious however. Friction and wear data often correlate poorly [5,25]. In addition, one can have friction without wear. Figures 5.39-5.40 showed, as expected, an increase in frictional force as the side load increased for all couplings and under both environmental conditions.

5.5.3 Apparent Coefficient of Friction

The second law of friction states that the friction force F is proportional to the normal load W, that is

$$F \alpha W$$

therefore,

$$F = \mu W, \qquad (5.1)$$

where μ is a constant known as the 'coefficient of friction'. It must be stressed that μ is a constant for a given pair of sliding materials under a given set of ambient conditions and varies for different materials and under different conditions.

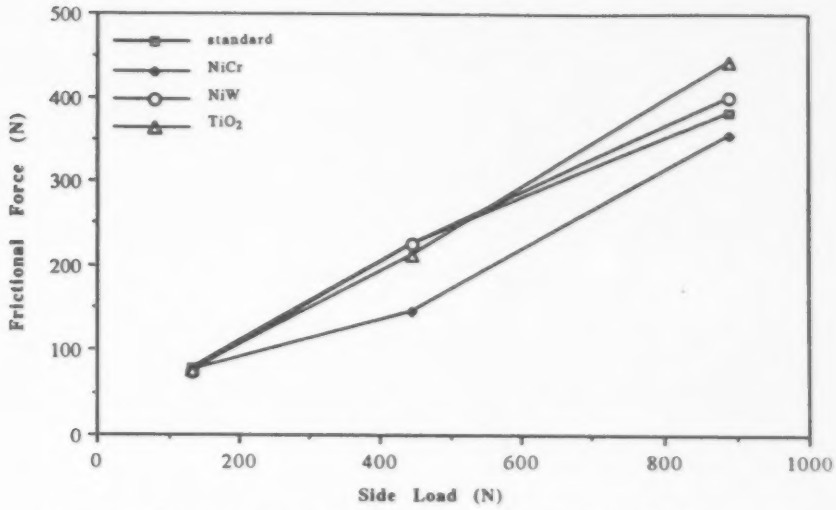

Figure 5.39. Frictional Force as a Function of Side Load-Water Environment

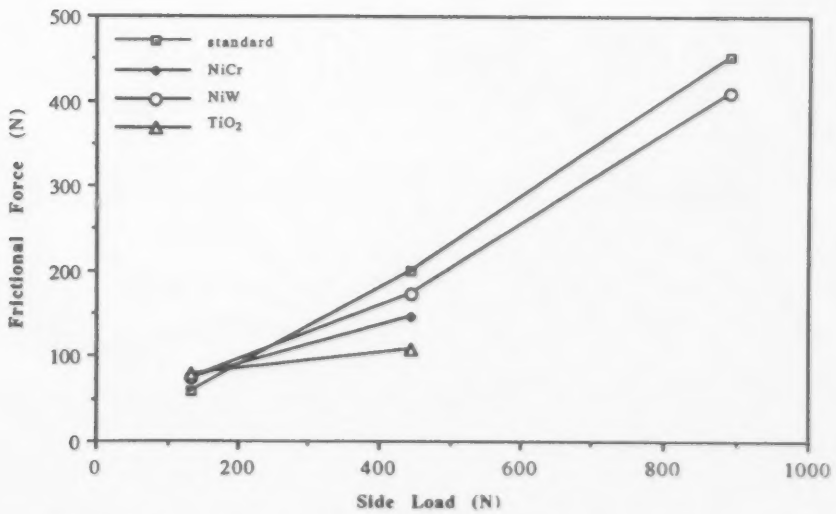

Figure 5.40. Frictional Force as a Function of Side Load-Water & Sand Environment

In the theory mentioned above, μ is constant. In the proposed wear study however, the mechanism is different. μ changes during the test (Figure 5.38) and is affected by the load, speed, wear modes etc. In short, equation 5.1 does not assume significant wear of material as occured in the present study. Therefore, the c.o.f. in this study will be called the 'apparent coefficient of friction'. When using two different environmental conditions, the results are not expected to be the same. Hirn [47] distinguished between lubricated and non-lubricated solids. He observed that the effect of velocity, surface area, and load differed in the two cases.

Water Environment

The results presented in Figure 5.41 show that with increasing load the general trend of the apparent coefficient of friction decreased. This behavior is similar to that of a journal bearing or to the tilted-pad bearings [48] which is illustrated in Figure 5.43. While the load increases, the angle α decreases, the trailing edge rises a little and the friction decreases. It should be noted that the use of a bearing system in this context is only to explain the behavior of the apparent coefficient of friction. The apparent coefficient of friction during individual tests consistently decreased when using loads under 445 N (see Figure 5.38 for example). Suh [12] explained this behavior as when a slider slides against a specimen (slider is harder than the stationary specimen), the asperities of the hard surface are gradually removed creating a mirror finish. In this case, the frictional force decreases because of the decrease in the plowing of

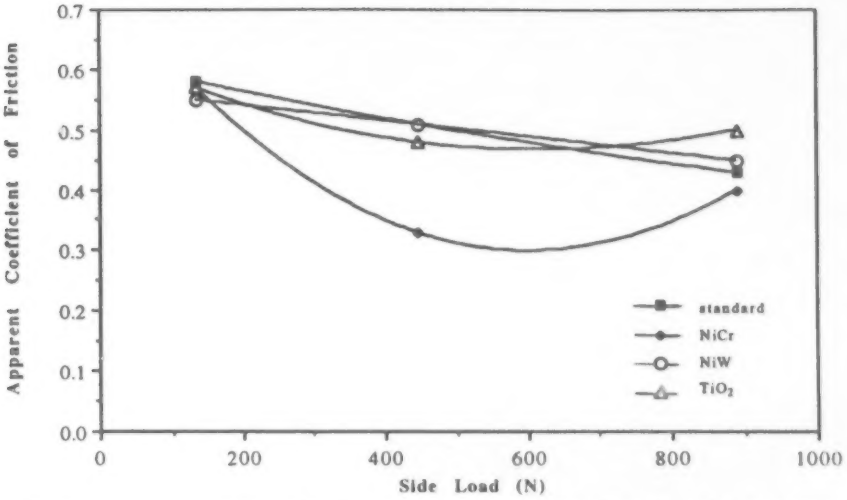

Figure 5.41. Apparent Coefficient of Friction of Tubing with Different Couplings at Various Side Loads- Water Environment

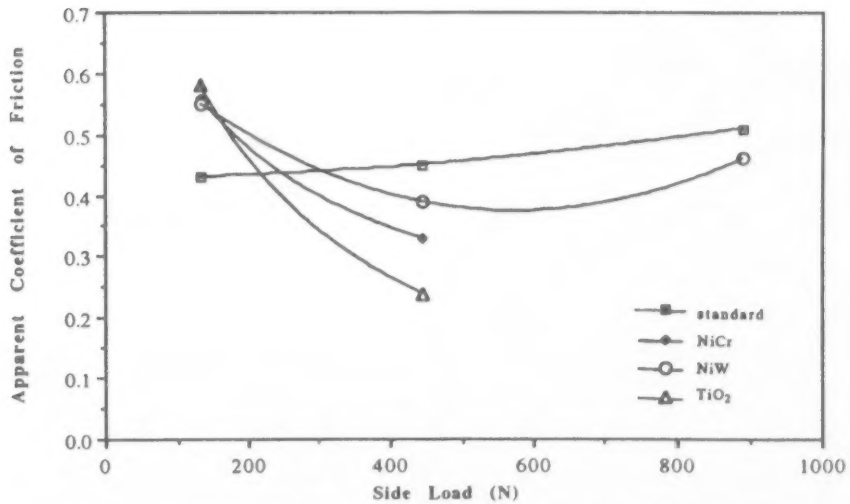

Figure 5.42. Apparent Coefficient of Friction of Tubing with Different Couplings at Various Side Loads - Water & Sand Environment

the surfaces by the wear particles and the reduction of surface asperities. Wear particles cannot plow since they cannot penetrate and anchor into the hard surface. Under 445 N and 890 N side loads, the apparent coefficient of friction decreased during the test using the TiO_2 coated coupling and was found to fluctuate for the remainder of the couplings. It is suggested that this was due to differences in surface roughness.

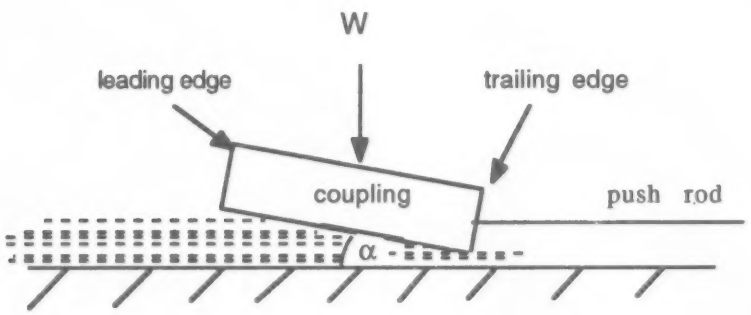

Figure 5.43 Test Sliding Condition for Tilted Pad Bearing

Water and Sand Environment

The standard coupling did not behave in the sand-water environment as it did in the water only environment. As the load increased, the apparent coefficient of friction increased. This may be due to the fact that the sand did not let the angle decrease but served as a barrier between the two surfaces as the load increased. At a low load,133.5 N, the sand rolled down (washed down with the

water) the tubing and served as a bearing for the coupling. In other words, the sand facilitated the sliding action of the coupling. At higher loads (445 N - 890 N), the sand grains became embedded in the tubing and in the standard coupling and resisted the sliding motion of the coupling. Hence, the value of the apparent coefficient of friction increased. The coated coupling showed the same behavior as it did in the water environment. This may be because of the hard coating effect on the sand. The coating crushed the sand and therefore, the sand did not have a major effect on the angle. The value of the apparent coefficient of friction during individual tests was inconsistent during the test with a sand-water environment and fluctuated as a function of surface roughness and abrasive particles.

5.6 Wear Rate

Water Environment

In general, the wear rate* of the couplings was reduced as the applied side load increased. This was a result of work hardening of the surface. Figure 4.44 illustrates the wear rate of all couplings at the end of a test. The wear rate of the coated couplings decreased with an increasing side load. The standard coupling showed a different behavior. For loads up to 445 N the wear rate decreased and then increased at 890 N. This may have been due to a change in the wear mode i.e. up to 445 N side load the coupling experienced

* Note that when describing the wear rate in the present study, it is a function of the load and the distance travelled.

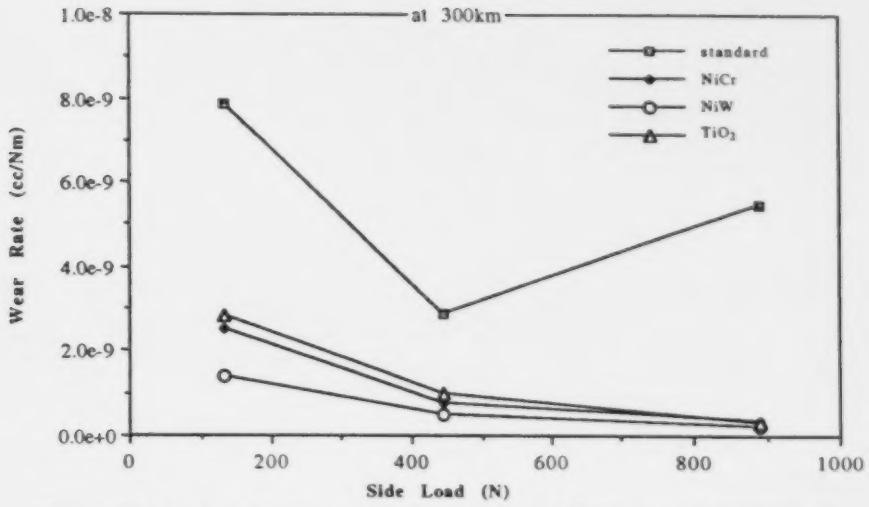

Figure 5.44. Wear Rates of All Couplings at 300 km as a Function of Side Load - Water Environment

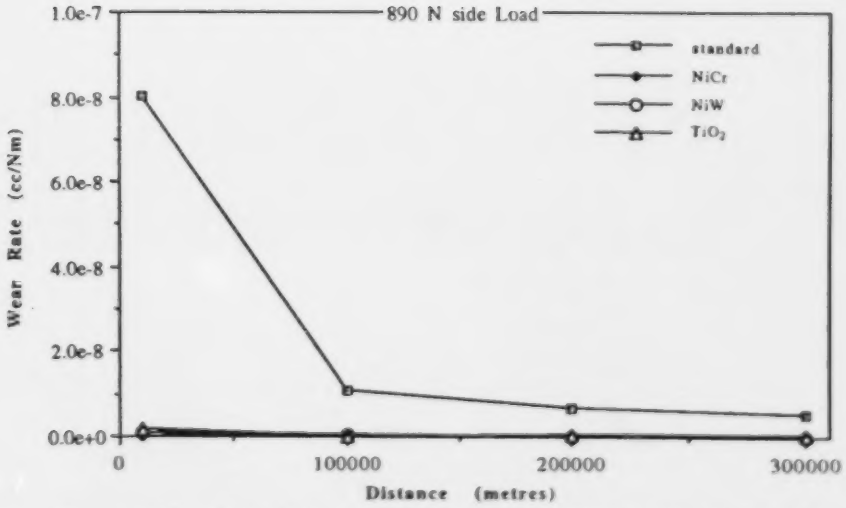

Figure 5.45. Wear Rates of All Couplings at 890 N Side Load as a Function of Distance - Water Environment

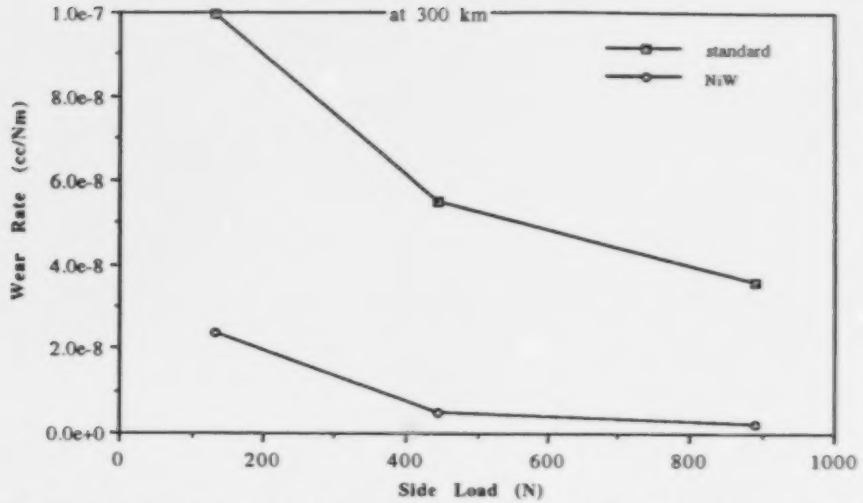

Figure 5.46. Wear Rates of Standard and NiCr Coated Couplings at 300 km as a Function of Side Load - Water & Sand Environment

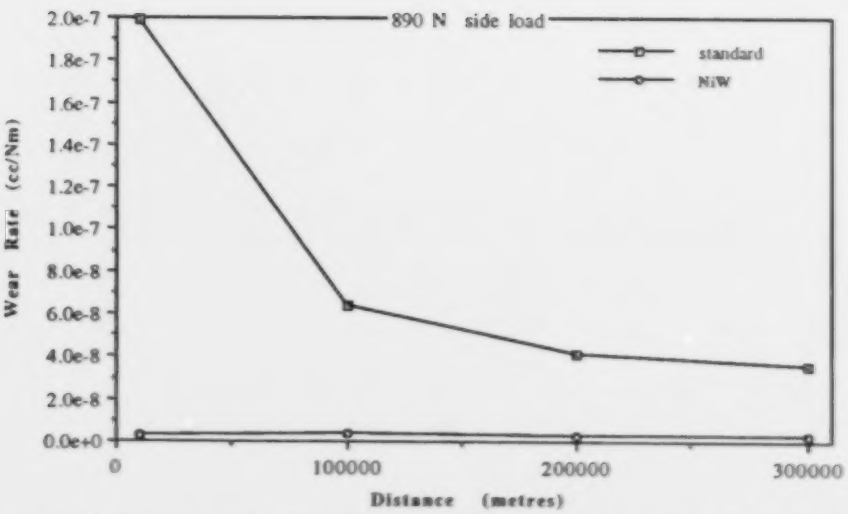

Figure 5.47. Wear Rates of Standard and NiCr Coated Couplings at 890 N Side Load as a Function of Distance - Water & Sand Environment

mild wear and at a side load of 890 N the wear mode was severe. Figure 5.45 shows the wear rate of couplings as a function of distance travelled at the highest side load, 890 N. The wear rate of the standard coupling at 10 km was much higher(8.01×10^{-8} cc/Nm) compared to 100 km - 300 km(5.48×10^{-9} cc/Nm). The reason for this was that the higher the contact area (from 100 km - 300 km) the lower the contact pressure. Hence, the lower the wear rate.

Water and Sand Environment

The performance of the NiW coated coupling (Figure 5.46-5.47) was better than that of the standard coupling. The wear rate of the standard coupling was 63 times (at 10 km) and 15 times (at 300 km) higher than the wear rate of the NiW coated couplings at the same distances using an 890 N side load. The difference in the wear rate of the standard coupling in the early stage of the test i.e. 10 km as compared to the end of the test i.e. 300 km (Figure 5.47) was due to the workhardening of the surface of the coupling.

5.7 Wear Rate and Friction Relationship

As mentioned in Section 5.5.2, friction and wear data often correlate poorly. From Figures 5.48a-d a general observation can be made. This observation suggests that the coated coupling wear rate decreased as the apparent coefficient of friction decreased. For the

standard coupling there is a transition point for the wear rate at 445 N. This may be due to changes in the wear mode. Simultaneously, the apparent coefficient of friction kept decreasing. The apparent coefficient of friction of all couplings (example: Figure 5.38) and the wear rate (Figure 5.45) decreased as a function of distance travelled due to work hardening. This leads to a conclusion that a harder surface does indeed reduce the wear rate. In a way, the apparent coefficient of friction also influences the wear rate. In cases of mild wear and as long as the wear mode does not change, the wear rate decreases as the apparent coefficient of friction decreases for all couplings. At higher loads, this conclusion applies only for the NiW coated coupling. For the rest of the couplings, the results and conclusions are inconclusive due to changes in wear modes.

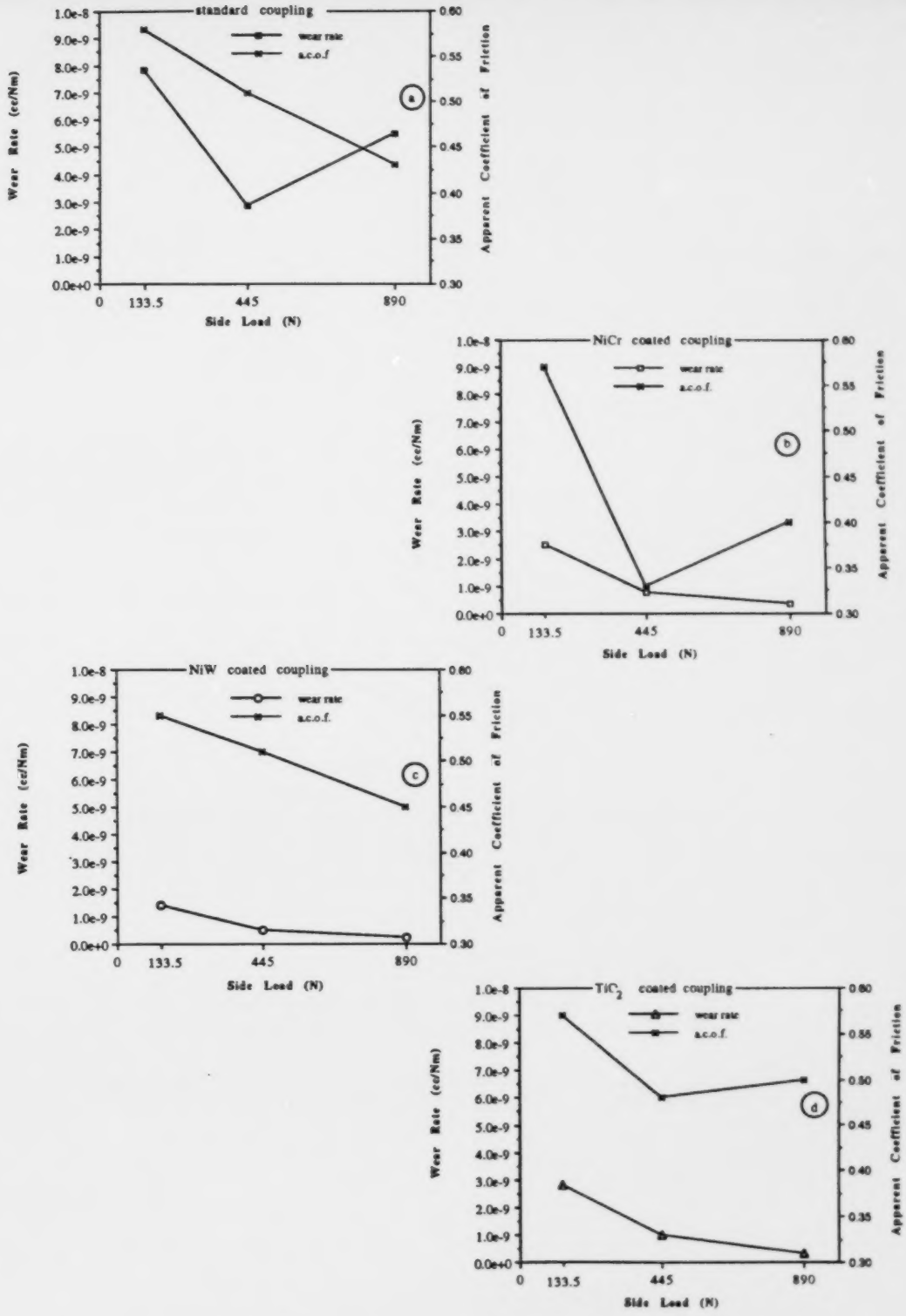

Figure 5.48. Wear Rate and Friction Relationship For All Couplings at 300 km as a Function of Side Load

5.8 Wear Modes

Both mild and severe modes were observed in the present study. Both were dependent on the nature of the surfaces in contact, the amount of side load and the type of environment.

Mild wear was observed in all tests using 133.5 N side load and water environment. Mild wear was also observed at all loads and with a water environment using the TiO_2 coated coupling. When mild wear occurred at low loads (133.5 N) the contact resistance between the two surfaces (the coupling and tubing) was high, the wear debris was fine and consisted mainly of metal oxide and the rubbed surfaces became polished.

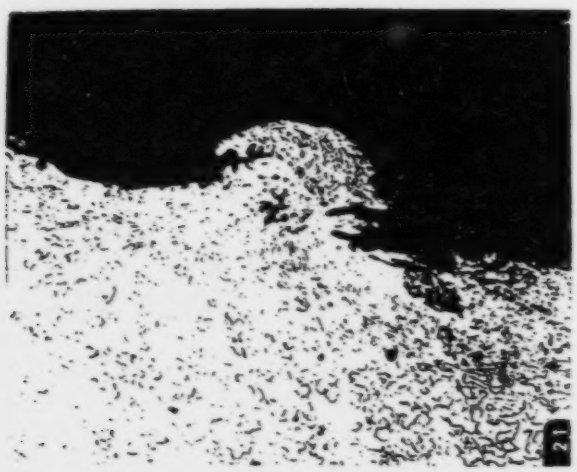

Figure 5.49. Transverse Surface of Tubing Using Standard Coupling Under 890 N Side Load After 300 km (x 240 , 2% Nital etchant)

At a side load of 445 N, during the first 1000 m, the tubing underwent severe wear with the NiCr and NiW coated couplings.

With the standard coupling, severe wear of the tubing was observed only during the first 10,000 m. For the remainder of the distance, up to 300,000 m, mild wear was observed. At a 890 N side load, severe wear of the tubing was observed for all distances with the standard coupling (Figure 5.49). In severe wear at high loads (445 N - 890 N), the contact resistance was low and the wear debris included coarse metallic particles and the rubbed surfaces were rough. During the first 10,000 m with the NiCr and NiW coated couplings, mild wear occurred, followed by a short duration of severe wear, followed by a return to mild wear. Mild wear occurred over the duration 10,000 m to 300,000 m.

In the sand-water environment at all loads, the wear of the tubing was continuously severe using standard and TiO_2 coated couplings. Mild wear of the tubing was observed under the same environment with NiCr and NiW coated couplings under a side load of 133.5 N, whereas severe wear was observed at side loads of 445 N and 890 N.

5.9 Analysis of Different Wear Mechanisms Using Scanning Electron Micrographs

The description of wear may be based upon the appearance of the worn surface. The wear of the sliding surfaces was controlled by one or more wear mechanisms. In order to gain a better understanding of what wear mechanism was involved in the process, the wear surfaces were inspected using a SEM technique. Various

tubing specimens were selected and micrographs of the worn surfaces were recorded. The results of these investigations were observed and are reported below.

Adhesion is characterized by the transfer of material from one surface to another. Plate 1 (Figures 1-8) shows the adhesive wear observed for different tubings using different couplings and side loads. Figure 1-3 shows smeared Nickel (bright areas) from the NiCr coated couplings under different side loads. In Figures 4-5, ceramic particles were released from the TiO_2 coated coupling as loose wear debris and they became embedded in the surface of the tubing. This explains one of the ways in which the third body abrasion caused wear in the coupling. Figure 6 shows a sand particle embedded in the tubing using a standard coupling. The sand source was from the sand-water environment. Figure 7 shows Co and W particles from the NiW coated coupling under a 445 N side load. In Figure 8, adhesion of nickel from the NiW coated coupling was found along with the abraded surface. This is an example of two mechanisms controlling the wear of the tubing under an 890 N side load.

Abrasive wear was seen in the form of gouging and surface cracks. This was the major wear mechanism with the water-sand environment. Plate 2 (Figures 9-16) shows the abrasive wear observed for different tubings. Abrasive wear appeared along with other mechanisms such as fatigue and adhesion. Figure 9 shows a combination of abrasion and fatigue in the form of a cracked surface

Plate 1: Adhesive Wear of Tubing

Fig. 1. TUBING vs. NiCr COUPLING
133.5 N , x 210
water only

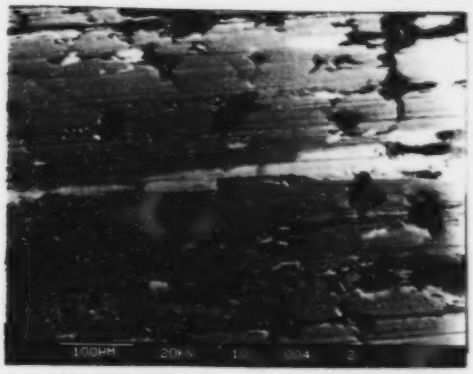

Fig. 2. TUBING vs. NiCr COUPLING
445 N , x 160
water only

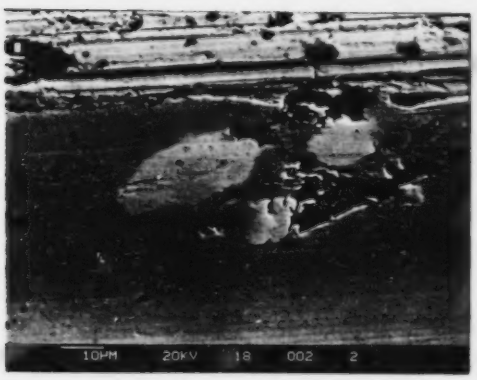

Fig. 3. TUBING vs. NiCr COUPLING
890 N , x 700
water only

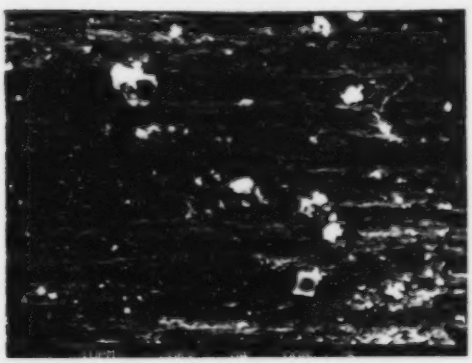

Fig. 4. TUBING vs. TiO2 COUPLING
445 N , x 600
water only

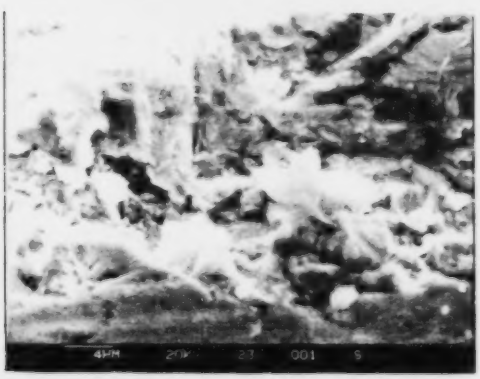

Fig. 5. TUBING vs. TiO2 COUPLING
445 N , x 2700
water & sand

Fig. 6. TUBING vs. STD. COUPLING
133.5 N , x 3500
water & sand

Plate 1: Adhesive Wear of Tubing (continued)

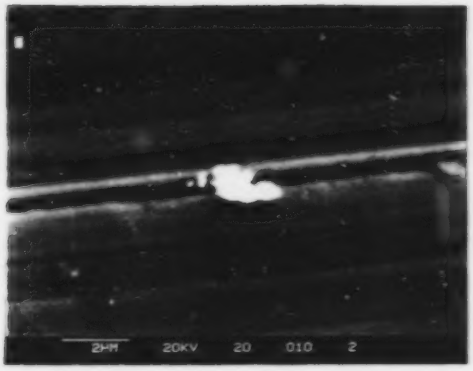

Fig. 7. TUBING vs. NiW COUPLING
445 N , x 7900
water only

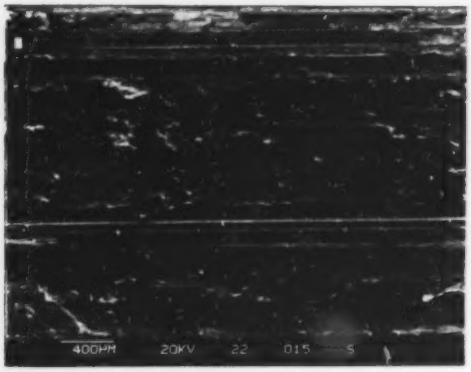

Fig. 8. TUBING vs. NiW COUPLING
890 N , x 30
water only

of tubing in a water-sand environment using a standard coupling. Figure 10 shows abrasive wear in the tubing using a NiCr coated coupling at a 890 N side load. In this test, adhesive wear was also observed as transfer of Nickel from the NiCr coated coupling (see Figure 3). Figure 11 shows partial abrasion of the contact surface along with the wear debris being removed. The back scattered image of the abraded wear surface shown in Figure 12 reveals that the gouges occurred parallel to the sliding motion due to the surface contact of the tubing with a harder asperity of the NiW coated coupling. The abrasive wear track was also found in the tubing using the TiO_2 coated coupling (Figure 13) and in the water-sand environment. This mainly was caused by the third body abrasive sand particles. Figure 14 shows a rough surface due to ploughing by a NiCr counterface in a water-sand environment. Figure 15 shows the abrasive wear of the tubing using the NiW coated coupling in the

Plate 2: Abrasive Wear of Tubing

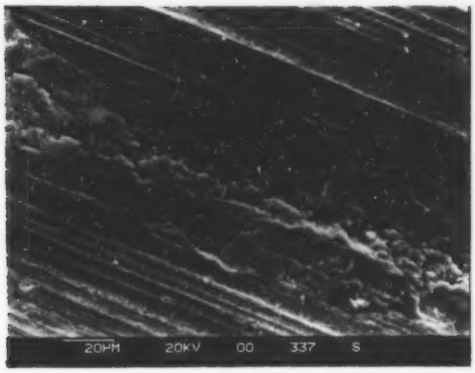

Fig. 9. TUBING vs. STD. COUPLING
133.5 N , x 3500
water & sand

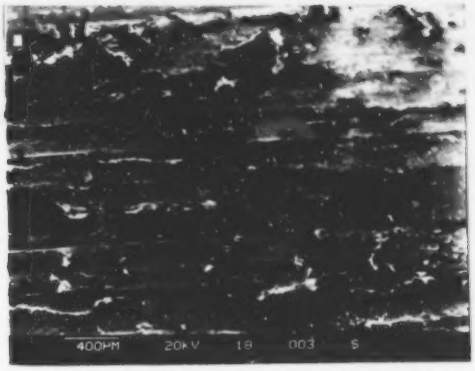

Fig. 10. TUBING vs. NiCr COUPLING
890 N , x 20
water only

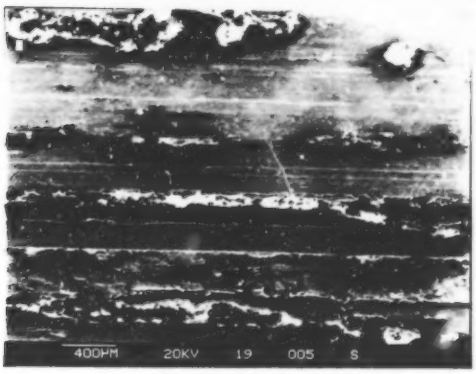

Fig. 11. TUBING vs. STD. COUPLING
445 N , x 20
water only

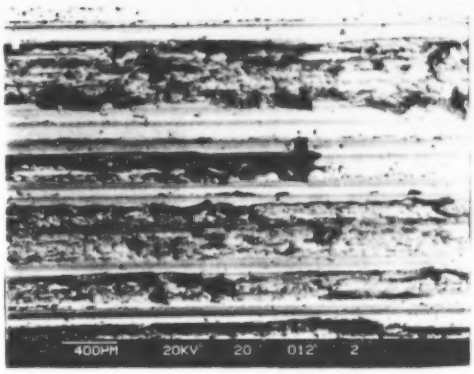

Fig. 12. TUBING vs. NiW COUPLING
445 N , x 30
water only

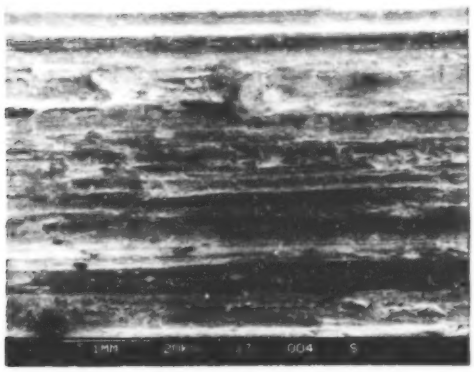

Fig. 13. TUBING vs. TiO2 COUPLING
445 N , x 20
water & sand

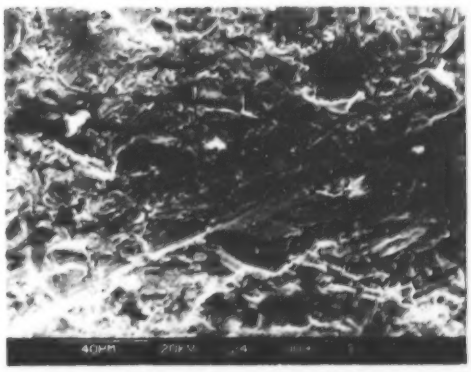

Fig.14. TUBING vs. NiCr COUPLING
445 N , x 3500
water & sand

Plate 2: Abrasive Wear of Tubing (continued)

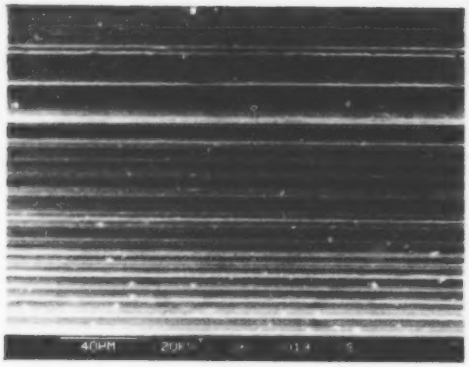

Fig. 15. TUBING vs. NiW COUPLING
890 N , x 540
water & sand

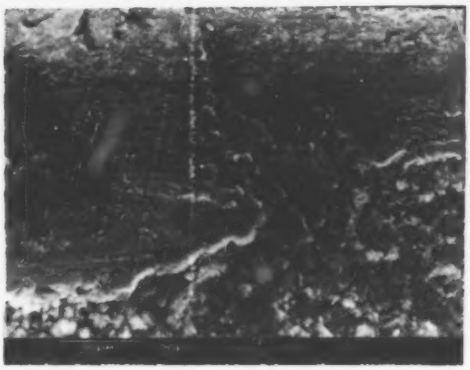

Fig. 16. TUBING vs. NiW COUPLING
890 N , x 1000
water & sand

water-sand environment. A closer view of the same location is shown in Figure 16 which shows that the abrasion was accompanied by surface cracks which occurred from the hard surface and the loading system (890 N).

Other wear mechanisms, such as fatigue, corrosion and delamination were observed and some are shown in Plate 3 (Figures 17-22). Fatigue failure of the surface of the tubing leading to cracks was observed in combination with corrosion that led to pits that were caused by the water environment. Figures 17-19 show a combination of corrosion and fatigue in the form of cracks, pits and oxidized surfaces. A typical oxidation morphology is shown in Figure 20 which was typical of all of the oxidated surfaces. Figure 21 shows surface fatigue cracks in the tubing surface caused by a NiW coated coupling under a side load of 445 N. The cracks occurred due to the

Plate 3: Other Wear Mechanisms of Tubing

corrosion-fatigue

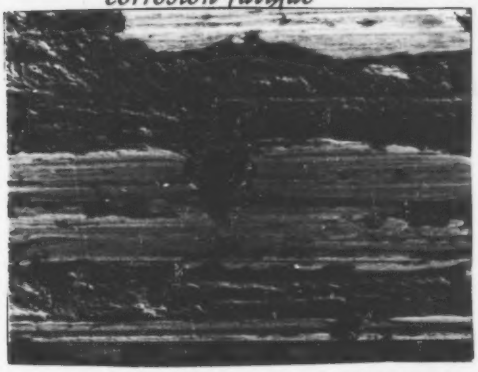

Fig. 17. TUBING vs. STD. COUPLING
133.5 N , x 120
water only

corrosion-fatigue

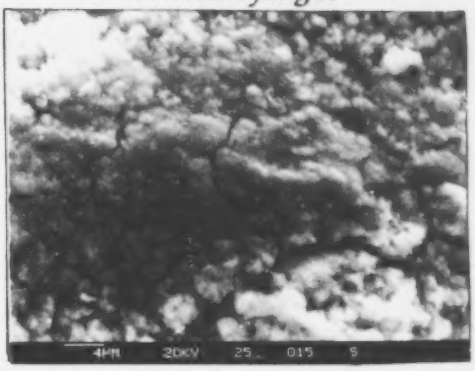

Fig. 18. TUBING vs. STD. COUPLING
890 N , x 2000
water & sand

corrosion-fatigue

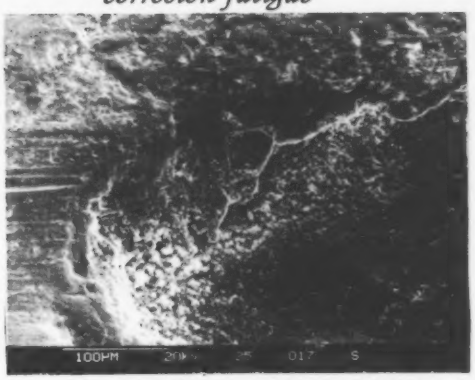

Fig. 19. TUBING vs. STD. COUPLING
890 N , x 240
water & sand

corrosion

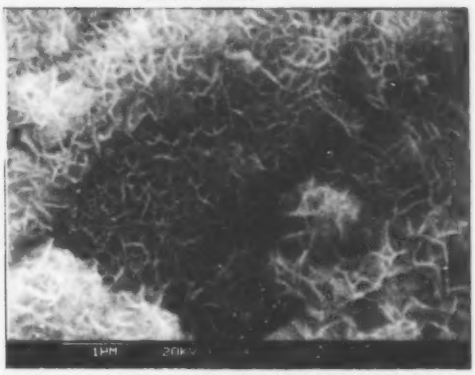

Fig. 20. OXIDATION MORPHOLOGY
X16000

fatigue

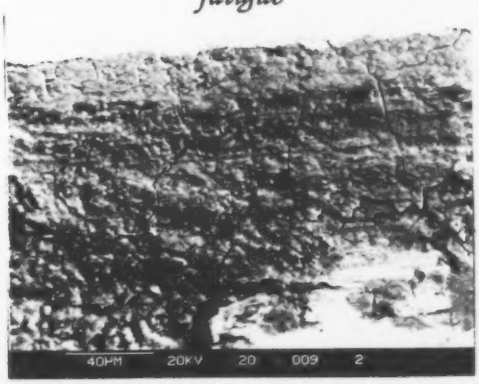

Fig. 21. TUBING vs. NiW COUPLING
445 N , x 520
water only

delamination

Fig. 22. TUBING vs. TiO2 COUPLING
445 N , x 1000
water & sand

brittle surface of the tubing once it became harder and cracked under cyclic loading. Figure 22 shows thin laminated sheets of material forming a junction before being sheared off.

Abrasion was the main wear mechanism in most of the tests, particularly in tests using a water-sand environment. Adhesion was the other main wear mechanism observed. This wear mechanism was observed only in the tests with water. S.E.M. analysis did not reveal any material transfer to the tubing in a sand-water environment. This confirms the prediction made by Bellow et al. [1] and shown in Section 5.4.2 that the sand prevented the effective transfer of metal particles.

5.10 The Effect of Sand Rates on The Wear of Coupling/Tubing

All the previous tests discussed used a controlled sand rate i.e. 165 g/day. The investigation performed involved the use of saturated sand slurries. In the oil field, however, sand rate can vary. Therefore, a brief study was performed to see if there was any relationship between the amount of sand and the degree of wear. The study presents the wear of tubing using standard couplings under 133.5 N side load. This type of coupling is the most common coupling used in the field. The tests included four different sand rates as follows: 0, 15, 165, and 180 g/day.

In Figure 5.50, the coupling weight loss was directly influenced by an increase in the sand rate i.e. the higher the sand rate the higher the weight loss of the standard coupling. The tubing behaved in the same manner as shown in Figure 5.51 where the wear of the tubing was measured in the form of average wall thickness loss.

The surface roughness of the tubing result did not correlate well with the degree of sand contamination as seen in Figure 5.52. The surface roughness decreased as a function of the distance travelled. This was observed for all sand rates evaluated. Figures 5.53-5.54 show the effects of different sand rates on the work hardening of the surface of the standard coupling. At each sand rate the hardness of the coupling and the tubing increased with distance travelled. It was also seen that the higher the sand rate, the greater the hardness of the coupling and tubing. When higher sand rates were used, the grooves were found to be deeper i.e. indentations were deeper and hence, greater hardness occurred.

From the apparent coefficient of friction (Figure 5.55), there did not appear to be any correlation with the degree of sand contaminates. On the other hand, the wear rate of the standard coupling at different sand rates showed a consistent reduction as the sliding distance increased. The wear rate was proportional to the sand rate i.e. the higher the sand rate the higher the wear rate (Figure 5.56). The relationship between the coupling surface hardness and the wear rate was evident i.e. as the surface hardness increased, the wear rate decreased.

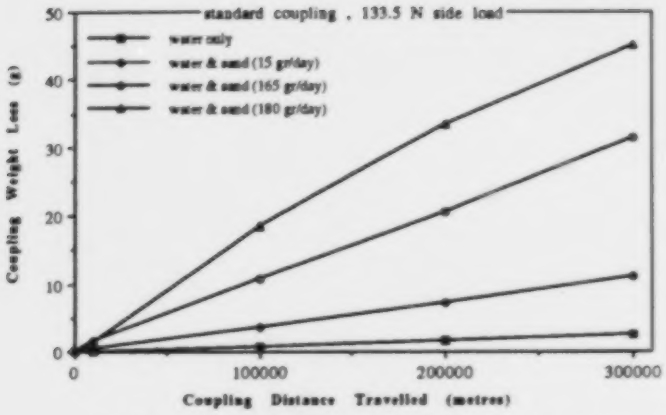

Figure 5.50. Coupling Weight Loss at Different Sand Rates

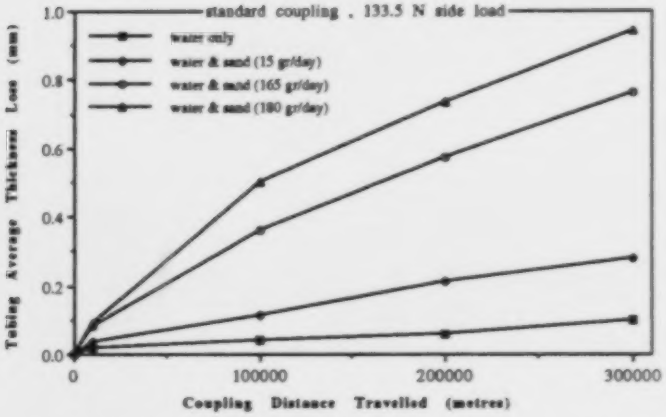

Figure 5.51. Tubing Average Thickness Loss at Different Sand Rates

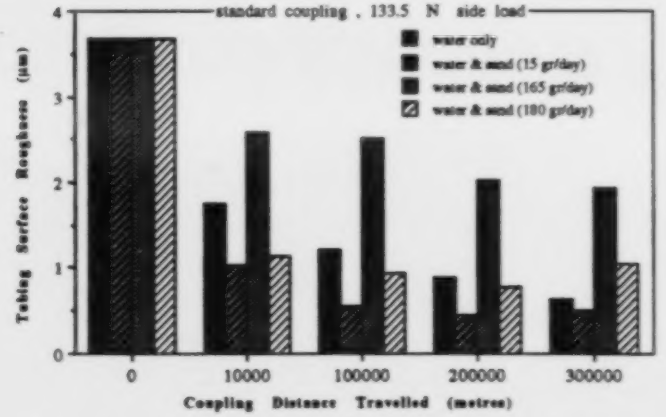

Figure 5.52. Tubing Surface Roughness at Different Sand Rates

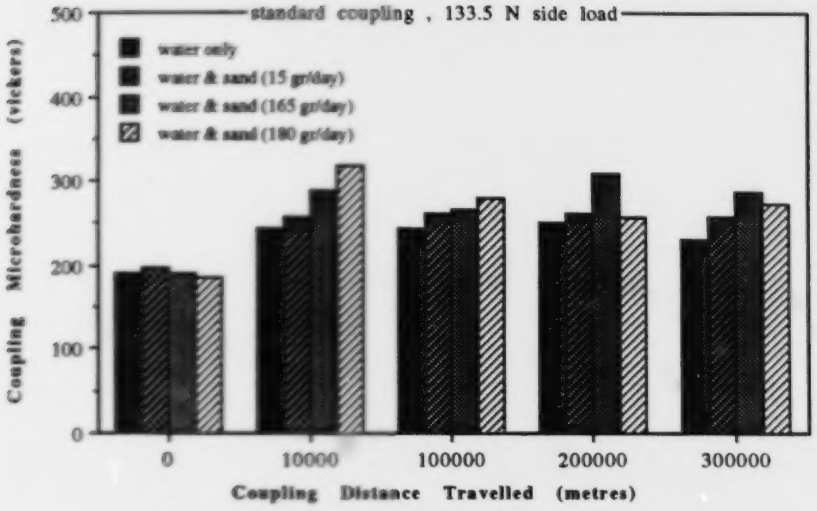

Figure 5.53. Coupling Microhardness at Different Sand Rates

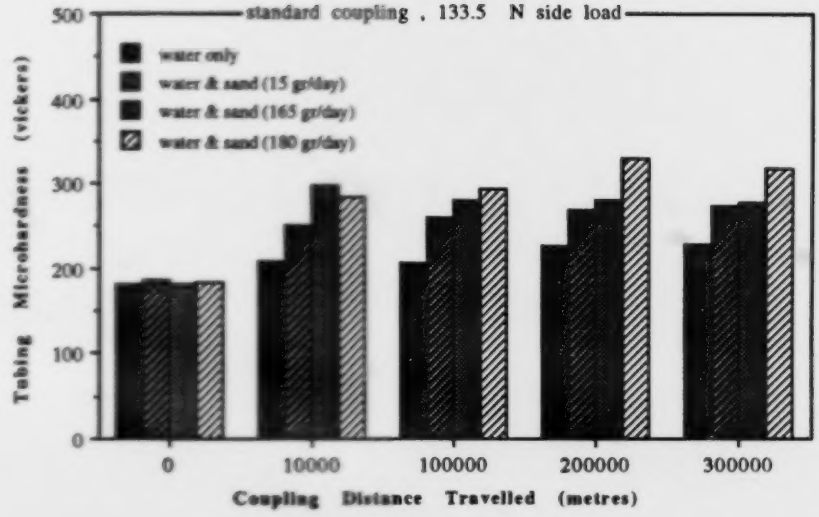

Figure 5.54. Tubing Microhardness at Different Sand Rates

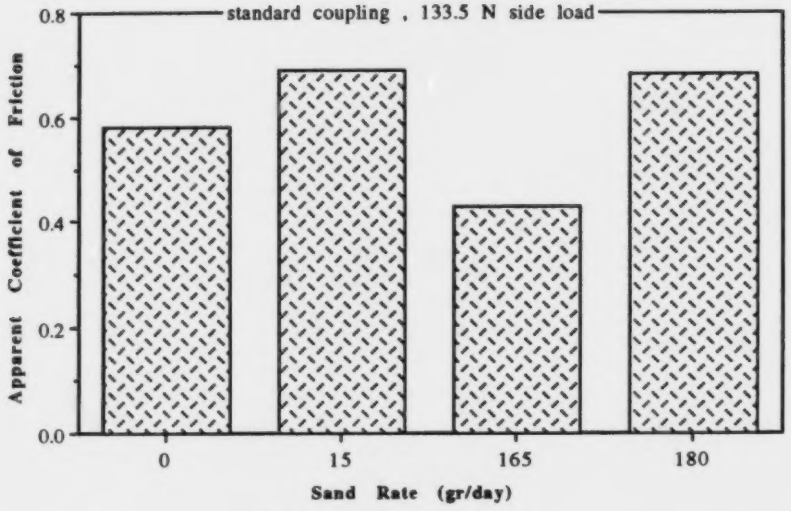

Figure 5.55. Apparent Coefficient of Friction vs Sand Rate

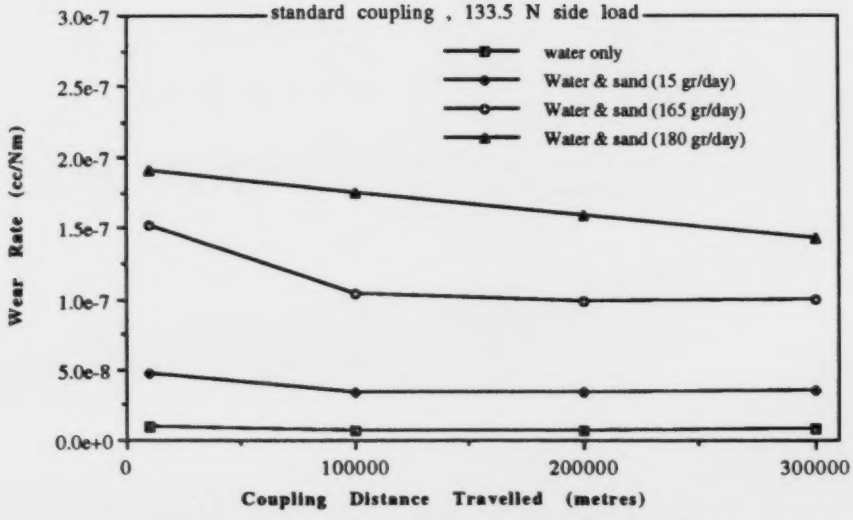

Figure 5.56. Coupling Wear Rate at Different Sand Rates

A summary of the correlation between the sand rate and the degree of wear as found in this brief study is presented in Table 5.1.

Table 5.1. Sand Rate and the Degree of Wear Relationship

	Coupling weight loss	Tubing thickness loss	Tubing surface roughness	Coup.&Tub. micro-hardness	Apparent coefficient of friction	Coup.&Tub. wear rate
Direct influence	x	x		x		x
No correlation			x		x	

5.11 The Advantages of Coating Materials

The use of hardmetal and ceramic coatings to improve wear resistance is increasing and will continue to expand because they offer certain economic and technical advantages over the use of uncoated couplings. The main advantage for the surface is to optimize wear and corrosion resistance, while the base material is optimized for strength purposes. Another advantage is to achieve a hard coating while retaining the ductility of the base material. Coating reduces the costs of making the coupling entirely out of Ni, Cr, W and Ti. Coatings are also economically advantageous since wear and corrosion resistance alloys are usually more expensive than low alloy structural steels. Furthermore, replacing the coating during rework or repair is usually less expensive than replacing the part. The question now is, how much it is going to cost to coat the standard couplings. Table 5.2 addresses this question. As shown,

variation in the prices of coated couplings depends upon the type of powder used and the number of couplings to be coated. The prices presented in Table 5.2 were suggested by 'Eutectic-Castolin'. The cost of coating the standard couplings needs to be added to the cost of the base material (Table 5.3).

Table 5.2. The Cost of Coating Couplings

Powder->	NiCr	NiW	TiO2
amount of powder (kg)	0.15	0.20	0.11
For only 1 coated coupling (prices are in $)			
price of powder/kg	33.00	99.23	118.30
labor/hr	45.00	45.00	45.00
price of powder/coupling	4.95	19.85	13.01
labor/coupling	15.00	15.00	11.25
total cost/unit	19.95	34.85	24.26
For 500 or more coated couplings			
price of powder/kg	24.75	74.42	88.73
labor/hr	22.50	22.50	22.50
price of powder/coupling	3.71	14.89	9.76
labor/coupling	7.50	7.50	5.63
total cost/unit	11.21	22.39	15.39
Coupling is 4"(100 mm) long and 1-3/4"(44 mm) diameter Coating thickness is 0.020"(0.508 mm)			

Table 5.3. The Cost of Standard Coupling

Amount	1	100	500 (one timer)	500 (frequantly)
Cost/unit ($)	12.00	10.80	9.00	6.75

Table 5.4. Comparison of Coupling Cost vs Performance

Type	Standard coupling	NiCr coated coupling	NiW coated coupling	TiO2 coated coupling
Price ($)	6.75	17.96	29.14	22.14
water environment (test results)*				
Coupling weight loss(g)	11.50	0.80	0.60	0.50
Tubing thickness loss(mm)	0.69	0.81	0.59	0.15
water & sand environment (test results)				
Coupling weight loss(g)	75.10	-	6.90	-
Tubing thickness loss(mm)	2.06	-	2.00	-
ratios **				
Price	1.00	2.66	4.32	3.28
water environment				
Coupling weight loss(g)	1.00	0.070	0.052	0.043
Tubing thickness loss(mm)	1.00	1.174	0.855	0.217
water & sand environment				
Coupling weight loss(g)	1.00	-	0.092	-
Tubing thickness loss(mm)	1.00	-	0.971	-

* Wear of coupling and tubing was taken at the end of the test i.e. 300 km and under 890 N side load

**All prices and performances of the coated couplings were compared to those of the standard coupling.
For example, the price of NiW coated coupling was 4.32 times higher than the price of the standard coupling but, the performance of the NiW coated coupling was better than that of the standard coupling by 19.23 times (or as presented in the table, while the weight loss of the standard coupling was 1 unit, the weight loss of the NiW coated coupling was 0.052 unit) in water environment and by 10.87 times in water & sand environment.

Table 5.4 shows the comparison of coupling cost versus performance. Although coating the coupling adds to the cost, the performance of the coated couplings justifies the expense. For example, as shown in Table 5.4, the cost of TiO_2 coated coupling is 3.28 times more expensive than the standard coupling, but its performance is better by 23 times in a water environment. Whereas in a water and sand environment, the TiO_2 coated coupling performed poorly. When considering both environments, the NiW coated coupling had the best overall performance. Even though the price of the NiW coated coupling is 4.32 times more expensive than the cost of the standard coupling its performance is better by 19.23 times in a water environment and by 10.87 times in a water and sand environment.

Two of the coated couplings contained Ni but the study did not attempt to determine the merits of Ni versus W versus Cr etc.. These were commercially available coatings on sucker rod couplings and because of this, it limited the analysis to these compositions. More or less, Ni, Cr or W may have an influence which could not be determined within the scope of the study.

Chapter 6

Conclusions and Recommendations

Wear may result whenever there is relative sliding of two materials in contact. The rate at which material is removed due to wear will depend upon the loading conditions and the environment. The purpose of the present study was to investigate the performance of the standard coupling, hardmetal and ceramic coated couplings and oil field tubing. The wear of the couplings and tubing was examined in both a water environment and in a water and sand environment (sand rate - 165 g/day).

The purpose of the present study was to obtain a reliable correlation between various variables and the wear behavior of couplings/tubing while evaluating the performance of tubing in contact with different types of couplings. Another purpose of the present study was to assist in gaining a better understanding of the controlling and participating wear mechanisms.

6.1 Conclusions

1. The TiO_2 coated coupling wore the least and caused the least damage to the tubing in the water environment condition. However, it showed the worst performance in the water and sand environment due to the breakdown of the coating material (ceramic).

2. Overall, the performance of the NiW coated coupling was the best in both environments and under different side loads. The NiW did not wear completely as did the NiCr and the TiO_2 coatings. In addition, it protected the base material (the standard coupling).

3. The operating variables had an expected influence on the wear of the couplings and tubing. In general, the following features were observed:

a). Higher side load caused an increase in wear of couplings and tubing.

b). Increasing sliding duration (distance) increased the wear of the couplings/tubing.

c). Increasing side load caused an increase in the tubing surface hardness which in turn reduced the wear rate.

d). Work hardening of the surface of the tubing occurred during the tests.

e). Surface hardness increased due to work hardening, and to the transfer of harder particles which enhanced the wear resistance of the tubing.

f). Surface roughness influenced the wear of couplings/tubing. Higher surface roughness increased the wear of all tubings and couplings.

g). The apparent coefficient of friction had an influence on the wear of couplings/tubing only in mild wear and as long as the wear mode did not change. The wear rate decreased as the apparent coefficient of friction decreased for all couplings. The same conclusion applies for the NiW coated coupling at higher loads (890 N). For the rest of the couplings, the results were inconclusive due to changes in the wear modes.

h). Mild wear was observed in all the wear tests using a 133.5 N side load and in a water environment. Mild wear was also observed in the test using the TiO_2 coated coupling under all loads in a water environment and in the tests using NiCr and NiW coated couplings under 133.5 N in a water and sand environment. Mild and severe wear alternated in the tests using NiCr and NiW coated couplings under 445 and 890 N side loads and under 445 N using a standard coupling all in water environments. Severe wear was observed during the tests using a standard coupling under a 890 N side load in a water environment and in all tests using standard and TiO_2 coated couplings in water and sand environments. Severe wear was also observed in the tests using 445 and 890 N with NiCr and NiW coated couplings in water and sand environments.

i). Introducing sand to the environment prevented the effective transfer of metal particles from the coated couplings onto the tubing. Where there was excessive grooving due to sand particles, the hardness of the tubing increased significantly.

j). As expected, introducing sand to the environment caused an increase in the wear of all coupling/tubing combinations.

4. Abrasion was the dominating wear mechanism in most of the wear tests, particularly in the tests using a sand-water environment. Adhesion, corrosion, fatigue and delamination were also observed on the S.E.M.

5. Increasing the sand flow rate increased the wear of couplings and tubing.

6.2 Recommendations

The present study examined the effectiveness of commercially available coupling coatings in withstanding wear in well conditions. Future research should focus on investigating and determining the optimum amounts of Ni, Cr, W, and/or Ti that should be utilized in the composition of the coating of the coupling in order to produce the best results i.e.wear resistance.

References

[1] Bellow, D.G., Owens, D.C. & Smuga-Otto, I. (1989) Wear of standard and hard-metal-coated couplings with oilfield tubing. Wear, 133, Elsevier Sequoia: Lausanne , 83-93

[2] Ko, P.L., Humphreys, K. & Matthews, C. (1989) Reciprocating-sliding wear of sucker rods and production tubing in deviated oil wells. Wear of Materials, LuDema, K.C. (ed.), ASME, 681-687

[3] Schumacher, W.J. (1991) Wear simulation of sucker rod couplings. Materials Performance, 30(9), NACE, 62-64

[4] Lancaster, J.K. (1972) Frictions and Wear. Polymer Science. Chapter 14. Jenkins, A.D. (ed.)

[5] Rigney, A.D. (1980) Introduction. Fundamentals of Friction and Wear of Materials. Materials Science Seminar. Rigney, D.A. (ed.), ASM, 1-12

[6] Jahnmir, S. (1978) On wear mechanisms and wear equations. Fundamental of Tribology. Conference on the Fundamentals of Tribology. Suh, N.P. & Sake, N. (eds.), MIT Press: Massachusetts, 455-467

[7] Buckley, D.H. (1981) Surface effects in adhesion, friction, wear and lubrication. Tribology Series 5, Elsevier: Amsterdam

[8] Kerridge, M. & Lancaster, J.K. (1956) The stages in a process of severe metallic wear. Proc. R. Soc.. 236A, Royal Society Burlington House Piccadilly London, 250-264

[9] Moore, A. M. (1980) Abrasive wear . Fundamentals of Friction and Wear of Materials. Materials Science Seminar. Rigney, D.A. (ed.), ASM, 73-118

[10] Hirano, H.H. and Levy, A.V. (1978) An investigation to two body abrasive wear. Fundamental of Tribology. Conference on the Fundamentals of Tribology. Suh, N.P. & Sake, N. (eds.), MIT Press: Massachusetts, 519-542

[11] Kruschov, M.M. (1957) Resistance of metals to wear by abrasions; related to hardness. Conference On Lubrication and Wear. Instn. Mech. Engineers : London, 655-659

[12] Suh, N.P. (1980) Update on the delamination theory of wear. Fundamentals of Friction and Wear of Materials. Materials Science Seminar. Rigney, D.A. (ed.), ASM, 43-71

[13] Suh, N.P. (1973) The delamination Theory of Wear, Wear, 25, Elsevier Sequoia: Lausanne ,111-124

[14] Archard, J.F. & Hirst, W. (1956) The wear of metals under unlubricated conditions. Proc. R. Soc.. 236A, Royal Society Burlington House Piccadilly London, 397-410

[15] Teer, D.G. & Arnell, R.D. (1975) Wear. Principles of Tribology. Chapter 5. Halling, J. (ed.), Macmillan Press: London

[16] Syniuta, W.D. & Corrow, C.J. (1970) A Scanning Electron Microscope Fractographic Study of Rolling-Contact Fatigue. Wear. [15], Elsevier Sequoia: Lausanne ,187-199

[17] Kragelsky, I.V. (1981) Friction, Wear, Lubrication - Tribology Handbook. I. Mir Publishers: Moscow, 102-118

[18] Hirst, W. & Lancaster, J. K. (1960) The Influence of Speed on Metallic Wear. Proc. R. Soc.. 259A, Royal Society Burlington House Piccadilly London, 228-241

[19] Glossary of Terms and Definitions in the Field of Friciton, Wear and Lubrication (1969). OECD Publications, Paris

[20] Jahnmir, S. & Suh, N.P. (1977) Mechanics of Subsurface Void Nucleation in Delamination Wear. Wear, 44, Elsevier Sequoia: Lausanne,17-38

[21] Alamsyah, C., Dillich, S.A. & Femia, A.P. (1989) Effect of initial surface finish on cam wear. Wear of Materials. Ludema, K.C. (ed.), ASME, 657-664

[22] Argon, A.S. Mechanical properties of near surface material in friction and wear. Fundamentals of Tribology. Conference on the Fundamentals of Tribology. Suh, N.P. & Sake, N. (eds.), MIT Press: Massachusetts,103-117

[23] Blau, P.J. (1989) Break-in, Run-in and Wear-in. Friction And Wear Transitions Of Materials. Chapter 5, Noyes Publications: New Jersey

[24] Kragelsky, I.V., Dobychin, M.N. & Kombalov, V.S. (1982) Friction And Wear Calculation Methods. Pergamon Press: Oxford

[25] Viswanath, N.S. (1992) An analysis of the wear of polymers. Unpublished doctoral dissertation, University of Alberta, Edmonton

[26] Poggie, R.A. & Wert, J.J. (1991) The influence of surface finish and strain hardening on near surface residual stress and the friction and wear behavior of A2, D2 and CPM-10V tool steel. Wear of Materials, ASME, 497-501

[27] Czichos, H. & Habig, K.H. (1986) Wear of medium carbon steel: A systematic study of the influences of materials and operating parameters. Wear, 110, Elsevier Sequoia: Lausanne, 389-400

[28] Jahmnir, S., Abrahamson, E.P. & Suh, N.P. (1975) In Proceedings Of The Third North American Metalworking Research Conference Carnegie-Mellon University. Edited by Shaw, M.C. Carnegie Press, Pittsburgh, 854

[29] Peterson, M.B. & Ramalingam, S. (1980) Coatings for tribological applications. Fundamentals of Friction and Wear of Materials. ASM, Rigney, D. (ed), 331-372

[30] Fang, L., Zhou, Q.D. & Li, Y.J. (1991) An explanation of the relation between wear and material hardness in three-body abrasion. Wear of Materials, ASME, 513-520

[31] Rabinowicz, E., Dunn, L.A. & Russel, P.G. (1961) A study of abrasive wear under three-body conditions. Wear, 4, Elsevier Sequoia: Lausanne, 345-355

[32] Misra, A. & Finie, I. (1981) Correlations between two-body and three-body abrasion and erosion of metals. Wear, 68, Elsevier Sequoia: Lausanne, 33-39

[33] Rabinowicz, E. (1965) Friction and Wear Of Materials. Chapter 8. John Wiley & Sons, New York

[34] Bowden, F.P. & Tabor, D. (1964) The Friction And Lubrication Of Solids. Clarendon Press, Oxford, London. Part 1, 1950, Part 2, 1964

[35] Bentley & Doquette, D.J. (1980) Environmental considerations in wear processes. Fundamentals of Friction and Wear Of Materials. Materials Science Seminar, Rigney, D.A. (ed), ASM, 291-329

[36] Dahalberg, E.P. (1956) Fatigue crack propogation in high strength 4350 steel in humid air. Trans. ASM Quarterly. 58, 46

[37] Appledorn, J.K., Goldman, I.B. & Tao, F.F. (1969) Corrosion wear by atmospheric oxygen and moisture. ASCE Trans. 12, 140

[38] Barwell, F.T. (1957-8) Wear of metals. Wear, 1, Elsevier Sequoia: Lausanne , 317-332

[39] Lancaster, J.K. (1980) Material-specific wear mechanisms: Relevance to wear modelling. Wear, 141, Elsevier Sequoia: Lausanne , 159-183

[40] Archard, J.F. (1968) Interdisciplinary approach to friction and wear. NASA Spec. Publ.. SP-181, 267-233

[41] Dally, J.W., Riley, W.F. & McConnell, K.G. (1984) Instrumentation For Engineering Measurements. John Wiley & Sons Inc.

[42] Wallbridge, N.C. & Dowson, D. (1987) Distribution of wear rate data and a statistical approach to sliding wear theory. Wear, 119, Elsevier Sequoia: Lausanne , 295-312

[43] Rabinowicz, E. (1980) Wear Coefficient - Metals ASME Wear Control Handbook. New York, 475-506

[44] Zum Gahr, K.H. (1987) Microstructure And Wear Of Materials. Tribology Series 10, Elsevier: Amsterdam

[45] Whitehous, D.J. (1978) Surface topography and quality and its relevance to wear. Fundamentals of Tribology. Conference on the Fundamentals of Tribology. Suh, N.P. & Sake, N. (eds.), MIT Press: Massachusetts, 17-52

[46] Kim, D.E. & Suh, N.P. (1991) On microscopic mechanisms of friction and wear. Wear of Materials. ASME, 475-480

[47] Hirn, G.A. (1854) Sur les principaux phenomenes que presentent les frottements mediats, et sur les diverses manieres de determiner la valeur mecanique des matieres employees au graissage des machines. Bull. Soc. Indust., 26, Mulhouse, 188-237

[48] Bowden, F.P. & Taber, D. (1973) Friction: An Introduction to Tribology. Doubleday & Co., New York

APPENDIX 1: Statistical Analysis

Complete sample of statistical analysis on all tests results using standard coupling/J55 tubing under 133.5 N side load in water environment.

Table A.1.1. Coupling Weight Loss

Weight Loss at 10 Km				
W.L. [g]	Dev.Ratio	MEAN=	0.10	
0.1	0.00	STDEV=	0.00	
0.1	0.00	SDOM=	0.00	
0.1	0.00	%ERROR=	0.00	
		From Chauvenet's Criterion		
		DRo for this case with n=3, is 1.38		
		If DR>DRo data point is rejected		
		*** No data point is rejected**		
		W.L.=0.10±0.0% [g]		
Weight Loss at 100 Km				
W.L. [g]	Dev.Ratio	MEAN=	0.73	
0.7	-0.50	STDEV=	0.06	
0.8	1.17	SDOM=	0.03	
0.7	-0.50	%ERROR=	4.11	
		*** No data point is rejected**		
		W.L.=0.73±4.11% [g]		
Weight Loss at 200 Km				
W.L. [g]	Dev.Ratio	MEAN=	1.47	
1.4	-0.58	STDEV=	0.12	
1.6	1.08	SDOM=	0.07	
1.4	-0.58	%ERROR=	4.76	
		*** No data point is rejected**		
		W.L.=1.47±4.76% [g]		
Weight Loss at 300 Km				
W.L. [g]	Dev.Ratio	MEAN=	2.47	
2.4	-0.58	STDEV=	0.12	
2.4	-0.58	SDOM=	0.07	
2.6	1.08	%ERROR=	2.83	
		*** No data point is rejected**		
		W.L.=2.47±2.83% [g]		

Table A.1.2. Tubing Average Thickness Loss

Thickness Loss at 10 Km				
TH. L. [mm]	Dev Ratio	MEAN=	2.00E-02	
0.02	0.00	STDEV=	3.29E-10	
0.02	0.00	SDOM=	1.90E-10	
0.02	0.00	%ERROR=	0.00	
		From Chauvenet's Criterion		
		DRo for this case with n=3, is 1.38		
		If DR>DRo data point is rejected		
		*** No data point is rejected**		
		TH.L.=2E-02±0% [mm]		
Thickness Loss at 100 Km				
TH. L. [mm]	Dev Ratio	MEAN=	3.67E-02	
0.03	-1.16	STDEV=	5.77E-03	
0.04	0.57	SDOM=	3.33E-03	
0.04	0.57	%ERROR=	9.09	
		*** No data point is rejected**		
		TH.L.=3.67E-02±9.09% [mm]		
Thickness Loss at 200 Km				
TH. L. [mm]	Dev Ratio	MEAN=	6.33E-02	
0.06	-0.57	STDEV=	5.77E-03	
0.06	-0.57	SDOM=	3.33E-03	
0.07	1.16	%ERROR=	5.26	
		*** No data point is rejected**		
		TH.L.=6.33E-02±5.26% [mm]		
Thickness Loss at 300 Km				
TH. L. [mm]	Dev Ratio	MEAN=	9.67E-02	
0.10	0.57	STDEV=	5.77E-03	
0.09	-1.16	SDOM=	3.33E-03	
0.10	0.57	%ERROR=	3.45	
		*** No data point is rejected**		
		TH.L.=9.67E-02±3.45% [mm]		

Table A.1.3 (a). Tubing Surface Roughness - Initial

Roughness [μin]**	Dev. Ratio				
140	-0.42				
155	0.48		MEAN=	147	
160	0.78		STDEV=	16.74	
175	1.67		SDOM=	3.06	
155	0.48		%ERROR=	2.08	
140	-0.42				
120	-1.61		From Chauvenet's Criterion		
185	2.27		DRo for this case with n=30, is 2.38		
180	1.97		If DR>DRo data point is rejected		
160	0.78				
160	0.78		*** No data point is rejected**		
140	-0.42				
140	-0.42		S.R.=147±2.08% [μin] or		
150	0.18				
150	0.18		**S.R.=3.675±2.08% [μm]**		
150	0.18				
140	-0.42				
130	-1.02				
135	-0.72		** three tests, each contains		
160	0.78		ten readings		
150	0.18				
145	-0.12				
140	-0.42				
145	-0.12				
155	0.48				
110	-2.21				
120	-1.61				
130	-1.02				
140	-0.42				
150	0.18				

Table A.1.3 (b). Tubing Surface Roughness - 10 Km

Roughness [μin]**	Dev. Ratio				
82	0.32		MEAN=	70	
100	0.97		STDEV=	22.90	
105	1.15		SDOM=	4.25	
85	0.43		%ERROR=	6.07	
62	-0.40				
80	0.25		From Chauvenet's Criterion		
90	0.61		DRo for this case with n=30, is 2.38		
75	0.07		If DR>DRo data point is rejected		
120	1.69				
80	0.25		*** One data point is rejected**		
60	-0.47				
60	-0.47		S.R.=70±6.07% [μin] or		
100	0.97				
70	-0.11		**S.R.=1.75±6.07% [μm]**		
75	0.07				
80	0.25				
60	-0.47				
70	-0.11		** three tests, each contains		
60	-0.47		ten readings		
35	-1.37				
20	-1.91				
65	-0.29				
90	0.61				
55	-0.65				
53	-0.72				
58	-0.54				
18	-1.98				
62	-0.40				
70	-0.11				
160	3.13	**Rejected**			

Table A.1.3 (c). Tubing Surface Roughness - 100 Km

Roughness [μin]**	Dev. Ratio				
95	1.48		MEAN=	48	
90	1.31		STDEV=	26.12	
80	0.98		SDOM=	4.85	
80	0.98		%ERROR=	10.10	
30	-0.71				
55	0.13		From Chauvenet's Criterion		
105	1.82		DRo for this case with n=30, is 2.38		
100	1.65		If DR>DRo data point is rejected		
62	0.37				
35	-0.54		*** One data point is rejected**		
50	-0.03				
36	-0.51		S.R.=48±10.10% [μin] or		
50	-0.03				
20	-1.04		**S.R.=1.2±10.10% [μm]**		
50	-0.03				
35	-0.54				
20	-1.04				
20	-1.04		** three tests, each contains		
20	-1.04		ten readings		
50	-0.03				
20	-1.04				
60	0.30				
21	-1.01				
38	-0.44				
45	-0.20				
27	-0.81				
27	-0.81				
32	-0.64				
44	-0.24				
130	2.66	**Rejected**			

Table A.1.3 (d). Tubing Surface Roughness - 200 Km

Roughness [µin]**	Dev. Ratio				
50	0.40		MEAN=	35	
105	2.26		STDEV=	25.11	
25	-0.44		SDOM=	4.66	
100	2.09		%ERROR=	13.31	
70	1.08				
70	1.08		From Chauvenet's Criterion		
40	0.07		DRo for this case with n=30, is 2.38		
55	0.57		If DR>DRo data point is rejected		
20	-0.61				
24	-0.47		*** One data point is rejected**		
28	-0.34				
32	-0.20		S.R.=35±13.31% [µin] or		
26	-0.40				
18	-0.67		**S.R.=0.875±13.31% [µm]**		
15	-0.78				
14	-0.81				
40	0.07				
25	-0.44		** three tests, each contains		
15	-0.78		ten readings		
20	-0.61				
18	-0.67				
42	0.13				
13	-0.84				
15	-0.78				
15	-0.78				
21	-0.57				
24	-0.47				
15	-0.78				
60	0.74				
125	2.94	**Rejected**			

Table A.1.3 (e). Tubing Surface Roughness - 300 Km

Roughness [μin]**	Dev. Ratio				
42	0.51		MEAN=	25	
70	1.71		STDEV=	13.60	
28	-0.09		SDOM=	2.57	
40	0.43		%ERROR=	10.28	
32	0.09				
40	0.43		From Chauvenet's Criterion		
20	-0.43		DRo for this case with n=30, is 2.38		
30	0.00		If DR>DRo data point is rejected		
15	-0.64				
12	-0.77		*** Two data points are rejected**		
28	-0.09				
9	-0.90		S.R.=25±10.28% [μin] or		
14	-0.69				
44	0.60		**S.R.=0.625±10.28% [μm]**		
38	0.34				
12	-0.77				
18	-0.51				
25	-0.21		** three tests, each contains		
12	-0.77		ten readings		
21	-0.39				
19	-0.47				
12	-0.77				
18	-0.51				
19	-0.47				
23	-0.30				
18	-0.51				
20	-0.43				
12	-0.77				
90	2.57	**Rejected**			
110	3.43	**Rejected**			

Table A.1.4 (a). Coupling Microhardness - Initial

VHN #1	Dev. Ratio #1	VHN #2	Dev. Ratio #2	VHN #3	Dev. Ratio #3
226	1.10	238	1.47	122	-2.17
172	-0.60	236	1.41	220	0.91
222	0.97	220	0.91	140	-1.60
222	0.97	194	0.09	216	0.78
192	0.03	180	-0.35	224	1.03
194	0.09	194	0.09	208	0.53
204	0.41	156	-1.10	210	0.59
218	0.84	192	0.03	176	-0.47
216	0.78	240	1.54	224	1.03
196	0.15	176	-0.47	192	0.03
196	0.15	244	1.66	250	1.85
192	0.03	192	0.03	224	1.03
190	-0.03	168	-0.73	172	-0.60
202	0.34	123	-2.14	236	1.41
196	0.15	222	0.97	180	-0.35
202	0.34	210	0.59	236	1.41
210	0.59	224	1.03	152	-1.23
194	0.09	150	-1.29	168	-0.73
198	0.22	156	-1.10	172	-0.60
200	0.28	176	-0.47	212	0.66
212	0.66	196	0.15	184	-0.22
242	1.60	200	0.28	139	-1.64
218	0.84	200	0.28	139	-1.64
192	0.03	186	-0.16	200	0.28
147	-1.38	210	0.59	254	1.97
210	0.59	220	0.91	220	0.91
136	-1.73	186	-0.16	216	0.78
164	-0.85	190	-0.03	208	0.53
166	-0.79	232	1.28	176	-0.47
144	-1.48	176	-0.47	192	0.03
166	-0.79	168	-0.73	200	0.28
166	-0.79	194	0.09	254	1.97
172	-0.60	196	0.15	139	-1.64
166	-0.79	130	-1.92	139	-1.64
176	-0.47	126	-2.04	184	-0.22
192	0.03	180	-0.35	224	1.03
204	0.41	164	-0.85	210	0.59
202	0.34	150	-1.29	250	1.85
156	-1.10	242	1.60	172	-0.60
142	-1.54	214	0.72	180	-0.35
188	-0.10	133	-1.82	152	-1.23
144	-1.48	160	-0.98	172	-0.60
268	2.41	172	-0.60	212	0.66
212	0.66	200	0.28	168	-0.73
242	1.60	192	0.03	236	1.41
210	0.59	152	-1.23	236	1.41
188	-0.10	168	-0.73	122	-2.17
188	-0.10	172	-0.60	224	1.03
178	-0.41	166	-0.79	140	-1.60
194	0.09	176	-0.47	220	0.91
MEAN=	191.10		From Chauvenet's Criterion		
STDEV=	31.85		DRo for this case with n=150, is 2.89		
SDOM=	2.60		If DR>DRo data point is rejected		
%ERROR=	1.36		***No data point is rejected**		
	MICROHARDNESS=191.1±1.36% (VHN)				

Table A.1.4 (b). Coupling Microhardness - 10 Km

VHN #1	Dev. Ratio #1	VHN #2	Dev. Ratio #2	VHN #3	Dev. Ratio #3
130	-2.16	202	-0.80	285	0.77
216	-0.53	192	-0.99	256	0.22
111	-2.52	174	-1.33	250	0.11
226	-0.35	200	-0.84	285	0.77
119	-2.37	280	0.67	260	0.30
136	-2.05	280	0.67	250	0.11
236	-0.16	214	-0.57	295	0.96
236	-0.16	265	0.39	265	0.39
158	-1.63	290	0.86	258	0.26
164	-1.52	214	-0.57	270	0.49
290	0.86	275	0.58	275	0.58
370	2.38	285	0.77	280	0.67
305	1.15	280	0.67	275	0.58
310	1.24	224	-0.38	275	0.58
152	-1.74	265	0.39	270	0.49
166	-1.48	275	0.58	256	0.22
138	-2.01	220	-0.46	248	0.07
265	0.39	158	-1.63	285	0.77
350	2.00	200	-0.84	260	0.30
168	-1.44	230	-0.27	188	-1.06
150	-1.78	305	1.15	265	0.39
138	-2.01	248	0.07	258	0.26
182	-1.18	252	0.15	250	0.11
305	1.15	242	-0.04	270	0.49
188	-1.06	206	-0.72	218	-0.50
190	-1.03	290	0.86	280	0.67
280	0.67	284	0.75	260	0.30
114	-2.46	295	0.96	280	0.67
335	1.71	290	0.86	270	0.49
275	0.58	186	-1.10	265	0.39
270	0.49	230	-0.27	250	0.11
232	-0.23	224	-0.38	285	0.77
200	-0.84	290	0.86	256	0.22
248	0.07	295	0.96	260	0.30
380	2.56	260	0.30	280	0.67
115	-2.44	280	0.67	285	0.77
275	0.58	218	-0.50	260	0.30
325	1.52	315	1.34	258	0.26
111	-2.52	265	0.39	275	0.58
126	-2.23	236	-0.16	256	0.22
280	0.67	275	0.58	285	0.77
135	-2.06	270	0.49	188	-1.06
244	-0.01	238	-0.12	258	0.26
285	0.77	204	-0.76	270	0.49
265	0.39	275	0.58	218	-0.50
182	-1.18	240	-0.08	250	0.11
256	0.22	280	0.67	265	0.39
300	1.05	246	0.03	260	0.30
240	-0.08	290	0.86	248	0.07
180	-1.21	260	0.30	270	0.49
MEAN=	244.29		From Chauvenet's Criterion		
STDEV=	52.93		DRo for this case with n=150, is 2.89		
SDOM=	4.32		If DR>DRo data point is rejected		
%ERROR=	1.77		*No data point is rejected		
	MICROHARDNESS=244.29±1.77% (VHN)				

Table A.1.4 (c). Coupling Microhardness - 100 Km

VHN #1	Dev. Ratio #1	VHN #2	Dev. Ratio #2	VHN #3	Dev. Ratio #3
310	1.75	204	-1.08	280	0.95
280	0.95	232	-0.33	180	-1.72
295	1.35	244	-0.01	206	-1.03
295	1.35	238	-0.17	202	-1.14
315	1.88	265	0.55	280	0.95
220	-0.65	256	0.31	280	0.95
280	0.95	230	-0.39	254	0.25
320	2.02	240	-0.12	226	-0.49
234	-0.28	218	-0.71	230	-0.39
138	-2.85	246	0.04	260	0.41
196	-1.30	258	0.36	232	-0.33
254	0.25	260	0.41	226	-0.49
204	-1.08	265	0.55	265	0.55
265	0.55	246	0.04	262	0.47
238	-0.17	270	0.68	258	0.36
265	0.55	268	0.63	224	-0.55
190	-1.46	250	0.15	220	-0.65
275	0.81	188	-1.51	295	1.35
216	-0.76	222	-0.60	232	-0.33
275	0.81	204	-1.08	220	-0.65
335	2.42	254	0.25	180	-1.72
244	-0.01	250	0.15	202	-1.14
256	0.31	226	-0.49	280	0.95
194	-1.35	250	0.15	226	-0.49
246	0.04	232	-0.33	260	0.41
285	1.08	212	-0.87	226	-0.49
260	0.41	256	0.31	260	0.41
228	-0.44	236	-0.23	224	-0.55
275	0.81	240	-0.12	295	1.35
192	-1.40	206	-1.03	220	-0.65
204	-1.08	285	1.08	232	-0.33
305	1.62	250	0.15	220	-0.65
265	0.55	224	-0.55	258	0.36
270	0.68	240	-0.12	265	0.55
254	0.25	256	0.31	232	-0.33
320	2.02	242	-0.07	230	-0.39
345	2.69	252	0.20	254	0.25
285	1.08	202	-1.14	280	0.95
310	1.75	230	-0.39	206	-1.03
335	2.42	224	-0.55	280	0.95
310	1.75	210	-0.92	285	1.08
345	2.69	222	-0.60	210	-0.92
242	-0.07	220	-0.65	268	0.63
254	0.25	184	-1.62	260	0.41
230	-0.39	170	-1.99	225	-0.52
224	-0.55	190	-1.46	235	-0.25
182	-1.67	184	-1.62	260	0.41
162	-2.20	256	0.31	270	0.68
182	-1.67	240	-0.12	255	0.28
196	-1.30	238	-0.17	262	0.47
MEAN=	244.51		From Chauvenet's Criterion		
STDEV=	37.42		DRo for this case with n=150, is 2.89		
SDOM=	3.06		If DR>DRo data point is rejected		
%ERROR=	1.25		***No data point is rejected**		
	MICROHARDNESS=244.51±1.25% (VHN)				

Table A.1.4 (d). Coupling Microhardness - 200 Km

VHN #1	Dev. Ratio #1	VHN #2	Dev. Ratio #2	VHN #3	Dev. Ratio #3
370	1.96	240	-0.25	238	-0.28
355	1.71	242	-0.22	260	0.09
320	1.11	246	-0.15	258	0.06
335	1.37	252	-0.05	280	0.43
405	2.56	275	0.35	194	-1.03
345	1.54	242	-0.22	194	-1.03
147	-1.83	212	-0.73	246	-0.15
242	-0.22	246	-0.15	250	-0.08
242	-0.22	184	-1.20	270	0.26
252	-0.05	210	-0.76	260	0.09
242	-0.22	180	-1.27	208	-0.80
420	2.81	210	-0.76	270	0.26
280	0.43	200	-0.93	258	0.06
275	0.35	212	-0.73	245	-0.17
335	1.37	254	-0.01	248	-0.11
220	-0.59	246	-0.15	252	-0.05
365	1.88	252	-0.05	238	-0.28
420	2.81	188	-1.14	221	-0.57
300	0.77	256	0.02	238	-0.28
244	-0.18	202	-0.90	248	-0.11
146	-1.85	224	-0.52	258	0.06
330	1.28	188	-1.14	246	-0.15
325	1.20	182	-1.24	218	-0.63
330	1.28	210	-0.76	232	-0.39
290	0.60	230	-0.42	235	-0.34
118	-2.33	188	-1.14	230	-0.42
154	-1.72	295	0.69	250	-0.08
350	1.62	265	0.18	280	0.43
164	-1.54	238	-0.28	280	0.43
340	1.45	254	-0.01	250	-0.08
182	-1.24	270	0.26	265	0.18
295	0.69	226	-0.49	275	0.35
340	1.45	242	-0.22	268	0.23
285	0.52	252	-0.05	218	-0.63
246	-0.15	280	0.43	228	-0.45
194	-1.03	242	-0.22	224	-0.52
330	1.28	222	-0.56	270	0.26
335	1.37	194	-1.03	282	0.46
142	-1.92	244	-0.18	265	0.18
350	1.62	180	-1.27	248	-0.11
420	2.81	224	-0.52	238	-0.28
216	-0.66	254	-0.01	260	0.09
320	1.11	234	-0.35	250	-0.08
285	0.52	265	0.18	270	0.26
240	-0.25	196	-1.00	260	0.09
110	-2.46	228	-0.45	230	-0.42
232	-0.39	234	-0.35	224	-0.52
228	-0.45	228	-0.45	224	-0.52
455	**3.41 R**	236	-0.32	247	-0.13
435	**3.07 R**	256	0.02	275	0.35
MEAN=	252.14		From Chauvenet's Criterion		
STDEV=	54.72		DRo for this case with n=150, is 2.89		
SDOM=	4.50		If DR>DRo data point is rejected		
%ERROR=	1.78		***Two data points are rejected**		
	MICROHARDNESS=252.17±1.78% (VHN)				

Table A.1.4 (e). Coupling Microhardness - 300 Km

VHN#1	Dev. Ratio #1	VHN #2	Dev. Ratio #2	VHN #3	Dev. Ratio #3
355	2.46	220	-0.24	224	-0.16
355	2.46	214	-0.36	210	-0.44
310	1.56	190	-0.84	236	0.08
335	2.06	232	0.00	210	-0.44
250	0.36	212	-0.40	216	-0.32
345	2.26	224	-0.16	212	-0.40
325	1.86	244	0.24	198	-0.68
218	-0.28	230	-0.04	184	-0.96
290	1.16	254	0.44	214	-0.36
325	1.86	222	-0.20	210	-0.44
242	0.20	236	0.08	188	-0.88
246	0.28	238	0.12	230	-0.04
305	1.46	224	-0.16	198	-0.68
345	2.26	242	0.20	172	-1.20
305	1.46	220	-0.24	224	-0.16
340	2.16	236	0.08	174	-1.16
325	1.86	220	-0.24	220	-0.24
285	1.06	216	-0.32	228	-0.08
162	-1.40	188	-0.88	236	0.08
214	-0.36	200	-0.64	226	-0.12
206	-0.52	226	-0.12	236	0.08
172	-1.20	234	0.04	238	0.12
190	-0.84	232	0.00	220	-0.24
345	2.26	270	0.76	210	-0.44
234	0.04	184	-0.96	216	-0.32
162	-1.40	200	-0.64	184	-0.96
244	0.24	232	0.00	242	0.20
172	-1.20	194	-0.76	251	0.38
128	-2.08	224	-0.16	218	-0.28
310	1.56	230	-0.04	212	-0.40
198	-0.68	230	-0.04	236	0.08
228	-0.08	246	0.28	244	0.24
320	1.76	206	-0.52	230	-0.04
370	2.76	210	-0.44	220	-0.24
158	-1.48	170	-1.24	224	-0.16
310	1.56	135	-1.94	228	-0.08
218	-0.28	202	-0.60	242	0.20
355	2.46	202	-0.60	248	0.32
340	2.16	222	-0.20	210	-0.44
224	-0.16	178	-1.08	208	-0.48
285	1.06	228	-0.08	202	-0.60
238	0.12	178	-1.08	200	-0.64
315	1.66	216	-0.32	225	-0.14
160	-1.44	152	-1.60	220	-0.24
204	-0.56	192	-0.80	240	0.16
220	-0.24	194	-0.76	212	-0.40
182	-1.00	192	-0.80	202	-0.60
140	-1.84	236	0.08	248	0.32
275	0.86	200	-0.64	230	-0.04
390	**3.16 R**	218	-0.28	231	-0.02
MEAN=	230.95		From Chauvenet's Criterion		
STDEV=	48.42		DRo for this case with n=150, is 2.89		
SDOM=	3.97		If DR>DRo data point is rejected		
%ERROR=	1.72		***One data point is rejected**		
	MICROHARDNESS=230.95±1.72% (VHN)				

Table A.1.5 (a). Tubing Microhardness - Initial

VHN #1	Dev. Ratio #1	VHN #2	Dev. Ratio #2	VHN #3	Dev. Ratio #3
122	-2.48	198	0.73	198	0.73
141	-1.67	202	0.90	148	-1.38
144	-1.55	216	1.49	176	-0.20
178	-0.11	172	-0.37	186	0.22
168	-0.53	186	0.22	188	0.31
138	-1.80	200	0.82	168	-0.53
178	-0.11	190	0.39	176	-0.20
194	0.56	214	1.41	196	0.65
180	-0.03	188	0.31	186	0.22
160	-0.87	184	0.14	166	-0.62
182	0.06	214	1.41	212	1.32
160	-0.87	188	0.31	198	0.73
127	-2.26	180	-0.03	172	-0.37
123	-2.43	184	0.14	192	0.48
158	-0.96	180	-0.03	192	0.48
144	-1.55	216	1.49	192	0.48
180	-0.03	204	0.98	184	0.14
178	-0.11	190	0.39	198	0.73
176	-0.20	220	1.66	176	-0.20
132	-2.05	200	0.82	206	1.07
172	-0.37	184	0.14	170	-0.45
107	-3.11	180	-0.03	184	0.14
192	0.48	186	0.22	204	0.98
152	-1.21	204	0.98	200	0.82
128	-2.22	192	0.48	210	1.24
168	-0.53	208	1.15	188	0.31
160	-0.87	194	0.56	202	0.90
162	-0.79	204	0.98	148	-1.38
160	-0.87	188	0.31	186	0.22
194	0.56	200	0.82	168	-0.53
160	-0.87	168	-0.53	196	0.65
184	0.14	184	0.14	166	-0.62
162	-0.79	212	1.32	198	0.73
109	-3.02	184	0.14	192	0.48
114	-2.81	190	0.39	192	0.48
160	-0.87	194	0.56	198	0.73
144	-1.55	186	0.22	176	-0.20
136	-1.88	200	0.82	202	0.90
176	-0.20	196	0.65	188	0.31
240	2.50	212	1.32	204	0.98
138	-1.80	180	-0.03	170	-0.45
142	-1.63	178	-0.11	184	0.14
178	-0.11	188	0.31	210	1.24
176	-0.20	208	1.15	200	0.82
164	-0.70	188	0.31	198	0.73
156	-1.04	196	0.65	176	-0.20
178	-0.11	174	-0.28	188	0.31
202	0.90	168	-0.53	176	-0.20
176	-0.20	214	1.41	186	0.22
194	0.56	186	0.22	212	1.32

MEAN=	180.67	From Chauvenet's Criterion	
STDEV=	23.70	DRo for this case with n=150, is 2.89	
SDOM=	1.94	If DR>DRo data point is rejected	
%ERROR=	1.07	***No data point is rejected**	
	MICROHARDNESS=180.67±1.07% (VHN)		

Table A.1.5 (b). Tubing Microhardness - 10 Km

VHN #1	Dev. Ratio #1	VHN #2	Dev. Ratio #2	VHN #3	Dev. Ratio #3
246	1.25	214	0.14	248	1.31
250	1.38	180	-1.02	194	-0.54
258	1.66	208	-0.06	218	0.28
248	1.31	194	-0.54	208	-0.06
246	1.25	208	-0.06	248	1.31
224	0.49	216	0.21	224	0.49
252	1.45	224	0.49	204	-0.20
210	0.01	190	-0.68	198	-0.41
206	-0.13	194	-0.54	208	-0.06
248	1.31	188	-0.75	176	-1.16
224	0.49	186	-0.82	208	-0.06
236	0.90	206	-0.13	228	0.63
218	0.28	210	0.01	188	-0.75
242	1.11	222	0.42	200	-0.34
290	2.76	202	-0.27	188	-0.75
238	0.97	200	-0.34	242	1.11
228	0.56	218	0.28	248	1.31
210	0.01	194	-0.54	254	1.52
208	-0.06	204	-0.20	254	1.52
224	0.49	206	-0.13	228	0.63
230	0.69	190	-0.68	232	0.76
156	-1.85	236	0.90	218	0.28
198	-0.41	184	-0.89	218	0.28
214	0.14	196	-0.47	210	0.01
198	-0.41	170	-1.37	200	-0.34
210	0.01	210	0.01	200	-0.34
202	-0.27	166	-1.51	194	-0.54
206	-0.13	196	-0.47	208	-0.06
242	1.11	188	-0.75	224	0.49
202	-0.27	190	-0.68	198	-0.41
188	-0.75	190	-0.68	176	-1.16
220	0.35	206	-0.13	228	0.63
210	0.01	260	1.73	200	-0.34
188	-0.75	210	0.01	248	1.31
188	-0.75	232	0.76	254	1.52
170	-1.37	214	0.14	200	-0.34
176	-1.16	196	-0.47	210	0.01
210	0.01	212	0.08	218	0.28
121	-3.05	218	0.28	232	0.76
118	-3.16	170	-1.37	254	1.52
162	-1.64	188	-0.75	228	0.63
135	-2.57	204	-0.20	248	1.31
196	-0.47	218	0.28	218	0.28
210	0.01	158	-1.78	248	1.31
111	-3.40	226	0.56	204	-0.20
145	-2.23	214	0.14	208	-0.06
202	-0.27	210	0.01	188	-0.75
222	0.42	224	0.49	242	1.11
204	-0.20	198	-0.41	242	1.11
186	-0.82	190	-0.68	305	**3.27 R**
MEAN=	209.15		From Chauvenet's Criterion		
STDEV=	28.10		DRo for this case with n=150, is 2.89		
SDOM=	2.30		If DR>DRo data point is rejected		
%ERROR=	1.10		***One data point is rejected**		
	MICROHARDNESS=209.15±1.10% (VHN)				

Table A.1.5 (c). Tubing Microhardness - 100 Km

VHN #1	Dev. Ratio #1	VHN #2	Dev. Ratio #2	VHN #3	Dev. Ratio #3
230	0.47	200	-0.25	190	-0.49
220	0.23	196	-0.35	200	-0.25
260	1.19	188	-0.54	202	-0.20
248	0.90	194	-0.40	210	-0.01
194	-0.40	200	-0.25	188	-0.54
315	2.52	202	-0.20	200	-0.25
260	1.19	194	-0.40	194	-0.40
258	1.14	180	-0.73	208	-0.06
175	-0.85	206	-0.11	216	0.13
111	-2.40	200	-0.25	218	0.18
185	-0.61	226	0.37	226	0.37
234	0.57	204	-0.16	216	0.13
120	-2.18	224	0.33	222	0.28
186	-0.59	172	-0.93	198	-0.30
183	-0.66	210	-0.01	206	-0.11
200	-0.25	238	0.66	224	0.33
156	-1.31	216	0.13	214	0.08
260	1.19	200	-0.25	202	-0.20
162	-1.17	202	-0.20	216	0.13
220	0.23	186	-0.59	244	0.81
101	-2.64	190	-0.49	226	0.37
199	-0.28	224	0.33	218	0.18
179	-0.76	208	-0.06	220	0.23
144	-1.60	242	0.76	210	-0.01
175	-0.85	204	-0.16	194	-0.40
280	1.67	194	-0.40	226	0.37
315	2.52	176	-0.83	206	-0.11
158	-1.26	180	-0.73	230	0.47
280	1.67	192	-0.45	214	0.08
170	-0.97	196	-0.35	242	0.76
160	-1.22	198	-0.30	214	0.08
168	-1.02	192	-0.45	224	0.33
220	0.23	200	-0.25	200	-0.25
164	-1.12	176	-0.83	216	0.13
265	1.31	226	0.37	240	0.71
170	-0.97	176	-0.83	218	0.18
158	-1.26	216	0.13	218	0.18
285	1.79	180	-0.73	212	0.04
175	-0.85	200	-0.25	236	0.61
194	-0.40	194	-0.40	236	0.61
285	1.79	196	-0.35	214	0.08
214	0.08	188	-0.54	202	-0.20
254	1.05	206	-0.11	224	0.33
240	0.71	188	-0.54	198	-0.30
111	-2.40	190	-0.49	226	0.37
133	-1.87	170	-0.97	236	0.61
345	**3.24 R**	214	0.08	232	0.52
335	**3.00 R**	210	-0.01	242	0.76
390	**4.32 R**	210	-0.01	204	-0.16
355	**3.48 R**	190	-0.49	238	0.66
MEAN=	206.49		From Chauvenet's Criterion		
STDEV=	34.03		DRo for this case with n=150, is 2.89		
SDOM=	2.82		If DR>DRo data point is rejected		
%ERROR=	1.37		***Four data points are rejected**		
	MICROHARDNESS=206.49±1.37% (VHN)				

Table A.1.5 (d). Tubing Microhardness - 200 Km

VHN #1	Dev. Ratio #1	VHN #2	Dev. Ratio #2	VHN #3	Dev. Ratio #3
355	2.04	172	-0.98	214	-0.29
236	0.07	190	-0.69	236	0.07
194	-0.62	214	-0.29	224	-0.13
275	0.72	202	-0.49	212	-0.32
290	0.96	198	-0.55	200	-0.52
360	2.12	210	-0.36	218	-0.22
240	0.14	222	-0.16	216	-0.26
300	1.13	230	-0.03	218	-0.22
400	2.78	275	0.72	240	0.14
365	2.20	194	-0.62	236	0.07
360	2.12	230	-0.03	244	0.20
184	-0.79	194	-0.62	214	-0.29
335	1.71	212	-0.32	224	-0.13
232	0.01	210	-0.36	202	-0.49
190	-0.69	200	-0.52	220	-0.19
250	0.30	208	-0.39	224	-0.13
258	0.44	236	0.07	220	-0.19
365	2.20	246	0.24	198	-0.55
355	2.04	232	0.01	254	0.37
130	-1.68	210	-0.36	226	-0.09
218	-0.22	228	-0.06	238	0.11
370	2.28	182	-0.82	236	0.07
148	-1.38	184	-0.79	204	-0.46
335	1.71	196	-0.59	232	0.01
224	-0.13	188	-0.72	242	0.17
335	1.71	220	-0.19	242	0.17
114	-1.94	190	-0.69	204	-0.46
152	-1.31	210	-0.36	238	0.11
265	0.55	200	-0.52	236	0.07
335	1.71	188	-0.72	232	0.01
174	-0.95	192	-0.65	226	-0.09
120	-1.84	192	-0.65	198	-0.55
254	0.37	212	-0.32	224	-0.13
390	2.61	176	-0.92	220	-0.19
158	-1.21	200	-0.52	224	-0.13
325	1.54	206	-0.42	244	0.20
166	-1.08	216	-0.26	240	0.14
168	-1.05	234	0.04	216	-0.26
180	-0.85	204	-0.46	200	-0.52
265	0.55	206	-0.42	224	-0.13
240	0.14	220	-0.19	214	-0.29
202	-0.49	200	-0.52	236	0.07
140	-1.51	206	-0.42	212	-0.32
405	2.86	196	-0.59	218	-0.22
122	-1.81	226	-0.09	236	0.07
135	-1.59	224	-0.13	214	-0.29
265	0.55	218	-0.22	224	-0.13
455	**3.69 R**	204	-0.46	220	-0.19
415	**3.03 R**	208	-0.39	220	-0.19
410	**2.94 R**	202	-0.49	198	-0.55
MEAN=	227.51		From Chauvenet's Criterion		
STDEV=	54.24		DRo for this case with n=150, is 2.89		
SDOM=	4.47		If DR>DRo data point is rejected		
%ERROR=	1.96		***Three data points are rejected**		
	MICROHARDNESS=227.51±1.96% (VHN)				

Table A.1.5 (e). Tubing Microhardness - 300 Km

VHN #1	Dev. Ratio #1	VHN #2	Dev. Ratio #2	VHN #3	Dev. Ratio #3
315	1.93	206	-0.51	196	-0.73
280	1.15	200	-0.64	232	0.07
330	2.27	200	-0.64	208	-0.46
182	-1.04	224	-0.10	210	-0.42
280	1.15	206	-0.51	212	-0.37
158	-1.58	216	-0.28	270	0.92
236	0.16	204	-0.55	224	-0.10
208	-0.46	210	-0.42	230	0.03
285	1.26	212	-0.37	214	-0.33
265	0.81	210	-0.42	242	0.30
236	0.16	224	-0.10	240	0.25
320	2.04	218	-0.24	244	0.34
168	-1.36	198	-0.69	246	0.39
184	-1.00	218	-0.24	240	0.25
236	0.16	204	-0.55	204	-0.55
295	1.48	194	-0.78	238	0.21
232	0.07	224	-0.10	202	-0.60
115	-2.54	234	0.12	280	1.15
135	-2.09	256	0.61	180	-1.09
350	2.71	232	0.07	244	0.34
256	0.61	212	-0.37	240	0.25
212	-0.37	216	-0.28	285	1.26
295	1.48	200	-0.64	242	0.30
194	-0.78	200	-0.64	236	0.16
315	1.93	210	-0.42	244	0.34
250	0.48	238	0.21	196	-0.73
140	-1.98	210	-0.42	208	-0.46
242	0.30	258	0.66	212	-0.37
330	2.27	242	0.30	224	-0.10
265	0.81	260	0.70	214	-0.33
220	-0.19	258	0.66	240	0.25
109	-2.68	236	0.16	246	0.39
194	-0.78	224	-0.10	204	-0.55
102	-2.83	265	0.81	202	-0.60
182	-1.04	224	-0.10	180	-1.09
325	2.15	222	-0.15	240	0.25
238	0.21	220	-0.19	242	0.30
197	-0.71	180	-1.09	244	0.34
275	1.04	200	-0.64	236	0.16
154	-1.67	214	-0.33	285	1.26
194	-0.78	224	-0.10	244	0.34
345	2.60	192	-0.82	280	1.15
325	2.15	210	-0.42	238	0.21
290	1.37	180	-1.09	240	0.25
122	-2.39	210	-0.42	244	0.34
132	-2.16	228	-0.02	242	0.30
180	-1.09	234	0.12	230	0.03
300	1.59	250	0.48	270	0.92
315	1.93	212	-0.37	210	-0.42
275	1.04	194	-0.78	232	0.07
MEAN=	228.68		From Chauvenet's Criterion		
STDEV=	44.72		DRo for this case with n=150, is 2.89		
SDOM=	3.65		If DR>DRo data point is rejected		
%ERROR=	1.60		*No data point is rejected		
	MICROHARDNESS=228.68±1.60% (VHN)				

APPENDIX 2: Summary of Results

Table A.2.1. Coupling Weight Loss [g] vs Distance Travelled at Various Side Loads-Water Environment

	Distance[m]-->	Initial	10000	100000	200000	300000
	Side Load[N]					
standard coupling	133.5	0	0.10	0.73	1.47	2.47
	445	0	0.30	1.10	2.10	3.00
	890	0	5.60	7.40	9.30	11.50
NiCr coated coupling	133.5	0	0	0.27	0.57	0.80
	445	0	0	0.30	0.50	0.80
	890	0	0	0.10	0.50	0.80
NiW coated coupling	133.5	0	0.10	0.16	0.37	0.60
	445	0	0.10	0.20	0.40	0.70
	890	0	0.10	0.30	0.40	0.60
TiO2 coated coupling	133.5	0	0.17	0.34	0.50	0.63
	445	0	0.10	0.40	0.65	0.75
	890	0	0.10	0.10	0.40	0.50

Table A.2.2. Coupling Weight Loss [g] vs Distance Travelled at Various Side Loads-Water & Sand Environment

	Distance[m]-->	Initial	10000	100000	200000	300000
	Side Load[N]					
standard coupling	133.5	0	1.60	10.90	20.60	31.40
	445	0	2.50	28.20	43.60	57.90
	890	0	13.90	44.50	58.20	75.10
NiCr coated coupling	133.5	0	0.40	3.90	6.00	9.70
	445	0	1.00	8.30	16.00	23.80
	890	-	-	-	-	-
NiW coated coupling	133.5	0	0.70	3.70	6.40	10.30
	445	0	0.40	3.00	5.80	7.10
	890	0	0.30	3.40	5.30	6.90
TiO2 coated coupling	133.5	0	2.80	12.90	18.90	28.20
	445	0	13.80	76.30	106.10	142.40
	890	-	-	-	-	-

Table A.2.3. Tubing Average Thickness Loss [mm] vs Distance Travelled at Various Side Loads-Water Environment

	Distance[m]-->	Initial	10000	100000	200000	300000
	Side Load[N]					
standard coupling	133.5	0	0.02	0.04	0.06	0.10
	445	0	0.02	0.06	0.10	0.14
	890	0	0.63	0.64	0.64	0.69
NiCr coated coupling	133.5	0	0.01	0.02	0.04	0.06
	445	0	0.06	0.13	0.17	0.23
	890	0	0.17	0.43	0.67	0.81
NiW coated coupling	133.5	0	0.01	0.03	0.04	0.05
	445	0	0.05	0.12	0.16	0.18
	890	0	0.12	0.37	0.49	0.59
TiO2 coated coupling	133.5	0	0.02	0.05	0.06	0.09
	445	0	0.02	0.05	0.09	0.11
	890	0	0.04	0.08	0.12	0.15

Table A.2.4. Tubing Average Thickness Loss [mm] vs Distance Travelled at Various Side Loads-Water & Sand Environment

	Distance[m]-->	Initial	10000	100000	200000	300000
	Side Load[N]					
standard coupling	133.5	0	0.08	0.36	0.57	0.76
	445	0	0.16	0.94	1.20	1.46
	890	0	0.67	1.42	1.72	2.06
NiCr coated coupling	133.5	0	0.01	0.20	0.33	0.46
	445	0	0.14	0.76	1.08	1.40
	890	-	-	-	-	-
NiW coated coupling	133.5	0	0.06	0.32	0.51	0.71
	445	0	0.11	0.76	1.25	1.48
	890	0	0.30	1.25	1.75	2.00
TiO2 coated coupling	133.5	0	0.04	0.29	0.38	0.52
	445	0	0.40	1.43	1.82	2.21
	890	-	-	-	-	-

Table A.2.5. Tubing Surface Roughness [μm] vs Distance Travelled at Various Side Loads-Water Environment

	Distance[m]-->	Initial	10000	100000	200000	300000
	Side Load[N]					
standard coupling	133.5	3.675	1.750	1.200	0.875	0.625
	445	3.675	2.328	1.698	2.300	1.038
	890	3.675	6.113	6.075	4.888	3.550
NiCr coated coupling	133.5	3.675	1.107	0.538	0.533	0.438
	445	3.675	1.975	2.050	0.975	0.500
	890	3.675	3.725	6.700	6.325	4.575
NiW coated coupling	133.5	3.675	1.600	0.695	0.625	0.575
	445	3.675	2.838	2.650	1.950	1.838
	890	3.675	5.243	5.225	3.588	5.413
TiO2 coated coupling	133.5	3.675	0.750	0.350	0.300	0.225
	445	3.675	0.675	0.425	0.400	0.325
	890	3.675	0.248	0.483	0.225	0.253

Table A.2.6. Tubing Surface Roughness [μm] vs Distance Travelled at Various Side Loads-Water & Sand Environment

	Distance[m]-->	Initial	10000	100000	200000	300000
	Side Load[N]					
standard coupling	133.5	3.675	2.570	2.500	2.020	1.920
	445	3.675	7.340	5.030	5.340	4.530
	890	3.675	6.580	4.660	4.510	5.580
NiCr coated coupling	133.5	3.675	0.210	0.240	0.260	0.470
	445	3.675	2.750	2.380	2.000	2.050
	890	-	-	-	-	-
NiW coated coupling	133.5	3.675	0.540	0.390	0.500	0.350
	445	3.675	2.420	4.180	2.310	2.030
	890	3.675	3.790	3.650	3.550	3.400
TiO2 coated coupling	133.5	3.675	1.790	1.250	1.060	1.620
	445	3.675	5.630	3.830	2.980	2.710
	890	-	-	-	-	-

Table A.2.7. Coupling Microhardness [VHN] vs Distance Travelled at Various Side Loads-Water Environment

	Distance[m]-->	Initial	10000	100000	200000	300000
	Side Load[N]					
standard coupling	133.5	191.10	244.29	244.51	252.17	230.95
	445	187.00	318.20	323.00	282.00	284.00
	890	187.00	282.50	287.00	297.40	296.28
NiCr coated coupling	133.5	639.00	642.00	664.00	667.00	649.00
	445	641.00	693.00	675.00	675.00	665.00
	890	648.00	624.00	626.00	636.50	621.00
NiW coated coupling	133.5	694.10	668.20	660.40	645.00	590.00
	445	700.80	656.60	654.60	641.00	527.40
	890	690.00	660.20	694.00	650.80	554.00
TiO2 coated coupling	133.5	615.00	675.00	707.00	739.00	723.00
	445	616.00	661.00	677.00	668.00	656.00
	890	616.00	620.00	622.00	643.00	662.00

Table A.2.8. Coupling Microhardness [VHN] vs Distance Travelled at Various Side Loads-Water & Sand Environment

	Distance[m]-->	Initial	10000	100000	200000	300000
	Side Load[N]					
standard coupling	133.5	189.68	289.08	267.56	308.36	286.84
	445	190.44	306.64	253.40	290.48	286.52
	890	187.20	325.24	286.56	323.04	315.76
NiCr coated coupling	133.5	634.60	595.80	615.00	595.00	567.60
	445	639.00	622.20	593.20	418.28	236.92
	890	-	-	-	-	-
NiW coated coupling	133.5	669.60	643.80	629.00	576.00	546.40
	445	692.20	632.71	622.60	630.60	627.40
	890	684.00	633.40	627.80	562.04	559.20
TiO2 coated coupling	133.5	615.00	336.88	256.56	266.16	320.76
	445	615.00	257.20	266.28	277.84	281.92
	890	-	-	-	-	-

Table A.2.9. Tubing Microhardness [VHN] vs Distance Travelled at Various Side Loads-Water Environment

	Distance[m]-->	Initial	10000	100000	200000	300000
	Side Load[N]					
standard coupling	133.5	180.67	209.15	206.49	227.51	228.68
	445	184.30	213.40	277.00	268.00	276.00
	890	178.00	283.50	291.00	288.40	286.30
NiCr coated coupling	133.5	191.00	203.00	215.00	210.00	212.00
	445	186.00	291.00	269.00	274.00	245.00
	890	186.20	285.50	311.90	362.70	342.70
NiW coated coupling	133.5	187.30	232.50	245.00	240.80	245.00
	445	190.00	332.00	288.00	252.00	234.00
	890	189.44	316.50	303.00	318.00	299.00
TiO2 coated coupling	133.5	189.00	211.00	211.00	202.00	205.00
	445	192.00	224.00	213.00	204.00	210.00
	890	188.60	228.00	208.30	204.10	193.00

Table A.2.10. Tubing Microhardness [VHN] vs Distance Travelled at Various Side Loads-Water & Sand Environment

	Distance[m]-->	Initial	10000	100000	200000	300000
	Side Load[N]					
standard coupling	133.5	180.92	298.32	279.36	280.32	277.28
	445	184.24	270.08	278.56	294.44	295.12
	890	179.44	276.52	290.08	292.04	292.96
NiCr coated coupling	133.5	182.68	221.76	227.76	229.80	235.40
	445	180.08	342.52	325.92	287.92	249.52
	890	-	-	-	-	-
NiW coated coupling	133.5	181.96	259.32	219.20	224.08	230.72
	445	183.36	340.20	291.16	332.44	332.00
	890	180.16	277.24	344.36	355.00	305.52
TiO2 coated coupling	133.5	177.80	306.08	297.80	272.92	268.12
	445	180.96	235.36	271.24	275.04	280.04
	890	-	-	-	-	-

Table A.2.11. Frictional Force [N] as a Function of Side Load-Water Environment

	Side Load[N]	Mean
standard coupling	133.5	77.43
	445	226.95
	890	382.70
NiCr coated coupling	133.5	76.10
	445	146.85
	890	356.00
NiW coated coupling	133.5	73.43
	445	226.95
	890	400.50
TiO2 coated coupling	133.5	76.10
	445	213.60
	890	445.00

Table A.2.12. Frictional Force [N] as a Function of Side Load-Water & Sand Environment

	Side Load[N]	Mean
standard coupling	133.5	57.40
	445	200.25
	890	453.90
NiCr coated coupling	133.5	74.76
	445	146.85
	890	-
NiW coated coupling	133.5	73.42
	445	173.55
	890	409.40
TiO2 coated coupling	133.5	77.43
	445	106.80
	890	-

Table A.2.13. Apparent Coefficient of Friction at Various Side Loads-Water Environment

	Side Load[N]	Range	Mean
standard coupling	133.5	0.52 - 0.64	0.58
	445	0.47 - 0.63	0.51
	890	0.37 - 0.48	0.43
NiCr coated coupling	133.5	0.37 - 0.74	0.57
	445	0.24 - 0.42	0.33
	890	0.38 - 0.45	0.40
NiW coated coupling	133.5	0.40 - 0.70	0.55
	445	0.43 - 0.56	0.51
	890	0.41 - 0.49	0.45
TiO2 coated coupling	133.5	0.50 - 0.71	0.57
	445	0.41 - 0.60	0.48
	890	0.33 - 0.63	0.50

Table A.2.14. Apparent Coefficient of Friction at Various Side Loads-Water & Sand Environment

	Side Load[N]	Range	Mean
standard coupling	133.5	0.33 - 0.59	0.43
	445	0.33 - 0.57	0.45
	890	0.40 - 0.67	0.51
NiCr coated coupling	133.5	0.46 - 0.68	0.56
	445	0.16 - 0.50	0.33
	890	-	-
NiW coated coupling	133.5	0.49 - 0.66	0.55
	445	0.32 - 0.50	0.39
	890	0.35 - 0.59	0.46
TiO2 coated coupling	133.5	0.41 - 0.76	0.58
	445	0.10 - 0.53	0.24
	890	-	-

Table A.2.15. Coupling Wear Rates [cc/Nm]-Water Environment

	Distance[m]-->	10000	100000	200000	300000
	Side Load[N]				
standard coupling	133.5	9.53E-09	6.96E-09	7.00E-09	7.85E-09
	445	8.58E-09	3.14E-09	3.00E-09	2.86E-09
	890	8.01E-08	1.06E-08	6.65E-09	5.48E-09
NiCr coated coupling	133.5	0	2.53E-09	2.67E-09	2.50E-09
	445	0	8.43E-10	7.02E-10	7.49E-10
	890	0	1.40E-10	3.51E-10	3.75E-10
NiW coated coupling	133.5	6.94E-09	1.11E-09	1.28E-09	1.39E-09
	445	2.08E-09	4.16E-10	4.16E-10	4.86E-10
	890	1.04E-09	3.12E-10	2.08E-10	2.08E-10
TiO2 coated coupling	133.5	2.27E-08	4.55E-09	3.34E-09	2.81E-09
	445	4.01E-09	1.61E-09	1.30E-09	1.00E-09
	890	2.01E-09	2.01E-10	4.01E-10	3.34E-10

Table A.2.16. Coupling Wear Rates [cc/Nm]-Water & Sand Environment

	Distance[m]-->	10000	100000	200000	300000
	Side Load[N]				
standard coupling	133.5	1.52E-07	1.04E-07	9.82E-08	9.97E-08
	445	7.15E-08	8.06E-08	6.23E-08	5.52E-08
	890	1.99E-07	6.36E-08	4.16E-08	3.58E-08
NiCr coated coupling	133.5	3.75E-08	3.65E-08	2.81E-08	3.03E-08
	445	2.81E-08	2.33E-08	2.25E-08	2.23E-08
	890	-	-	-	-
NiW coated coupling	133.5	4.86E-08	2.57E-08	2.22E-08	2.38E-08
	445	8.32E-09	6.24E-09	6.03E-09	4.92E-09
	890	3.12E-09	3.54E-09	2.76E-09	2.39E-09
TiO2 coated coupling	133.5	3.75E-07	1.73E-07	1.26E-07	1.26E-07
	445	5.54E-07	3.06E-07	2.13E-07	1.90E-07
	890	-	-	-	-

Table A.2.17. Summary of Results of Different Variables at Different Sand Rates Using Standard Coupling/ J55 Tubing Under 133.5 N Side Load

Distance[m]->	Initial	10000	100000	200000	300000
Sand Rate[g/day]					
	coupling weight loss [g]				
0	0.00	0.10	0.73	1.47	2.47
15	0.00	0.50	3.60	7.20	11.10
165	0.00	1.60	10.90	20.60	31.40
180	0.00	2.00	18.40	33.40	45.10
	tubing thickness loss [mm]				
0	0.00	0.02	0.04	0.06	0.10
15	0.00	0.04	0.11	0.23	0.28
165	0.00	0.08	0.36	0.57	0.76
180	0.00	0.09	0.50	0.73	0.94
	tubing surface roughness [μm]				
0	3.68	1.75	1.20	0.88	0.63
15	3.68	1.03	0.55	0.45	0.50
165	3.68	2.57	2.50	2.02	1.92
180	3.68	1.14	0.95	0.77	1.04
	coupling microhardness [VHN]				
0	191.10	244.29	244.51	252.17	230.95
15	196.76	257.50	263.04	262.40	257.80
165	189.68	289.08	267.56	308.36	286.84
180	186.70	317.30	280.50	258.90	272.50
	tubing microhardness [VHN]				
0	180.67	209.15	206.49	227.51	228.68
15	185.60	250.00	259.40	269.20	274.30
165	180.92	298.32	279.36	280.32	277.28
180	184.00	285.00	294.00	328.60	317.40
	coupling wear rate [cc/Nm]				
0	0	9.53E-09	6.96E-09	7.00E-12	7.85E-09
15	0	4.77E-08	3.43E-08	3.43E-08	3.53E-08
165	0	1.52E-07	1.04E-07	9.82E-08	9.97E-08
180	0	1.91E-07	1.75E-07	1.59E-07	1.43E-07
apparent coefficient of friction (mean value)					
0	0.58				
15	0.69				
165	0.43				
180	0.68				